Impact of renewable power penetration on power market operation

Zhao, Qian

2012

Zhao, Q. (2012). Impact of renewable power penetration on power market operation. Doctoral thesis, Nanyang Technological University, Singapore.

https://hdl.handle.net/10356/54909

https://doi.org/10.32657/10356/54909

Impact of Renewable Power Penetration on Power Market Operation

Zhao Qian

School of Electrical and Electronic Engineering

A thesis submitted to the Nanyang Technological University
in fulfillment of the requirement for the degree of
Doctor of Philosophy

2012

Acknowledgements

I would like to give my sincere gratitude and indebtedness to my supervisors, Prof. Lalit Goel and Prof. Peng Wang for their invaluable encouragement, support and guidance. The advices, criticism and support from Prof. Goel are thankfully acknowledged. His enthusiasm toward life and work has given me deep impression and will affect my future research and work a lot.

Special thanks and appreciation goes to my co-supervisor, Prof. Wang who has provided me valuable advices in my research work of my PhD study. He has also contributed a lot to this research work. His rigorous and conscientious attitude toward research impressed me very much. His concern for both my research and life are greatly acknowledged.

Prof. Yi Ding has given me valuable suggestion on my research work. I am very grateful for his patience in helping me solving research problems.

Financial support provided by Nanyang Technological University is sincerely appreciated for supporting me through my PhD study. I am thankful to the technicians Mr. Lim Kim Peow, Ms. Ng-Tan Siew Hong Jennifer, Mr. Yeoh Tiow Koon, Mr. Lee Ting Ye and Ms. Chew-Sim Annie for their technical support in the usage of computers, software and other equipment.

Great thanks are given to my parents who told me not to give up when I was troubled and who always support me in my life. Thanks also given to my brother and friends who always support me in my life and study.

Summary

The power market provides more choices for both power suppliers and consumers. The objective of each market participant is to maximize its benefit while minimizing the cost through purchasing or selling energy. In a conventional vertically integrated system, the electricity prices are determined uniformly by the system operators. In a restructured power system, however, the electricity prices are determined by clearing the power market. The system reliability is not only related to system configurations and component outage properties, but also affected by the electricity prices. Nodal prices and nodal reliability are adopted in the power market for pricing the energy and for evaluating customers' reliability. In deregulated power systems, the provision and pricing of ancillary services are determined in the ancillary service market.

Renewable energy have being utilized widely as substitutes for fossil fuels due to their clean generation process and abundance. Penetration of renewable sources, however, introduces additional variables to the existing power system due to their intermittent nature. The variation of renewable energy and participation of renewable energy providers in power market operation will affect the nodal prices and nodal reliability. New techniques need to be developed to understand and assess the behavior of renewable energy, and to quantify their impacts on power market operation.

The main aim of the research project was to investigate restructured power system operation and the impacts of the renewable energy penetration on market operations. The existing theories and methods to evaluate reliability performances and electricity prices have been studied. Renewable energy penetrations in deregulated power systems have been investigated. Since the fluctuations in unpredictable renewable power affect reserve deployment, the reserve market and deployment have also been

investigated. Contingency reserve models and an energy and reserve co-optimization market clearing process have been proposed. The impacts of contingency reserves on system reliability risks have been analyzed using an analytical method. The generation and reliability models of solar generation systems in terms of photovoltaic (PV) arrays and wind generation in terms of wind turbine generators (WTG) have been developed. The variations of renewable power have been examined using the auto-regressive and moving average time series method. Considering the stochastic and chronological nature of solar power, the pseudo sequential Monte Carlo simulation method has been utilized to evaluate the impacts of PV power on system reliability performances and reserve deployments. The bidding strategies of wind power providers have been investigated based on short-term forecasts. The impacts of wind power providers' bidding strategies on nodal price and nodal reliability have also been examined.

Table of Contents

Acknowledgements I
Summary II
Table of Contents IV
List of Symbols VII
List of Figures VIII
List of Tables IX
Chapter 1 Introduction 1
1.1 Conventional Power System 2
1.2 History of Power System Deregulation 3
1.3 Restructured Power Systems 8
1.3.1 Market participants 8
1.3.2 Market models 11
1.3.3 Ancillary services market 12
1.4 Renewable Power Penetrations 13
1.4.1 Renewable energy 13
1.4.2 Renewable power penetrations in restructured power systems 14
1.5 Power System Reliability 16
1.6 Objectives and Contributions 17
1.6.1 Impacts of reserve on system reliability 17
1.6.2 Impacts of renewable energy on nodal reliability 19
1.6.3 Impacts of renewable energy on energy price and customer reliability 20
1.7 Organization of the Thesis 21
Chapter 2 Power System Economics and Reliability 22
2.1 System Economic Operation 22
2.1.1 Economic Dispatch (ED) 22
2.1.2 Optimal Power Flow (OPF) 27
2.2 Power System Reliability Evaluation 34
2.2.1 Component models 34
2.2.2 System reliability evaluation 36
2.3 Nodal Price and Nodal Reliability 43
2.3.1 Nodal price 46
2.3.2 Customer reliability and load curtailment 46
2.3.3 Nodal price and nodal reliability 48
2.4 Conclusions 48
Chapter 3 Renewable Power Generation 50
3.1 Wind Energy Conversion System 50
3.1.1 Wind speed 51
3.1.2 Relation between power output and wind speed 55
3.2 Solar Energy Conversion System 56

3.2.1 Solar radiation 57
3.2.2 Electrical characteristic of PV panel 61
3.3 Market Behavior of Wind Power 62
3.4 Conclusions 63
Chapter 4 Impacts of Contingency Reserve on Energy Market 64
4.1 Introduction 64
4.2 Contingency Reserve and Energy Market Model 68
4.2.1 Contingency reserve pricing scheme 69
4.2.2 Market model 70
4.3 Reliability Modeling 72
4.3.1 Customer cost 73
4.3.2 Contingency formulation 74
4.3.3 Nodal price and nodal reliability risks 75
4.4 Case Studies 77
4.4.1 RBTS Studies 77
4.4.2 RTS Studies 84
4.5 Conclusions 89
Chapter 5 Impacts of Solar Power Penetration on Deregulated Power Systems 90
5.1 Introduction 91
5.2 PV Generating System 95
5.2.1 PV panel output 95
5.2.2 PV array power output 97
5.2.3 PV array reliability 98
5.2.4 PV power penetration 98
5.3 Problem Formulation 99
5.4 Proposed Method for Reliability and Reserve Evaluation 101
5.4.1 Markov Models 101
5.4.2 Pseudo-Sequential Monte Carlo Simulation 101
5.4.3 Nodal Reliability and Reserve Indices 105
5.5 Case Studies 107
5.6 Conclusions 111
Chapter 6 Impacts of Wind Power Penetration on Deregulated Power Systems 112
6.1 Introduction 112
6.2 Penetration of Wind Power 116
6.2.1 Wind turbine power output 116
6.2.2 Trading wind power 119
6.3 Contingency Reserve Modeling 120
6.3.1 Customer reserve requirements 121
6.3.2 Contingency reserve deployment 121
6.4 Reliability Modeling 122
6.5 Problem Formulation 122
6.6 Case Studies 125
6.6.1 Nodal indices without reserve and wind power 126
6.6.2 Impacts of contingency reserve 127

6.6.3 Impacts of wind power.....129
6.7 Conclusions.....135
Chapter 7 Conclusions and Recommendations 136
7.1 Conclusions.....136
7.2 Future Work 138
References.....140
Author's Publications.....151

List of Abbreviations

ISOs	Independent System Operators
OPF	Optimal Power Flow
ED	Economic Dispatch
UC	Unit Commitment
CASIO	California Independent System Operator
PJM market	Pennsylvania-New Jersey-Maryland market
RBTS	Roy Billinton Test System
RTS	Reliability Test System
PV	Photovoltaic
WTG	Wind Turbine Generator
WPPs	Wind Power Providers
LOLP	Loss Of Load Probability
LOLE	Loss Of Load Expectation
MTTF	Mean Time To Failure
MTTR	Mean Time To Repair
TTF	Time To Failure
TTR	Time To Repair
FOR	Forced Outage Rate
CDFs	Customer Damage Functions
ARMA	Auto-Regressive and Moving Average
UCR	Unit Commitment Risk
NUCR	Nodal Unit Commitment Risk
NEI	Nodal Energy Interruption
CR	Contingency Reserve
LOC	Loss Opportunity Cost
ORR	Outage Replacement Rate
NL	Net Load
EENS	Expected Energy Not Supplied
EEIC	Expected Energy Interruption Cost
LOLF	Loss Of Load Frequency

List of Figures

Fig. 1.1 Vertically integrated power industries....3
Fig. 1.2 Competitive wholesale power market....10
Fig. 1.3 Global total wind capacity installation [18]....13
Fig. 1.4 Global total PV capacity installation for recent years [20, 21]....14
Fig. 2.1 Single line diagram of the RBTS....32
Fig. 2.2 Two-state Markov model of a single component....35
Fig. 2.3 Conceptual tasks in generating capacity reliability evaluation....36
Fig. 3.1 Wind energy conversion system power output model....51
Fig. 3.2 Prediction and measurement of hourly wind speed....55
Fig. 3.3 Power output curve of wind turbine generator....55
Fig. 3.4 Solar energy conversion system power output model....57
Fig. 3.5 Prediction and measurement of hourly solar radiations for one week....60
Fig. 3.6 PV panel output curves....61
Fig. 4.1 Single line diagram of the modified RBTS....78
Fig. 4.2 *NUCR* for different CR allocation for the RBTS....81
Fig. 4.3 NEI at node 3 for different contingency states for the RBTS....82
Fig. 4.4 *NEI* at node 6 for different contingency states for the RBTS....83
Fig. 4.5 Nodal prices of node 18 of RTS at representative contingency states....86
Fig. 4.6 *NUCR* for different CR allocation of the RTS....88
Fig. 5.1 Relation between PV panel output power and solar radiation....96
Fig. 5.2 PDF of PV array power output....98
Fig. 5.3 PDF of PV array power output prediction error....98
Fig. 5.4 *LOLP* at different load nodes....108
Fig. 5.5 *EEIC* at different load nodes....110
Fig. 6.1 The relation between wind speed at hour *t-1* and hour *t*....118
Fig. 6.2 Flowchart of the simulation to determine wind power impacts on power market....125
Fig. 6.3 Nodal energy prices of different nodes for 24 hours....126
Fig. 6.4 *NUCR* for 24 hours....127
Fig. 6.5 Nodal Price at node 3 for 24 hours....127
Fig. 6.6 *NUCR* at node 3....128
Fig. 6.7 Nodal Prices for node 3 at hour 6....129
Fig. 6.8 Power curve of GE 1.5 MW WTG....130
Fig. 6.9 Expected nodal prices at node 3 with different WPP bidding strategy....133
Fig. 6.10 *NUCR* at node 3 with different WPP bidding strategies....134
Fig. 6.11 Nodal Price at node 3 for different outage states at hour 6....135

List of Tables

Table 2.1 Generation cost data 33
Table 2.2 Generation Output 33
Table 2.3 Nodal price at each bus 34
Table 2.4 Customer sector interruption cost ($/kW) 45
Table 4.1 Customer CR requirement for the RBTS 78
Table 4.2 Generator Reserve bids 79
Table 4.3 CR allocation 79
Table 4.4 Nodal price ρ_i^0 ($/MWh) for the normal state for the RBTS 80
Table 4.5 Expected Nodal price $\overline{\rho}_i$ ($/MWh) for the RBTS 80
Table 4.6 Standard deviations of nodal price σ_i ($/MWh) for the RBTS 80
Table 4.7 Percentage NUCR reduction $\Delta NUCR_i$ (%) for the RBTS 82
Table 4.8 Comparison of NRCC and NRCC' for the RBTS 83
Table 4.9 $ENIC_i$ ($/h) for the RBTS 84
Table 4.10 $ENREC_i$ ($/h) for the RBTS 84
Table 4.11 Customer CR requirement for the RTS 85
Table 4.12 Expected Nodal price $\overline{\rho}_i$ and corresponding standard deviation σ_i for the RTS 87
Table 4.13 $ENIC_i$ and $ENREC_i$ for the *RTS* 88
Table 5.1. Temperature Characteristics of PV Panel 95
Table 5.2. Electrical Characteristics 96
Table 5.3 Nodal PV install capacity (MW) 107
Table 5.4 EENS (MWh/yr) 109
Table 5.5 Reserve Commitments (MW) 111
Table 5.6 Reserve Utilization (MWh/yr) 111
Table 6.1 Correlation Coefficients of Continuous Hours 117
Table 6.2. Technical Data 129
Table 6.3 Probability Density Distribution of Wind Power at Hour 6 and Hour 15 131
Table 6.4 Wind power providers' bidding power and real power output 132
Table 6.5 Expected Nodal Price $\overline{\rho}_{ei}^t$ and Standard Deviation σ_{ei}^t at Hour 15 133

Chapter 1 Introduction

Power systems have been undergoing deregulation in recent decades. The purpose of deregulation is to ensure economic and reliable operation of power systems. Power markets started to exist in many countries as a result of deregulation. Competition is introduced to the conventional power system by opening the operation of generation, transmission and distribution by different companies. In a power market which is also called a deregulated power system, the electricity price is not determined by a sole system operator but by the market participants that contain both generation service providers and energy consumers. Since customers have choices to choose the energy service quantity and quality, the reliability performances vary among different customers. Operating reserves are important ancillary services to ensure the reliable operation of power systems. In a power market, the dispatch and pricing of operating reserve is determined according to customers' requirement and generation providers' reserve bids. The issues of energy and reserve pricing, dispatching and customers' reliability evaluation in the new environment are addressed in this thesis.

Renewable energies are clean and abundant compared to dwindling fossil fuels. Many countries have been implementing renewable generations to substitute conventional power generations. The issues with renewable generation are the variability and uncertainty of the renewable energy sources such as wind or solar. The intermittent characteristic of renewable energies makes it difficult to evaluate the capacity and energy contributions of renewable generation systems when incorporating them into existing power systems. The variations of renewable energy also require additional balancing reserves. The pricing of energy and customers' reliability performances will also be affected with renewable energy penetrations. Evaluating the impacts of renewable energy penetration on system energy pricing, reserve requirement and reliability performances is the main focus in this research work.

1.1 Conventional Power System

In conventional power systems, the vertically integrated utilities manage and control the generation, transmission and distribution of electricity, and formulate the monopoly operation [1-3]. Large power systems which cover wide geographical areas are subdivided into control zones. The security, reliability, and economics of the control zones are maintained and optimized by the integrated utility. An energy management system carries out functions such as load forecasting, state estimation, generation dispatch, reserve management, reactive power control, unit commitment, automatic generation control and contingency and preventive controls. Each control zone is responsible to regulate the frequency, and different zones are inter-connected by tie-lines to exchange powers. Fig. 1.1 illustrates the vertically integrated power industry. The generators and transmission providers/wholesalers belong to one corporation, which may also include distributors. Customers are supplied by one company and have fewer choices. Different systems are connected by tie lines.

In conventional power systems, the electricity prices are determined by an independent government regulatory body. Utilities maximize profits by minimization of costs subject to the minimum reliability standards. The pricing adjustment considering generation providers' and customers' requirements takes place through a public hearing process to ensure a fair and stable rate for customers and utility. However, such a process is inflexible and customers have limited choices. The single pricing for bundled services is not efficient since the cost for individual service may not be economically accounted for.

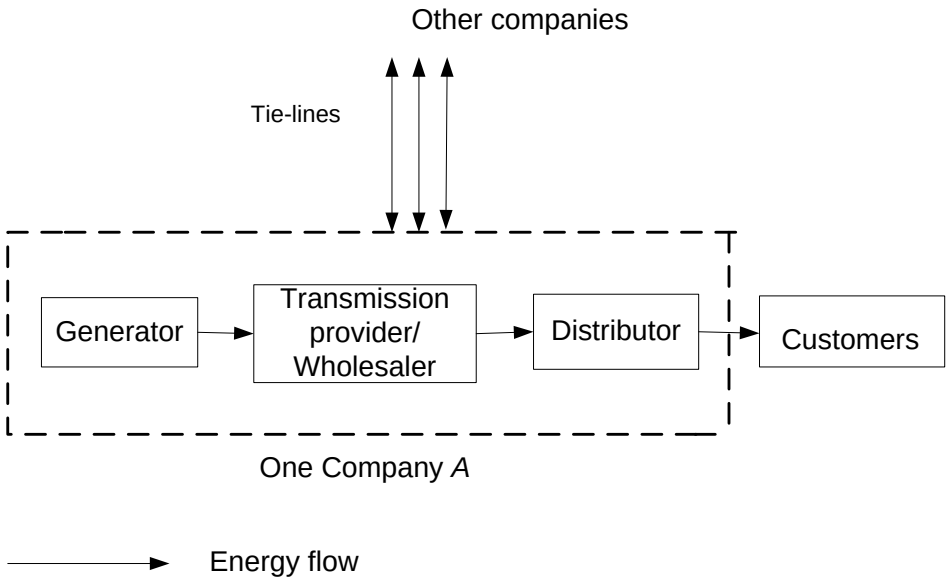

Fig. 1.1 Vertically integrated power industries

1.2 History of Power System Deregulation

The electric utility industry emerged at the beginning of the twentieth century when alternating current transmission enabled long distance transmission of electricity [4]. As perceived by many power utility executives, electricity supply constitutes a natural monopoly. The economic scale of electricity generation makes it possible for limited generation providers to monopolize the provision of power and attain the maximum profits with lowest cost [2]. Development of new technologies and benefits of properly distinct pricing of different service, however, promotes the unbundling process of conventional power systems [2]. Therefore a need was felt to import competition into the power system and pass the benefits of cost minimization to electricity consumers [3].

In many countries, electricity utility industries were formulated to be state-owned monopolies. The major motivation to deregulation was the inefficiency of the monopoly and energy conservation goals of the states. Since early 1980s, electricity industries began the deregulation process under a series of government policies. The

formulations of some of the existing electricity markets are introduced in the following paragraphs. The countries selected in the following are existing power markets that have been operating for a long time and have well developed operating procedures which serve as good examples for other under-developing market. The reasons behind the deregulation and major changes that lead to the deregulation of the power market have been briefly introduced below.

United States

During the 1970s, the high oil prices and inflation increased energy costs. Aiming for energy self-sufficiencies, the United States began to promote energy conservation programs and renewable energies such as wind, solar and geothermal. New legislation was settled and encapsulated in the Public Utility Regulatory Policy Act (PURPA) of 1978 [4]. PURPA started the deregulation of electricity industry in the United States. The electricity generation was opened to competition under PURPA.

The legislative act of 1992 Energy Policy Act (EPACT) began the first step to create a framework for a competitive wholesale electricity generation market and establish the exempt wholesale generator (EWG) as a new category of electricity producer [5]. The Federal Energy Regulatory Commission (FERC) issued Order 888 [6] and Order 889 [7] in 1996 played an important role in opening the transmission services to competition. FERC Order 888 also promoted the unbundling of electricity services and competition of the wholesale bulk power marketplace.

The FERC Order 2000 issued in 1999 further required the transmission owners to join the Regional Transmission Organizations (RTO) to reform transmission services [8]. The RTO members were responsible for the operation and expansion of their transmission systems, and for eliminating the discrimination in accessing transmission services to meet the needs of market operations. The Energy Policy Act of 2005 provided incentives to utilize renewable energy sources [9]. FERC Order 890

increased customers' ability to access new generating resources by eliminating barriers and requiring transparent and non-discriminated transmission operation and planning services [10].

With significant efforts in promoting the electricity utility deregulation, many major electricity markets were created in the United States. The California market (1996), New York Market, Pennsylvania-New Jersey-Maryland (PJM) market [11], Electric Reliability Council of Texas (1996), New England Market (1971), and Midwest Market (1996) are some of the major power markets in the United Sates [1].

United Kingdom [12]

The former electricity industry was owned and operated by the state in UK. The Central Electricity Generating Board (CEGB) was responsible for providing electricity generation and transmission services. The Thatcher government elected in 1979 started the privatization of nationalized industries in the economic reforms. The major goal of privatization was to achieve efficiency through reduction of state roles in economic decisions.

The Electricity Act of 1983 provided private generation producers access to state grids which was prohibited before. Then, the Electricity Act of 1989 led to the restructuring of the electricity industry. The CEGB was reformed into four organizations: two power producers, a transmission company and a distribution company. The restructured system evolved to the present UK electricity market structure through gradual privatization. The National Grid Company (NGC) operates the transmission services and the England and Wales Electricity Pool. The private generation producers trade electricity in the pool. Large users and other consumers also gained rights to choose electricity providers in the power pool after competition was introduced into the electricity market.

Australia and New Zealand [12, 13]

Before deregulation, the Australia electricity industry comprised vertically-integrated state utilities which are low efficient. The nation's over-participation in the electricity industry and pressure on government from debt and money restraints had driven the deregulation of Australia electricity industry to competitive marketplace.

The 1991 restructuring of the Australia electricity market resembled both UK and US models at national and state levels respectively. Reforms recommended by the Industry Commission led to privatization of the formerly state-owned electricity utility. The major contents of the reforms are: restructuring the vertically integrated electricity industry into separate generation, transmission, distribution sectors; privatizing and corporatizing the separate electricity transmission and distribution sectors; including competition into generation; combining the distributed state transmission units to a single national grid. In 1996, the National Electricity Code established the market rules and procedures for the national electricity market.

In 2001, the Australian National Electricity Market (NEM) was created as a competitive wholesale marketplace with the National Electricity Market Management Company (NEMMCO) as the market operator. There were three types of trading: the spot market trading on a half-hourly basis, the vesting contracts and the bilateral contracts [13].

The New Zealand electricity market (NZEM) started operation in 1996 [13]. The Electricity Market Company has assumed the role of the market operator. The NZEM is cleared based on a day-ahead settlement while spot market participation is not compulsory. The market participants submit bids of different services like energy or reserves to the market and can modify their bids up to four hours before the real time dispatching. The energy and reserve are cleared simultaneously. Prices are determined half-hourly and vary by load nodes which reflect the transmission losses and system constraints. In the NZEM, Trans Power operates the national grids and ensures the

secure operation of the system.

Singapore [14]

The driving forces behind the reform of the Singapore power system include promoting a competitive and reliable electricity industry and the restructuring experiences of other international electricity companies. The entrepreneurial industry also required the efficient and competitive electricity supply to increase their competitiveness internationally. The reforms began in 1995 when the formerly nation-owned Public Utilities Board (PUB) who supplied water, electricity and gas was corporatized. The Singapore Power (SP) company was created as the main holding company for other electricity service companies. such as generation companies: PowerSenoko Power and PowerSeraya; transmission company: PowerGrid; and electricity supply and utility support company : SP Services Ltd. The Singapore Power Pool started operation in 1998 as a wholesale electricity market. The PowerGrid was responsible as the pool administrator and system operator. The pool is a day-ahead market without real time spot market at the wholesale level. In 2000, the electricity utility ownerships were further separated and a market operator was established. The real-time market was also created with the liberalization of the retail markets.

The Energy Market Authority (EMA) was created in 2001 to take the responsibility of regulating the electricity and gas industries. In 2003 the National Electricity Market of Singapore (NEMS) began to trade electricity and other services. EMA is the power system operator and Energy Management Company (EMC) is the operator of the wholesale electricity market which is cleared every half-hour. The generators and large users or retailers can also trade energy through bilateral agreements.

Conclusions

The major reasons behind the deregulation for most existing power markets are to reduce generation and operating cost, while providing reliable power supply to

consumers. Although most power markets have been well developed, as more and more renewable energy systems are penetrated in the existing power markets and new operating scenarios like micro-grid are proposed, new market policies and clearing procedures will need to be developed to accommodate these developments, and the impacts of these developments also need to be examined.

1.3 Restructured Power Systems

1.3.1 Market participants

As the electricity industry is evolving into the competitive structure, the scope of activities of existing system participants has been redefined. New entities are created to take different roles in the new environment according to the market type [13]. There may be differences of the specific definition, but the general roles and types of market entities include the following [13, 15]:

Generation companies (Gencos)

The generation companies own the generating facilities or power purchase contracts. The Gencos can sell energies in the wholesale marketplace or through contracts with large consumers. They can also sell the reactive power and operating reserve in the ancillary services markets. The prices at which Gencos sell their power are not regulated. Gencos are also referred to as Independent Power Producers (IPPs).

Transmission companies (Transcos)

The transmission companies take the roles of building, maintaining and operating the power grids in certain geographical regions. Transcos are responsible for transmitting electricity reliably and efficiently from the Gencos to customers. Transcos must provide non-discriminating and transparent services to all transmission users. Their costs are recovered from the transmission tariffs collected from transmission usage and congestion charges. Transcos are regulated by federal or state level authorities.

Distribution companies (Discos)

The distribution companies own and operate the distribution systems which connect the transmission system and end users in a geographical area. Discos are also responsible for managing the distribution system outages and maintaining power quality.

Retailers

Retailers are new entities in the deregulated environment. Retailers obtain permits from regulation authorities to buy and resell electricity. The retailers can trade energy and ancillary services in the marketplace. They make deals with the sellers to purchase electricity and re-sell to customers.

Customers

Customers are the end-users of electricity and are connected to the distribution system or the transmission system according to their capacity. Customers have more choices of electricity providers. They can purchase electricity and ancillary services from wholesale marketplaces, Gencos or local distribution companies.

Independent system operators (ISOs)

In a deregulated environment, without vertically integrated utilities, the security and economic operation of the power system should be the responsibility of operators that are independent of the other market participants. ISOs are established to take this responsibility. ISO is an independent authority which does not own generating or transmission resources. ISOs conduct activities such as managing system congestions, coordinating maintenance scheduling and planning system expansions. ISOs also have the authority to make dispatch and commitment schedules according to the market clearing results. They also ensure that the market information is transparent and available to all the participants in order to promote an efficient and competitive market environment.

There are two major structures of ISOs with different objectives and responsibilities. One structure referred to as MinISO has modest authority and ensures a secure operation of the power market. This structure of ISO coordinates the transmission of the market cleared power within the constraints of the power system. The ISO has no market role and has limited control over the generating schedules. One example of this structure of ISO is the California ISO. Another structure of ISO referred to as MaxISO integrates with the power exchange (PX). PX is an independent, non-profit and non-government entity that ensures the competitive operation of the power market. PX clears the power market based on the biddings from power providers and consumers. This structure of ISO dispatches the energy and reserves based on the optimal power flow (OPF) model. The market participants are required to submit their cost, availability and other information. Based on this information, the ISO determines the dispatch schedules to maximize the social welfare, and also manage the congestions. This structure of ISO has wider authority and control. The examples of this structure are the National Generating Companies (NGC) in UK and the PJM ISO in the US.

The competitive wholesale power market model is shown in Fig. 1.2 [3].

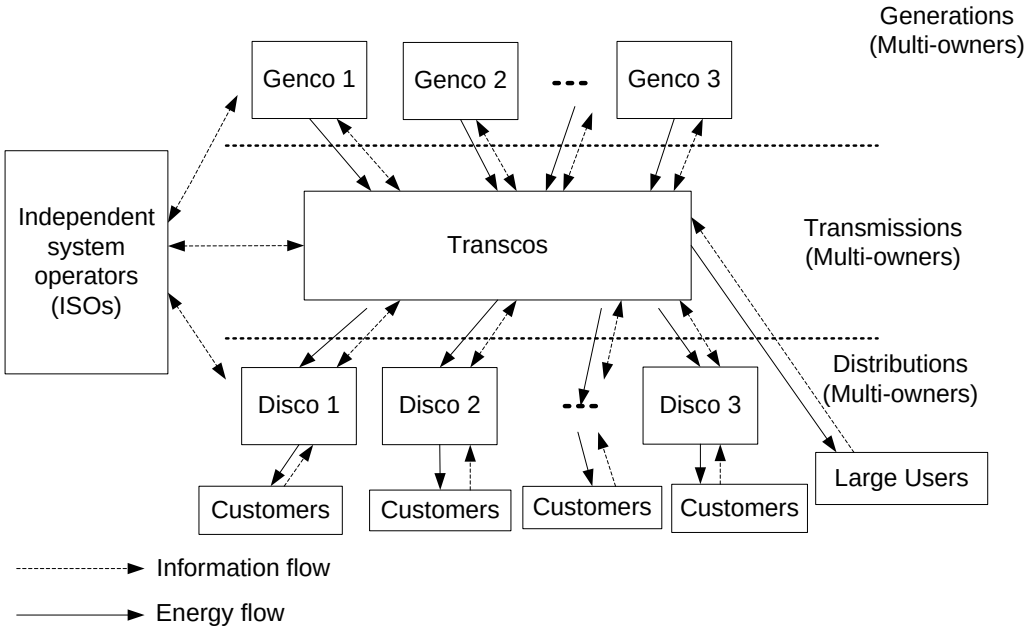

Fig. 1.2 Competitive wholesale power market

1.3.2 Market models

Through deregulation, the vertically integrated electricity industry is open for competition at the generation, transmission and distribution levels. The market driven electricity pricing schemes are expected to reduce the operation cost through competition. Different market structures are created to provide various choices for participants. Three major market structures and their operational aspects in existing power markets are introduced below [1, 15].

Poolco Model

This model describes the power market as a centralized marketplace that clears the market for suppliers and buyers. The suppliers will compete to supply energy by submitting competitive biddings into the market. The customers also submit bids of the amount that they are willing to pay for buying electricity. The ISOs perform the economic dispatch and determine a single market price for any predetermined period based on the bids. The suppliers with high electricity price might lose the opportunity to supply energy while the customers with low price may not get the required demand. The ISOs also provide price signals and other market information to all the participants. This market structure is designed to induce the suppliers to increase their generation efficiency through competitive biddings.

Bilateral Contracts model

In the bilateral contracts market, the electricity and services providers trade directly with the buyers through negotiations without ISO. The bilateral contracts set the transaction details including amount and prices. These details are submitted to ISO for improvement subject to the constraints of the transmission system. The bilateral contracts model provides a flexible way for participants to choose suppliers or consumers. However, the disadvantage is the high transaction cost through negotiations.

Hybrid Model

The hybrid model combines the features of the above two market structures. It provides maximum flexibility for market participants to trade in pool or directly from the individual entities. The hybrid model can induce the creation of variety of services and options to meet customers' needs. The disadvantage is the high system operation cost with various transactions. The California market and PJM market are typical examples of the hybrid model.

The Poolco model provides the optimization process considering all market participants and is utilized in this thesis for customer reliability and renewable energy impacts analysis.

1.3.3 Ancillary services market

Ancillary services refer to those activities on transmission grids that are necessary to maintain secure and reliable power transmission and ensure the required quality of power such as voltage and frequency levels [13, 15]. In conventional power systems, the ancillary services are integrated with energy and managed centrally by system operators. Due to deregulation, system operators have no control over the individual generators. They need to purchase ancillary services from the providers. The major ancillary services include: frequency control which is achieved through automatic generation control (AGC) or manual adjustment; reserve which is able to respond to demand changes or generation shortfalls and maintain the real time power balances; reactive power and voltage control which are necessary to ensure the security of energy consumption; black start capability services which are provided when major breakdown occurs.

The ancillary services are cleared simultaneously or sequentially depending on the market designs. In a sequentially cleared market, ancillary services are cleared first for the highest quality service, and then the second to the lowest quality services.

Participants who were rejected in the high quality market can re-bid their services in the low quality markets. In the simultaneously cleared market, the ancillary services with different qualities are cleared simultaneously. The market participants can only bid once to the pool. Market operators determine the quantity and price of different services according to an optimization algorithm. The substitutability of services with different quality is also considered in the clearing process.

1.4 Renewable Power Penetrations

1.4.1 Renewable energy

Renewable forms of energy such as wind and solar are widely utilized as substitutes for fossil fuels due to dwindling resources and environmental concerns [16].

Wind power installation has been growing rapidly in the last few decades. Wind turbine generator (WTG) is the major technology that converts wind energy into electric power. The capacity of commercial WTG ranges from a few hundred kW to over 2 MW [17]. The global cumulative installed wind capacity from 1996-2011 is shown in Fig. 1.3 [18]. Till the end of 2011, the total global wind capacity installation has exceeded 238GW. In Denmark, Germany and Spain, wind power can meet more than 20% of the total consumption [18].

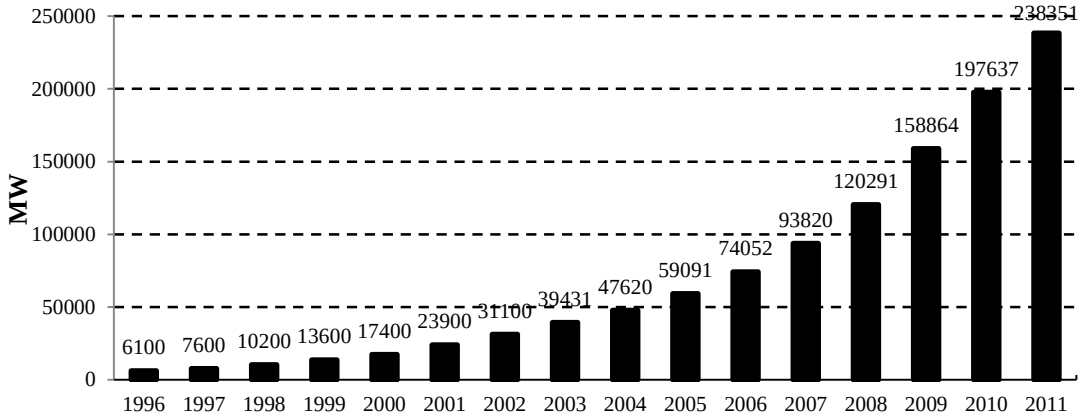

Fig. 1.3 Global total wind capacity installation [18].

Solar power has also been growing rapidly due to its abundance and accessibility, unlike wind power which is usually generated using large wind turbines. Two major solar power generating technologies include photovoltaic (PV) panels and concentrated solar power (CSP) [19, 20]. PV panels use semiconductor technology to convert solar radiation into electric power. CSP uses mirror or lenses to generate thermal energy by concentrating sunlight. The thermal energy is used directly or indirectly to heat engines to produce electric power. PV panels are mainly utilized to supply homes or businesses while CSP mainly generates electricity for large power stations. A broad application of PV panels is possible since PV panels can be installed on rooftops or building facade and supply demand directly. Fig. 1.4 shows the cumulative installed PV capacity from 1996-2010 [20, 21]. Around 40 GW PV capacities have been installed till the end of 2010.

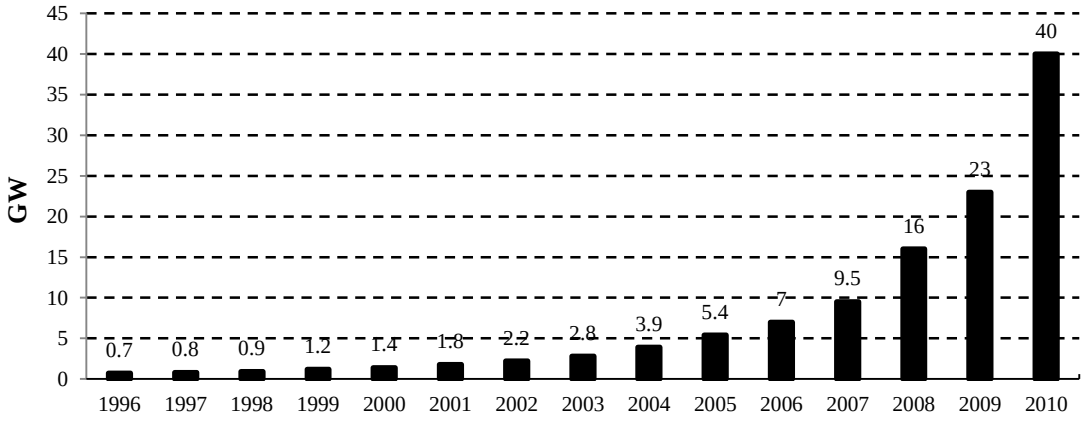

Fig. 1.4 Global total PV capacity installation for recent years [20, 21]

1.4.2 Renewable power penetrations in restructured power systems

Renewable energy including solar, wind and hydro energy are also competitive under government support and traded in energy markets in some countries [22, 23]. Different from conventional generations, renewable energy are intermittent and stochastic energy sources. The penetration of renewable energy, therefore, will bring new variables and problems to the existing system.

The renewable energy forms are being preferred due to economic and environmental factors. The unit commitment and dispatch of generation and reserve should explicitly consider the variable nature of renewable energy [24-30]. The wind power penetration will also affect the transmission planning and distribution system reliability [31, 32]. Since the power output of WTG is affected by the variant wind speeds, wind generation cannot be treated in the same way as conventional power sources. A comprehensive introduction on wind power penetrations in power system is presented in [33]. New techniques are developed to evaluate the adequacy benefits of adding WTG to the existing power system [34-37]. New techniques to investigate the impacts of renewable power on power system reliability have also been developed [38, 39]. The unpredictable variation of renewable energy increases the uncertainty of system operation, and additional reserves are required to meet the fluctuations [40]. The short term or long term reserve requirements with wind power penetrations are evaluated in [41-45]. As the penetration of renewable power increase, system reliability will be affected due to the random variation of renewable sources. To evaluate the reliability benefits and risks of utilization of renewable energy, techniques that can incorporate the random and chronological characteristics are developed [46-51]. Some techniques developed for conventional power systems can also be extended to use in the new environment.

In the market operation, trading renewable energies and the corresponding impacts on market prices and operations are of interest to many researches. Trading wind power has been investigated in many European markets like UK [52], Nordic [53], German [54], and in United States markets like California [55-57]. A case study of imbalance cost of PV power when they participate in Amsterdam Power exchange (APX) spot market is studied in [58]. A study of renewable penetration in Australian National Electricity Market (NEM) is presented in [59]. In the day-ahead or spot market, the short term predictions are of great importance for wind power providers (WPPs). WPPs may suffer imbalance cost due to the unpredictable variation of wind power [53,

60]. Behavior of WPPs can also impact the energy prices and reserve utilizations in power markets [41, 61, 62].

1.5 Power System Reliability

One important objective of power system operation is to supply electricity to the customer reliably and economically. Reliability analysis is therefore important in maintaining healthy operation and expansion planning of a certain power system. In conventional power systems, reliability is centrally determined and regulated by the system operator. Reliability issues and evaluation methods have been investigated by researchers [63-65]. Congestion management and load shedding are determined by system operators seldom considering different customers' preferences. Uniform reliability levels are applied to all customers. Customers accept electricity prices that are determined by the system operator with limited choices. In deregulated power systems where customers participate in the market operation, the traditional reliability determination method cannot be directly applied. The variations in customers' reliability and price preferences should be recognized. Since customers can adjust their demand facing electricity price variations, the correlation between prices and customers' reliability performances should also be considered. Nodal reliability and nodal prices are developed to evaluate customers' reliability and prices in the power market [66-69].

Nodal prices are influenced by the load characteristic at the node, generating unit location, available generating capacity, and transmission limits. Price spikes occur at certain nodes in the power market when inadequacy of generating capacity and transmission congestion are caused by system component faults [70]. Customers weigh between the interruption cost and the cost of accepting the high price and the corresponding revenues. Customers can reduce demand at any contingency state which affects their reliability.

The ancillary services market is created as a result of unbundling of energy and ancillary services [13, 15, 71]. The reserves and other services are priced and customers can purchase these services in order to improve or maintain their reliability levels. The system reserves provide additional energy in contingency states and balance the demand variations. Customers' reliability is affected by reserve requirement and deployment in deregulated power systems [72-74].

Therefore the reserve market should provide more choices for customers to optimize their benefits. New energy and reserve co-optimized market should be designed to allow participation of customer.

1.6 Objectives and Contributions

1.6.1 Impacts of reserve on system reliability

Objective

In conventional power systems, system operators procure the energy and reserve to meet demand and maintain the reliability level of the entire system. The overall social benefits are optimized by the system operators with less consideration of individual customers' requirements. The process may be inefficient due to the uniform pricing for services with different qualities. The unbundling of generation services in the new deregulated system promotes the differential pricing of generation services. The existence of the ancillary services market can also provide more choices for customers to optimize their reliability performances.

Operating reserves and contingency reserves are important ancillary services to maintain customers' reliability. The issues that need to be addressed for evaluating the benefits and costs of using reserves include: the pricing of energy and reserves, deployment of reserves with different quality, impacts of reserve on reliability, the reserve requirement for reliable market operation, customers' reserve preferences, and coupling between energy and reserve, etc [15, 75-86]. The reserve market was

developed in [76] and pricing and procurement of reserve were investigated considering the impacts on system reliability in deregulated power systems. An OPF model is proposed in [78] for pricing the energy and reserve in a co-optimized market. The locational marginal prices (LMPs) are utilized for pricing the energy and regulation up/down reserves. The properties and the coupling between the LMPs are investigated. The decision of provision of one service (for example, reserve) results in the loss of opportunity to provide another type of service (for example, energy). The lost opportunity costs therefore should be considered in the market design [77]. The optimal reserve allocation and dispatch are investigated in deregulated power systems in [81]. To achieve the economic and reliable operation goals, a probabilistic reserve requirement tool was developed considering the procurement cost and reliability of units [84]. The energy and reserve were priced differentially by the reliability implication and benefits of the pricing policy were demonstrated through case studies in [83].

In deregulated power systems, nodal reliability evaluation allows customers to choose their reliability level within the capability of the system. The main objective in this part of research is to design and investigate new market mechanism that allows customers to maintain their desired reliability by participating in the reserve market.

Contributions

Techniques to evaluate the benefit of customers' reliability requirements have been developed in this thesis. The energy and reserve co-optimized market that can take into consideration individual customers' reserve requirement has been designed. The reserve allocations and deployment are optimized so that customers who have higher reliability requirements will pay more for reserves and maintain higher reliability levels. The nodal price and nodal reliability are evaluated to examine the benefits of the proposed method. The reserve utilization and reliability cost are also evaluated for different customer reserve requirements.

1.6.2 Impacts of renewable energy on nodal reliability

Objectives

The unpredictability and chronological variation of renewable energy will affect the reserve commitment and deployment in power systems. In a deregulated power system, nodal reliability is closely related to reserve allocation and deployment. Therefore the impact of renewable penetration on nodal reliability is an important issue that needs to be addressed. To properly account for the stochastic nature of renewable energies, time variant models have been investigated in previous studies [48, 87]. Reliability and cost of traditional power systems including renewable energy are also evaluated in [88, 89]. These techniques, however, were developed for traditional power systems and did not explicitly evaluate customers' risks and benefits with renewable energy penetration.

The main objective in this part of research is to develop new method that can evaluate the impacts of renewable penetration on the reserve deployments, and as a result on customers' reliability, considering the intermittent characteristics of renewable energy and the correlation between renewable energy and load.

Contributions

In the new environment, energy and reserve are dispatched considering customers' reliability requirements. The impacts on energy and reserve dispatch due to utilization of solar energy have also been investigated in this thesis. The market, cleared hourly or daily, has explicitly considered the variant solar energy. The evaluation techniques have been developed using Monte Carlo simulation to incorporate the chronological fluctuations and prediction errors of solar energy. The correlation between load and solar power is also important. If the correlation is positive, less reserve and energy are needed. The proposed techniques have also taken into consideration the correlation issue.

1.6.3 Impacts of renewable energy on energy price and customer reliability

Objective

Renewable energy providers can also bid in the power market to maximize their benefits. Due to the variable nature of renewable energies, imbalance costs will be imposed on renewable energy providers to induce them to make more accurate predictions for reliable operation of the power system. Providers then will develop various bidding strategies to maximize their benefits by participating in market operations. Renewable energy providers' bidding strategies and their impacts on the market operation have been investigated in [53, 55]. The renewable energy variations include the chronological variation of renewable sources and the prediction errors. The responsibility of minimizing prediction errors can be attributed to system operators or renewable energy providers depending on the market design.

The renewable energies are price takers in the power market due to their small proportion in the energy market. However, their biddings can affect the energy market clearing due to the substitution of conventional generation. Their bidding strategies also affect the reserve deployment since the bidding variation needs to be balanced by reserves. The main objective in this part of research is to develop new technique that can evaluate the market clearing procedure considering the biddings of renewable energy and also evaluate the corresponding impact on customer reliability and energy prices.

Contributions

Different wind power providers' bidding strategies have been investigated in this thesis. Based on the short-term wind power prediction models, wind power providers' bidding strategies are analyzed in the market operation. A market clearing procedure that includes biddings from wind power has been developed. The resulting impacts on nodal price and nodal reliability have been evaluated under different wind power bidding strategies.

1.7 Organization of the Thesis

In this chapter, the background and motivations of the research have been presented. The objectives and contributions of this thesis have also been presented. The organization of the thesis is as follows:

The economic operation of power system optimal power flow techniques are introduced in Chapter 2. The reliability analyses techniques used in conventional power systems and deregulated power systems are described.

In Chapter 3, the intermittent characteristics of renewable energy sources and the electric power generation of renewable energy are presented. The market participation of renewable energy is also introduced.

Chapter 4 investigates the contingency reserve pricing and deployment through a two-step market clearing process. Customers' participation in reserve and energy market is explicitly considered. The nodal price and nodal reliability risks are evaluated for the proposed market.

The impacts of solar power on nodal reliability and reserve deployments are evaluated in Chapter 5. The stochastic and chronological variations of solar power are incorporated in the proposed evaluation technique using pseudo sequential Monte Carlo simulation.

In Chapter 6, the bidding of wind power providers and its impacts on market price and system reliability are examined.

The conclusions of the research and some recommendations for future work are presented in Chapter 7.

Chapter 2 Power System Economics and Reliability

In this chapter, power system economic operation is addressed. Pricing issues and reliability evaluation techniques are presented in both conventional power systems and deregulated power systems. Reliability evaluation techniques using analytical and Monte Carlo simulation methods are introduced. The economic and reliability benefits that can be achieved through deregulation are discussed.

2.1 System Economic Operation

The economic dispatch (ED) is executed over a 5-15 minutes period to dispatch real and reactive power to supply load with minimum cost [2]. Since different generation schedules can affect the power flow as well as generation cost, the problem of finding the generation schedule with minimum generation cost while satisfying the power flow equations of the system is defined as the optimal power flow (OPF) problem [13, 90]. The OPF optimizes the power flow solution of large scale power systems. The objective function of OPF may include economic costs, system security and other objectives.

2.1.1 Economic Dispatch (ED)

ED in conventional power system [2]

In conventional power systems, the system utilities are vertically integrated. The main task of the system operation is to minimize the total cost of the generators while satisfying the system demand. The rates that the utility charges its customers are set by an independent government regulatory body, such that minimizing the generation cost can provide the maximum profits [2]. The power output of any generator should not exceed its rating nor should be below its minimum output necessary for stable boiler operation. The generation should also compensate for the transmission system

losses. ED is modeled as a nonlinear optimization problem as shown below.

The objective function is given by

$$\min C_t = \sum_{i=1}^{n_g} C_{gi}\left(P_{gi}\right) \tag{2.1}$$

where the value of C_{gi} is calculated as:

$$C_{gi} = \alpha_i + \beta_i P_{gi} + \gamma_i P_{gi}^2 \tag{2.2}$$

subject to power balance constraints:

$$\sum_{i=1}^{n_g} P_{gi} = P_D + P_{loss} \tag{2.3}$$

generator output limit:

$$P_{gi}^{\min} \le P_{gi} \le P_{gi}^{\max} \tag{2.4}$$

where:

C_t	Total cost for all the generators.
n_g	Set of generators.
P_{gi}	Real power output of generator *i.*
C_{gi}	Cost function for generator *i.*
P_D	Total demand of power system.
P_{loss}	System loss.
$P_{gi}^{\min}$	Lower limit of real power output of generator *i*.
$P_{gi}^{\max}$	Upper limit of real power output of generator *i*.

The Lagrangian function is constructed to minimize the objective function subject to the constraints of Equations (2.3)-(2.4).

$$L = C_t + \lambda\left(P_D + P_{loss} - \sum_{i=1}^{n_g} P_{gi}\right) + \mu_{gi}^{\min}\left(-P_{gi} + P_{gi}^{\min}\right) + \mu_{gi}^{\max}\left(P_{gi} - P_{gi}^{\max}\right) \tag{2.5}$$

where λ, $\mu_{gi}^{\min}$ and $\mu_{gi}^{\max}$ are the Lagrangian multipliers for energy balance constraint, lower limit and upper limit of generator constraints respectively.

According to Karush-Kuhn-Tucker (KKT) condition, the following conditions should be satisfied for the optimal solution. For $\forall i$, there is:

$$\frac{\partial L}{\partial P_{gi}} = \frac{\partial C_t}{\partial P_{gi}} + \lambda\left(\frac{\partial P_{loss}}{\partial P_{gi}} - 1\right) - \mu_{gi}^{\min} + \mu_{gi}^{\max} = 0 \tag{2.6}$$

$$\frac{\partial L}{\partial \lambda} = P_D + P_{loss} - \sum_{i=1}^{n_g} P_{gi} = 0 \tag{2.7}$$

$$\frac{\partial L}{\partial \mu_{gi}^{\min}} = -P_{gi} + P_{gi}^{\min} = 0 \tag{2.8}$$

$$\frac{\partial L}{\partial \mu_{gi}^{\max}} = -P_{gi} + P_{gi}^{\max} = 0 \tag{2.9}$$

By solving Equations (2.6)-(2.9), it can be concluded that:

$$\lambda = \frac{\frac{\partial C_t}{\partial P_{gi}} - \mu_{gi}^{\min} + \mu_{gi}^{\max}}{\left(1 - \frac{\partial P_{loss}}{\partial P_{gi}}\right)} \left(for\ \forall\ i\right) \tag{2.10}$$

The inequality constraints are only active when either the lower or upper limit is reached. Under this condition, the inequality constraints hold at the lower or upper limit. If all the generators operate within their output limits, the inequality constraints are not active and their corresponding Lagrangian multipliers satisfy: $\mu_{gi}^{\min} = \mu_{gi}^{\max} = 0$, when (2.10) is reduced to:

$$\lambda = \frac{\frac{\partial C_t}{\partial P_{gi}}}{\left(1 - \frac{\partial P_{loss}}{\partial P_{gi}}\right)} \left(for \forall i\right) \tag{2.11}$$

From (2.11), all the generators operate at equal marginal cost which equals the λ at the optimal generation dispatch. From an economic point of view, Lagrange multiplier λ is the system marginal cost with respect to 1MW increase of system demand. When generator limit is active or the system loss as a function of generator output is implemented, (2.11) does not hold. From an economic point of view, the

values of $\mu_{gi}^{\min}$ and $\mu_{gi}^{\max}$ represent the sensitivity of system cost with respect to the corresponding generator output limits. This follows the Karush-Kuhn-Tucker necessary condition. $\left(1-\frac{\partial P_{loss}}{\partial P_{gi}}\right)$ is known as the penalty factor for generator *i*'s contribution to the transmission losses. Generators have different marginal cost considering transmission losses and output limits. This contributes to electricity price variation for different power suppliers in the power market.

ED in power market [2]

In the deregulated power system, generation companies are independent utilities. There is no predefined electricity price. Under perfect market condition, each generation company provides supply bids which specify the quantity of power they are offering and the corresponding price they are demanding from the market. The customers also bid to purchase electricity. The electricity price in the power market is determined by the market clearing process based on the bids from energy suppliers and consumers.

The economic dispatch becomes decentralized in a power market. Each participant in the market wants to maximize its own profits. Assume that the known electricity price is ρ, then the objective function for generation company *i* to maximize its profit is:

$$Max_{Pgi}\left\{\rho P_{gi}-C_{gi}\left(P_{gi}\right)\right\} \tag{2.12}$$

The object of load is maximizing its own profit. The objective function is

$$Max_{Pdi}\left\{B_{di}\left(P_{di}\right)-\rho P_{di}\right\} \tag{2.13}$$

where $B_{di}\left(P_{di}\right)$ is the benefit function of load *j* .

Equations (2.12) and (2.13) are subject to the same constraints of ED as in the conventional power system.

The optimal solutions for this problem are calculated using the same method as the

ED in conventional system explained earlier. It is assumed that the generator limits are not violated and that the system transmission loss is constant. In a perfect market, the optimization of all participants' benefits will converge to a single market price ρ, and the following results can be obtained with the number of n_d loads:

$$\frac{\partial C_{g1}}{\partial P_{g1}} = \cdots = \frac{\partial C_{gn_g}}{\partial P_{gn_g}} = \frac{\partial B_{d1}}{\partial P_{d1}} = \frac{\partial B_{dn_d}}{\partial P_{dn_d}} = \rho \tag{2.14}$$

The result is similar with that using the conventional economic dispatch. Under perfect market conditions, both the presently unconstrained economic dispatch and a competitive market process will lead to the same amount of power being traded and the total social welfare. This proves that in a perfect market, the optimization of the profit of each participant is equivalent to the optimization operation of the whole system. However, in the real market, some large generation companies may exert market power to maximize their own profits which will result in loss of social welfare.

It should be noted that the transmission losses have not been considered in the above discussion. The implementation of transmission losses will introduce the penalty factor as mentioned before. The price will deviate due to participant's contribution to the transmission losses. The nodal price is calculated as:

$$\rho_i = \frac{\dfrac{\partial C_{gi}}{\partial P_{gi}}}{\left(1 - \dfrac{\partial P_{loss}}{\partial P_{gi}}\right)} \left(for\ generation\ bus\ i \right) \tag{2.15}$$

$$\rho_j = \frac{\dfrac{\partial C_{dj}}{\partial P_{dj}}}{\left(1 - \dfrac{\partial P_{loss}}{\partial P_{dj}}\right)} \left(for\ load\ bus\ j \right) \tag{2.16}$$

The variances of nodal prices are caused by the transmission losses. The prices defined in (2.15) and (2.16) reflect the bundled energy price for meeting demand and compensating the share of transmission loss.

2.1.2 Optimal Power Flow (OPF)

System loads were assumed to be aggregated load in the economic dispatch introduced above, and no transmission limits were considered. Therefore, the resulting generation dispatch is likely to violate the physical law such as Kirchhoff's Law which determines the power flow of the system. By implementing the system security constraints in addition to the generator output limits in the optimization problem, OPF can avoid such a problem. Thus basically, OPF is a static, linear or nonlinear optimization problem of determining control variables while satisfying the set of power constraints [90, 91].

The objective of OPF is to minimize the system generation cost in the normal state. It can take other forms as well. In reactive power planning, the objective of OPF is to minimize the transmission losses. In energy and reserve co-optimized markets, the objective of OPF can be the total cost of reserve and energy. It can also be expressed as the minimum of load shedding in contingency conditions as well as minimum of the generation shift from an optimal generation point. The control variables which are being determined in the problem can be real and reactive power outputs of generators, the transformer tap ratios and phase shifts, switched capacitor settings, power exchanges between operating areas, etc [78, 92].

By setting the generation dispatch as an OPF problem, two main goals can be achieved. Firstly, the incremental cost of the system can be calculated more accurately with the implementation of the operation limits in operation cost minimization. In the power market, it provides the power providers with more useful information for choosing their bidding strategy. Second, the OPF solutions provide the consumers with the dispatch schedules that not only minimize the system operation cost, but also guarantee the safe operation of the power system. In addition, OPF can also implement the constraints of contingency operation. The OPF can dispatch the system in a defensive manner so that it can force the system to operate when contingency

occurs. This is known as “security-constrained OPF” [92].

Utilization of the OPF method to determine individual load point indices has been well documented [4, 67, 68, 78, 91, 93]. The objectives of the OPF problem are determined based on the practical application. In order to determine the electricity price for each bulk load point, the OPF problem is formulated with the objective of minimizing the system operation cost.

In addition to economic operation, a secondary goal of the OPF method is to determine the system marginal cost. The marginal cost data can aid in the pricing of MW transactions, and in pricing ancillary services such as voltage support through MVAR support. The marginal cost can be interpreted as an approximation of the spot price. In solving the OPF problem, the marginal cost can be determined as a by-product.

The solutions of OPF methods have many advantages over solutions of traditional ED which provide the marginal cost for each generating unit [90]. The OPF methods are capable of performing all the control functions necessary for the system operation. The ED determines the generator output such that the cost for generation is minimized for a certain load level. In addition to this, the OPF methods control the power flow on the transmission lines so that the transmission limits are not violated. The OPF methods can also control the transformer tap ratio and phase shift angle and the bus voltage magnitudes. The OPF methods ensure the economic and secure operation of power systems.

Problem Formulation

The traditional OPF minimizes the system generation cost. The objective function is defined as:

$$\min f = \sum_{i \in n_g} C_{gi} \tag{2.17}$$

The objective function is the sum of the generation cost from all generators in the system. The equality constraints of the problem are shown in (2.18) and (2.19) which are determined according to the physical laws. They ensure that the power flow equations are satisfied and that the net injection of real and reactive power is zero at each bus.

$$P_i = 0 = P_{gi} - P_{di} - \sum_{j=1}^{N} V_i V_j \left|Y_{ij}\right| \cos\left(\theta_i - \theta_j - \delta_{ij}\right) \tag{2.18}$$

$$Q_i = 0 = Q_{gi} - Q_{di} - \sum_{j=1}^{N} V_i V_j \left|Y_{ij}\right| \sin\left(\theta_i - \theta_j - \delta_{ij}\right) \tag{2.19}$$

Inequality constraints of the problem represent the physical limits of the electric device and the necessary operating limits for the safe operation of a power system. The generation output limits are expressed below.

$$P_{gi}^{\min} \le P_{gi} \le P_{gi}^{\max} \tag{2.20}$$

$$Q_{gi}^{\min} \le Q_{gi} \le Q_{gi}^{\max} \tag{2.21}$$

The ramp rate limits are

$$\Delta P_{gi}^{\min} \le \Delta P_{gi} \le \Delta P_{gi}^{\max} \tag{2.22}$$

The voltage magnitude of each bus should be maintained within certain limits for a secure operation of the power system.

$$V_i^{\min} \le V_i \le V_i^{\max} \tag{2.23}$$

The transmission line carrying capability relates to thermal rating of conductors and should be set to a specific level due to system security concerns. The OPF limits the apparent power flow of transmission line *ij* in a certain range.

$$\left|S_{ij}\right| \le S_{ij}^{\max} \tag{2.24}$$

Transformer tap ratio t_{ij} and phase shift angles α_{ij} are also limited within a certain range.

$$t_{ij}^{\min} \le t_{ij} \le t_{ij}^{\max} \tag{2.25}$$

$$\alpha_{ij}^{\min} \le \alpha_{ij} \le \alpha_{ij}^{\max} \tag{2.26}$$

where:

i, j	Bus index
N	Set of buses.
Y_{ij}	Element of the system admittance matrix.
δ_{ij}	Angle associated with Y_{ij}.
P_{gi}, Q_{gi}	Real and reactive power generations respectively at bus *i*.
P_{di}, Q_{di}	Real and reactive loads respectively at bus *i.*
P_i, Q_i	Net real and reactive powers injected respectively at bus *i.*
$P_{gi}^{\min}$, $P_{gi}^{\max}$	Lower and upper limits respectively on the real power of generator at bus *i.*
$Q_{gi}^{\min}$, $Q_{gi}^{\max}$	Lower and upper limits respectively on the reactive power of generator at bus *i.*
ΔP_{gi}	Ramp real power of generator at bus *i.*
$\Delta P_{gi}^{\min}$, $\Delta P_{gi}^{\max}$	Lower and upper limits respectively on the real power ramp rate of generator at bus *i.*
V_i	Voltage magnitude of bus *i*.
$V_i^{\min}$, $V_i^{\max}$	Lower and upper limits respectively of the voltage magnitude of bus *i*.
S_{ij}	Apparent power on transmission line from *i* and *j*.
$S_{ij}^{\max}$	Maximum limit of apparent power on transmission line from *i* and *j*.
$t_{ij}^{\min}, t_{ij}^{\max}$	Lower and upper limits respectively of transformer tap ratio.
$\alpha_{ij}^{\min}, \alpha_{ij}^{\max}$	Lower and upper limits respectively of phase shift angles.

Algorithm

Many algorithms have been developed to solve the OPF problem [94-96]. The sequential quadratic programming (SQP) algorithm was adopted in this research. The SQP algorithm has the advantage of efficiency, accuracy, and percentage of successful solutions over other methods [97]. The algorithm mimics the Newton's method to solve constrained optimization problem similar to what is done for the unconstrained optimization. For each major iteration, an approximation is made for the Hessian of the Lagrangian function using a quasi-Newton updating method. This is then used to generate a QP sub-problem whose solution is used to form a search direction for a line search procedure.

Solutions

Based on the formulation of the OPF problem, the solutions are widely used to determine electricity prices [91]. The Lagrange multipliers are the negatives of the derivative of the function that is being minimized with respect to the enforced constraint [91]. The resulting multiplier can be represented as the marginal cost for meeting that constraint. Therefore, the Lagrange multipliers for equality constraints of real and reactive power balance at bus *i*: μ_i^P and μ_i^Q can be interpreted as the marginal cost for supplying the load at bus *i* in $\$/MWh$ and $\$/MWARh$ respectively.

If the inequality constraint is satisfied, the corresponding multiplier should be zero, otherwise it is said that the inequality constraint is active, and the value of the multiplier can be perceived as the cost for violating the constraint. The Lagrange multipliers of transmission constraints can help system operators in transmission planning. For example, if the multiplier λ_{ij} of a power flow constraint of a transmission line between buses *i* and *j* is not zero, then the transmission line is operating at its limit. This implies that the specific transmission line may have significant economic impact on the power system. Line capacity increase may thus

improve the economic operation of the system.

The Roy Billinton Test System (RBTS) is used to illustrate the techniques of nodal price evaluation using the OPF method. Detailed information on the RBTS is given in [98]. The single line diagram of the RBTS is shown in Fig. 2.1. The generation cost for each unit is shown in Table 2.1.

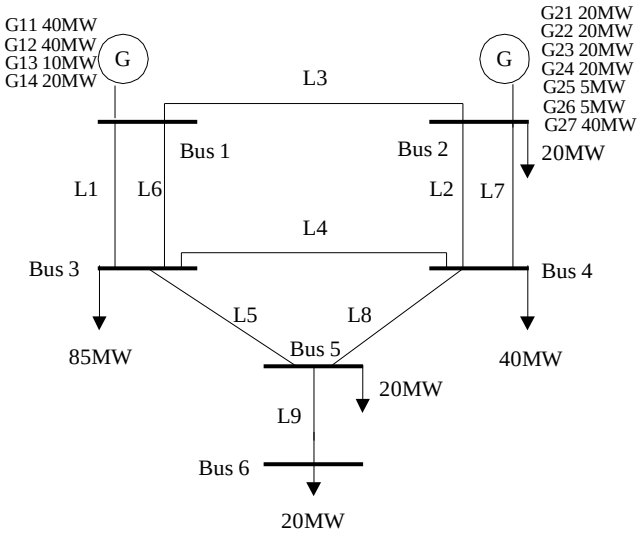

Fig. 2.1 Single line diagram of the RBTS

An OPF problem is formulated using the data given in Table 2.1 with the objective of minimizing the system operating cost. The operational constraints such as the voltage limits, generation output limits and transmission limits are included in order to accurately determine the generation output and system marginal cost. The results of the OPF problem are shown in Table 2.2.

Table 2.1 Generation cost data

Generator Index	Generator Cost Function ($/hr)	Real Power limit (MW)	Reactive Power Limit (MVAR)
G11	$0.096P_{g11}^2+10P_{g11}+90$	$0\le P_{g11}\le 40$	$-15\le Q_{g11}\le 17$
G12	$0.096P_{g12}^2+10P_{g12}+90$	$0\le P_{g12}\le 40$	$-15\le Q_{g12}\le 17$
G13	$0.1P_{g13}^2+11.5P_{g13}+80$	$0\le P_{g13}\le 10$	$0\le Q_{g13}\le 7$
G14	$0.11P_{g14}^2+12.5P_{g14}+100$	$0\le P_{g14}\le 20$	$-7\le Q_{g14}\le 12$
G21	$0.0403P_{g21}^2+4.75P_{g21}+80$	$0\le P_{g21}\le 20$	$-7\le Q_{g21}\le 12$
G22	$0.0403P_{g22}^2+4.75P_{g22}+80$	$0\le P_{g22}\le 20$	$-7\le Q_{g22}\le 12$
G23	$0.0403P_{g23}^2+4.75P_{g23}+80$	$0\le P_{g23}\le 20$	$-7\le Q_{g23}\le 12$
G24	$0.0403P_{g24}^2+4.75P_{g24}+80$	$0\le P_{g24}\le 20$	$-7\le Q_{g24}\le 12$
G25	$0.051P_{g25}^2+4.85P_{g25}+80$	$0\le P_{g25}\le 5$	$0\le Q_{g25}\le 5$
G26	$0.051P_{g26}^2+4.85P_{g26}+80$	$0\le P_{g26}\le 5$	$0\le Q_{g26}\le 5$
G27	$0.052P_{g27}^2+4.65P_{g27}+80$	$0\le P_{g27}\le 40$	$0\le Q_{g27}\le 17$

Table 2.2 Generation Output

Generator Index	Real Power Output (MW)	Reactive Power Output (MVAR)
G11	21.57	2.66456
G12	21.57	2.66456
G13	10	3.26499
G14	7.47	2.55165
G21	20	-2.29233
G22	20	-2.29233
G23	20	-2.29233
G24	20	-2.29233
G25	5	1.92979
G26	5	1.92979
G27	40	-8.31175

The nodal prices of real power at each bus are shown in Table 2.3. The nodal prices at different buses vary marginally from each other, around 14$/MWh.

Table 2.3 Nodal price at each bus

Bus Number	Real Power Price ($/MWh)
1	14.14
2	13.35
3	14.57
4	14.51
5	14.67
6	14.80

2.2 Power System Reliability Evaluation

Irrespective of whether the power system is a conventional power system or a restructured power system, the main objective of system operation is to supply customers as reliably and economically as possible. The basic reliability evaluation methods are introduced in this section. Three commonly used methods for reliability evaluation are: the probability method, the frequency and duration method, and the Monte Carlo simulation method [63]. These methods are generic and can be applied to any power system. However, they have different properties that suit different applications, which will be explained in this section.

2.2.1 Component models

System reliability relates to the randomly occurring failures of system components. The random behavior of the system component operation is known as a stochastic process. Based on the criterion of whether the system moves from one state to another in discrete time or continuous time, the process is classified as discrete or continuous, and accordingly referred to as a Markov Chain or a Markov Process. However, the system must satisfy certain conditions to be modeled using the Markov approach. Firstly, the system should be memoryless so that the future states of the system are independent of the past states except the immediately preceding one. Secondly, the system should be stationary. This indicates that the system behavior is the same irrespective of the point of time being considered, i.e, the probability of transition of

the system from one state to another dose not depend on time, but on the time interval. Thus the Markov approaches are applicable only to systems whose behavior is described by Poisson and Exponential distributions. For system components, a constant hazard rate ensures that the system state transitions remain constant at all points of time. Markov models for system components are established and reliability analysis is then conducted using the Markov process [63].

The failure and repair characteristics of the system components can be represented using exponential distributions. Therefore the system behavior can be modeled as a Markov process. The reliability model of the system must have the ability to show the system states and the transitions from one state to another. The state space is formulated as a discrete function which represents the state the system resides in and the duration. For a single component, the Markov model is shown in Fig. 2.2. The component has two states: UP(0) and DOWN(1). λ and μ are the system failure rate and repair rate respectively. However, if a unit has one or more derated states, it can be represented as a three or higher state Markov model.

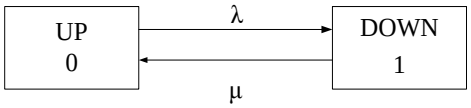

Fig. 2.2 Two-state Markov model of a single component

Given the failure and repair rates, the density functions of the components' operating and failure states are represented by $f_0(t)$ and $f_1(t)$ respectively:

$$f_0(t) = \lambda e^{-\lambda t} \tag{2.27}$$

$$f_1(t) = \mu e^{-\mu t} \tag{2.28}$$

The relationship between the mean time to failure (*MTTF*) and the failure rate is expressed in (2.29). The relationship between the mean time to repair (*MTTR*) and the repair rate is expressed in (2.30).

$$MTTF = \frac{1}{\lambda} \tag{2.29}$$

$$MTTR = \frac{1}{\mu} \tag{2.30}$$

The generating unit and transmission line reliability models can be developed using the Markov model.

System state is the aggregated state of all the system components. The state of each component should be determined in order to determine the system state. The availability of a system component at steady state p_0 and the unavailability p_1 are calculated as [63]:

$$p_0 = \frac{\mu}{\mu + \lambda} \tag{2.31}$$

$$p_1 = \frac{\lambda}{\mu + \lambda} \tag{2.32}$$

2.2.2 System reliability evaluation

Probability method

The probability method for reliability evaluation basically evaluates a given system generation configuration's adequacy. The loss of load probability (LOLP) or loss of load expectation (LOLE) is the most widely used probabilistic technique. The basic approaches for adequacy evaluation are similar and mainly include three parts as shown in Fig. 2.3. The generation and load models shown in Fig. 2.3 are combined to form the system risk model. The generation model is the convolved model of all the generation units in the system.

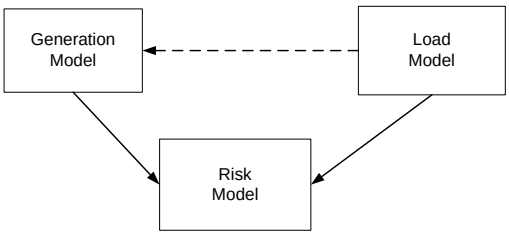

Fig. 2.3 Conceptual tasks in generating capacity reliability evaluation

Each generation unit can be modeled using the Markov model introduced before. All the parameters for each state can form a table designated as the capacity outage probability table (COPT) [63]. For a system that contains different types of generation units, the generation model can be obtained by multiplying the corresponding capacity probability. The load model is the aggregated model of the entire load in the system.

Loss of load occurs when the load exceeds the available generation capacity. By combining the capacity outage probability table and the load model, the LOLE can be calculated using the following equation:

$$LOLE = \sum_{i=1}^{n} p_i \times t_i \left(A_{ci} < L \right) \tag{2.33}$$

where p_i is the probability of state i, t_i is the time during which capacity A_{ci} is less than load L, and n is the number of states.

The units of LOLE are in days if the daily peak load variation curve is used or in hours if the load duration curve is used.

In order to use probability techniques in power systems, the following assumptions were made. First, the calculated indices do not include transmission line constraints. The transmission reliability is not included either. Second, since the calculated reliability indices are the overall adequacy of the generation system, they cannot reflect the generation deficiency at any particular customer load point. The third one relates to the characteristic of the indices. The LOLE represents the expected number of days (or hours) in a given period that the loads exceed the available generating capacity. It does not, therefore, reflect the frequency of occurrence of an insufficient capacity or its duration.

Frequency and duration method

The probability of the system staying in one state can be calculated using Markov

techniques described before. The frequency and duration method for system capacity evaluation is introduced to calculate the frequency of encountering a system state and the duration of the state. The frequency and duration method can incorporate the transmission line into overall or composite system evaluation, and it is also possible to evaluate the reliability indices for each customer and load point.

The additional data needed are the state frequency and duration. The basic technique of the frequency and duration method can be described using the Markov process of a single repairable component. The state space diagram of the component is shown in Fig. 2.2. The probability of the operating state and failure state are calculated using Equations (2.31) and (2.32) respectively.

The probability of residing in a certain state equals the mean residence time of the state divided by the mean cycle time for that state to happen. It can be extended to a multi-state system. The probability of residing in state *i* is:

$$p_i = \frac{m_i}{T} \tag{2.34}$$

where p_i is the probability of state *i*, m_i is the mean time of staying in state *i*, and *T* is the mean time of encountering state *i*.

For a repairable unit described in Fig. 2.2, the mean time between failures (MTBF) is described as the mean duration of encountering a system state which is the sum of MTTF and MTTR as in Equation (2.35). The state probability indices are calculated using Equations (2.36) and (2.37):

$$MTBF = MTTF + MTTR \tag{2.35}$$

$$p_0 = \frac{MTTF}{MTBF} = \frac{1}{\lambda \cdot MTBF} = \frac{f}{\lambda} \tag{2.36}$$

$$p_1 = \frac{MTTR}{MTBF} = \frac{1}{\mu \cdot MTBF} = \frac{f}{\mu} \tag{2.37}$$

where *f* is the frequency of encountering a system state and is the reciprocal of *MTBF*.

The extension of the equation is based on Equations (2.29) and (2.30).

In a more general sense, the frequency of a particular condition can be described as the mathematical expectation of encountering the boundary wall surrounding that condition. So the frequency of encountering the state can be expressed as the product of probability of that state and the rate of entering the state. From the frequency balance concept introduced in [63], the frequency of entering a state equals the frequency of leaving that state. The following equation can be derived from Equations (2.36) and (2.37).

$$f = \lambda \cdot p_0 = \mu \cdot p_1 \tag{2.38}$$

However, the concept is only applicable to the long term behavior of the system (steady state) and not valid for time dependent system probabilities and frequencies.

Then the duration of residing in the state is determined as:

$$m_i = p_i \cdot T_i = \frac{p_i}{f_i} = 1/\lambda_i^d \tag{2.39}$$

where λ_i^d is the departure rate of state *i*.

Compared to the probability method which only provides static adequacy evaluation of different system configurations and expansions, the frequency and duration method evaluates the transition of system states and provides frequency and duration indices in addition to the probability indices. However, these two methods lead to virtually identical expansion plans for a given reliability index.

Monte Carlo simulation method

The probability and frequency and duration methods described above are analytical methods. The analytical method represents the system by a mathematical model and evaluates the reliability indices from this model using direct numerical solutions. In

most cases, this is sufficient for the system operators and planners to make objective decisions. The results obtained from the analytical method are expectation indices. The simulation methods estimate the reliability indices by simulating the real system operation process and random behavior. Therefore it can include more aspects such as outage and repairs of elements represented by general probability distributions, dependent events and component behavior, queuing of failed components, and load variation, etc., in solving the problem.

Monte Carlo simulation simulates a system process by generating random variables based on the probability of the system model parameters [99]. It has been widely used in system analysis. There are basically two types of stochastic simulations: random and sequential [63]. The random approach simulates the basic intervals of the system states by choosing intervals randomly. The sequential approach simulates the system lifetime in a sequential manner. When there are some system problems for which one time interval has significant effects on the next interval, the chronological property of the system will have significant impacts on the reliability indices. In another condition, if the probability distribution and frequency of the state duration are needed in the system, these can only be evaluated explicitly if the chronology of the system behavior is simulated. The random approach on the other hand has more restrictive application requirements. For systems that can use both approaches, the random approach is computationally more efficient.

Modeling generation unit states using Monte Carlo simulation is based on the state probability of the unit. For a unit which has two states with probability of p_0 and p_1 as shown in Fig. 2.2, a random number U in the range (0, 1) is generated. If $U < p_1$, then the unit is deemed to be in the down state, otherwise the unit is deemed to be available. For a unit that has derated state with probability of p_2, if $U < p_1$, the unit is deemed to be in the totally down state and if $p_1 < U < p_1 + p_2$, the unit is

deemed to be in the derated state, otherwise, the unit is in available state.

After the state of the unit has been determined, the duration of the state is sampled.

In case of the exponential distribution, the duration *T* determined from the random number is discussed in [63] and given as the following:

$$T = -\frac{1}{\lambda}\ln U \tag{2.40}$$

where λ is the transition rate of the state.

Consequently, for a two-state unit described in Fig. 2.2, the random values of time to failure (TTF) and time to repair (TTR) are calculated by:

$$TTF = -\frac{1}{\lambda}\ln U\left(if\ \ p_1 < U < 1\right) \tag{2.41}$$

$$TTR = -\frac{1}{\mu}\ln U\left(if\ U < p_1\right) \tag{2.42}$$

The time to repair of a component is usually modeled as a normal distribution or a log-normal distribution in reliability evaluation [100]. In this case, the duration of a specific state is calculated using different equations. Two independently normally distributed variables X_1 and X_2 can be generated from two uniformly distributed variables U_1 and U_2 as:

$$X_1 = \sqrt{-2\ln U_1}\cos\left(2\pi U_2\right) \tag{2.43}$$

$$X_2 = \sqrt{-2\ln U_1}\sin\left(2\pi U_2\right) \tag{2.44}$$

The repair durations following normal distributions are given by X_1 or X_2.

For repair durations for the a log-normal distribution, the mean μ and variance σ^2 are determined as:

$$\mu = \ln\left(\frac{E^2}{\sqrt{V+E^2}}\right) \tag{2.45}$$

$$\sigma^2 = \ln\left(\frac{V + E^2}{E^2}\right) \tag{2.46}$$

where E and V are the mean and variance of the log-normal distribution.

The repair duration for the log-normal distribution can be calculated by:

$$T = e^{\mu+\sigma Z} \tag{2.47}$$

where z is a random variable generated from the standard normal distribution. The results are obtained under the assumption that the deviation equals one-third of the MTTR.

The operating cycle of the modeled component can be created using random number generators and the probability distribution of the TTF and TTR. The failure time and repair time are represented in the operating cycle.

The variation of load is represented in two ways: chronological or nonchronological. The chronological load model is a sequential load level in order of occurring time or expected time to occur. The nonchronological load model enumerates all the load levels and then represents the load level in a descending order to form a daily peak load duration curve (DPLDC) if the daily peak value is used or a load duration curve (LDC) if the hourly load is used. The chronological model is easy to use in Monte Carlo simulation by superimposing on the simulated chronological generation capacity. The nonchronological load model is treated in a different way. One method is to divide the load into limited steps to produce a multistep load model. The probability of step i, p_i is determined as the ratio of duration of load level d_i and the total period of interest T, i.e., $p_i = d_i / T$. Then the load level in Monte Carlo simulation can be determined by generating a uniformly distributed random number in the same way as the determination of a generating unit state.

The expected reliability indices $E(Q)$ for Q which can be loss of load or loss of energy

and others are determined as:

$$E(Q) = \frac{1}{N}\sum_{j \in N} x_j \tag{2.48}$$

where N is the number of sample states, x_j is an indicator that states the value of the examined index at each simulation state as:

$$x_j = \begin{cases} 0 \ \ if \ \ the \ state \ \ j \ is \ in \ up \ state \\ Q_j \ \ if \ \ the \ state \ \ j \ is \ in \ down \ state \end{cases} \tag{2.49}$$

The variances and distribution of the examined indices can also be obtained from Monte Carlo simulation. The accuracy level of Monte Carlo simulation is evaluated by its coefficient of variation which is also used as the convergence indicator.

Compared to the probability method and the frequency and duration method, the Monte Carlo simulation method can provide the distribution of calculated indices. The computation burden in Monte Carlo simulation is independent of the system size and is favorable in large systems.

2.3 Nodal Price and Nodal Reliability

In traditional vertically integrated power systems, customers have no choice in selecting power suppliers, and the price is fixed for customers at different nodes. In a power market, customers have more choices to choose power suppliers and they pay higher price for higher reliability of supply. Customers can also adjust their demand based on energy price and their reliability requirements [67]. The participation of demand side in power system operation has changed the way electricity prices are determined. The investigation of demand behavior can provide suppliers useful information for adjusting their bidding strategy and generation schedule.

In restructured power systems, nodal prices provide useful economic information that reflects the transmission and generation cost. The nodal or bulk load point reliability can provide information regarding the risk corresponding to the specific point [66].

With the participation of customer, the nodal price in contrast reflects the cost that the customer is willing to pay for the corresponding reliability level. Therefore nodal reliability and nodal price are correlated in a deregulated power system. The market participants can use this information to determine their bidding strategies and maximize their benefits. For system planners and investors, it provides them with great insight into the appropriate time and location for adding new generating units and transmission lines [66].

In a traditional power system, customers receive uniform price and reliability that is centrally managed by the system operators and planners. Customers have no choices to choose their reliability. When a contingency occurs, load shedding and generation re-dispatch decisions are made by the system operators to release the network violation without considering customers' different reliability requirements. The reliability evaluation techniques in a conventional power system are well developed and examined thoroughly [63-65]. The customer choice is not included in these techniques. In a deregulated power system, customers can choose to purchase reliable service to improve their reliability. It can be realized by assigning different customer benefit functions. Since it is hard to measure directly, the reliability benefits are evaluated indirectly as interruption cost of customers in many systems [66, 101]. Customer damage function (CDF) is one surrogate of interruption cost which is widely used in North America, while the value of lost load (VOLL) is used in UK and other European countries [63].

Customer interruption costs have been investigated by many researchers [63]. The approaches can be categorized into three main types: various indirect analytical evaluations, case studies of blackouts, and customer surveys. Among these methods, customer survey is widely used by the utilities due to its direct reflection of customer's response to supply interruption. The customer interruption cost dependents on the characteristic of customer and the interruption. Customer characteristics include types of load, nature of customer activities, size of operation, demographic

data, demand, energy requirements, and energy dependency as a function of time of the day, etc. It is also demonstrated that a customer will reduce demand when the price of electricity is higher than the customer marginal cost at contingency state [67]. Interruption characteristics include the duration, frequency, and time of occurrence of interruptions, the influence of the interruption, etc.

Based on customer surveys, customer interruption cost is determined for different customer categories. The Standard Industrial Classification (SIC) system of customer identification is widely used in determining the customer category. One convenient way to display customer interruption cost is the sector customer damage functions. Surveys have been conducted by the University of Saskatchewan and Canadian electric power utilities to estimate customer interruption costs [63]. The sector customer damage functions (CDFs) which are functions of electricity interruption have been determined from the survey data [63], and are shown in Table 2.4.

Table 2.4 Customer sector interruption cost ($/kW)

User Sector	Interruption Duration (mins) & Cost ($/kW)				
	1 min	20 min	60 min	240 min	480 min
Larger User	1.005	1.508	2.225	3.968	8.240
Industrial	1.625	3.868	9.085	25.16	55.81
Commercial	0.381	2.969	8.552	31.32	83.01
Agriculture	0.060	0.343	0.649	2.064	4.120
Residential	0.001	0.093	0.482	4.914	15.69

The nodal prices in a power market vary with customer load pattern and the load level. Customers can reduce their demand if the nodal price is too high. On the other hand, customers can also increase the demand if the price is low. In some cases, customer pays a higher price for higher reliability while others are willing to pay a lower price with lower reliability requirement. The design of market process and reliability evaluation should consider the correlation between nodal price and nodal reliability.

2.3.1 Nodal price

There are two electricity pricing methods in existing power markets [4]: the last accepted bid and the spot pricing method. The last accepted bid method collects market participants' bid blocks containing energy and prices. The aggregated supply curve is created by aggregating the supply bid in price ascending orders. The demand curve is created in the same way in price descending orders. The supply curve and demand curve are plotted against each other, and the price and energy at the cross point of these two curves are the market clearing price (MCP) and clearing energy respectively. All supply bids whose bidding price is higher than the MCP and demand bids whose bidding price is lower than MCP are rejected. This method is convenient and requires less computation effort. England, Wales, and New Zealand markets are examples of this type [4].

The basic theory of spot pricing is introduced in [102]. The participants in this method supply the cost curve to the market. The market operators determine the energy price based on the minimization of the total system cost. The participants accept the clearing price from the system optimization results. Australia, PJM market in eastern US and New England market in the US are examples of markets using the spot pricing method [4].

To accurately charge demand and reflect cost of providing energy considering locational effects, spot pricing can provide the uniform price, zonal price or nodal price [103]. The spot pricing method can ensure both the economic and secure operation in power systems and is therefore utilized in this thesis.

2.3.2 Customer reliability and load curtailment

In conventional power systems, customers are purely price takers and in contingency state when load shedding is needed, system operators determine the location and amount of load being curtailed. The reliability of supplying load is thus centrally

controlled by system operators to maximize the entire system benefit. In the new system environment, customers can maximize their own benefits by choosing suppliers and enhance their own reliability by purchasing reliability services such as transmission rights and higher load shedding priority. This can help them to hedge the risk of being shed in contingency states. Alternatively, the customer can choose to reduce its demand when the price is extremely high during system component failures [66]. For a certain customer, reducing demand may be much more beneficial than paying for a high electricity price. In such a case, the load shedding is determined by the customer. So the behavior of a customer in the market is modeled as an optimization of its own benefit. The objective function is the benefit minus the cost of load shedding. For customer *i*, at contingency state *j*, the load curtailment is determined by solving the following optimization problem:

$$Max\ \phi = B\left(P_{di}^{0}\right) - C\left(P_{di}^{j} - P_{di}^{0}\right) - \rho^{j} \times P_{di}^{j} \tag{2.50}$$

where P_{di}^{0} represents the equilibrium demand at the normal state, $\left(P_{di}^{j} - P_{di}^{0}\right)$ is the load curtailment at state *j* due to high electricity price or system network violation, P_{di}^{j} represents the demand at state *j*, ρ^{j} is the electricity price at state *j*, $B\left(P_{di}^{0}\right)$ is the customer benefit function for normal state, and $C\left(P_{di}^{j} - P_{di}^{0}\right)$ is the customer cost due to demand curtailment at state *j*.

When customer benefit $B\left(P_{di}^{0}\right)$ is constant, the problem becomes minimization of the curtailment cost and cost of purchasing energy. The problem then takes the following form:

$$Min \prod = C\left(P_{di}^{j} - P_{di}^{0}\right) + \rho^{j} \times P_{di}^{j} \tag{2.51}$$

The problem minimizes customers' interruption cost and energy cost subject to system operational constraints. Thus the solutions are correlated with the system economic operation solutions.

2.3.3 Nodal price and nodal reliability

The relationship between nodal reliability and nodal price can provide important information for market participants. Nodal prices at contingency states will deviate from normal state severely as presented in [66-68]. The contingency states occur randomly in system operation. In order to examine the price behavior for all system conditions, the expected nodal price is used. It is calculated as an expected value for all the system operation states according to the frequency and probability of the state. It is shown in [67] that the price fluctuation usually occurs at the weak load node and for these nodes, the expected nodal prices have significant deviations from the normal price. Hence it is very important to analyze the expected nodal price to give market participants the information of overall nodal price behavior.

The contingency state can be determined using the contingency enumeration and state selection method. The probability and frequency of each contingency state are evaluated using the same method for solving the bulk power systems [63]. The loss of load for each node is determined by proportional load shedding. Then the reliability index can be calculated for each node. The OPF techniques described in [68] are utilized to determine the nodal prices and the load curtailment with the objective of optimizing system benefits.

2.4 Conclusions

This chapter has presented system economic operation and reliability evaluation methods typically used in power systems. The techniques used in evaluating the electricity price and system reliability have been discussed.

One objective of system operation is to supply load at minimum cost. In both conventional and restructured power systems, the objective is realized by using economic dispatch (ED). However, the resulting generation dispatch of ED must satisfy the load demand and system losses and at the same time obey the system

power flow equations. The optimal power flow (OPF) is introduced to fulfill this requirement. OPF is a nonlinear optimization problem used in system economic operation to realize different operation objectives. In normal operation, the objective of OPF is to minimize the total generation cost. In a restructured power system, the participation of demand has changed the objective of OPF by including benefit function of load. The economic implication of the solutions of OPF makes it possible to use the results of OPF to determine the nodal prices. An example is also given in this chapter to illustrate the technique.

The reliability of power supply is an important part of system operation both in conventional and restructured power systems. Basic system reliability evaluation concepts and techniques are presented in this chapter. The characteristics of system components make it possible to use Markov models to represent the operation. Three system reliability evaluation methods are introduced in this chapter. These methods can be applied in both conventional and restructured power systems.

Nodal price and nodal reliability in deregulated power systems are also discussed. The spot pricing method and OPF techniques are utilized in determining nodal indices.

Chapter 3 Renewable Power Generation

With the extensive utilization of renewable energy in existing power systems, these resources should be properly investigated in order to optimize the benefits of renewable penetration on the power system. In order to understand and quantify the renewable power variations, renewable power generations are investigated and presented in this chapter. The market behavior of wind power providers is also presented.

3.1 Wind Energy Conversion System

A wind energy conversion system (WECS) converts the wind energy at a specific site into electric energy. In order to evaluate the potential benefits of adding WECS to a power system, a distinctive model of WECS which can take into account the intermittent and diffusive nature of the energy source as well as the failure and repair characteristic of the WECS needs to be developed.

The model of a wind turbine generator (WTG) contains three main factors that affect the generation output [46]. The first one is the random nature of the wind speed which must be included in a probabilistic model that reasonably approximates the wind characteristic at a particular location. The second factor is the relation between power output and wind speed. This relation can be described using the operating parameters of the WTG being considered. The commonly used parameters are the cut-in wind speed, cut-out wind speed, and the rated wind speed. The third factor is the probability of unavailability of the wind turbine which is expressed by the unit forced outage rate (FOR) [46].

A WECS contains two main parts: the wind source and the actual wind turbine units. Fig. 3.1 shows the WECS model for reliability analysis.

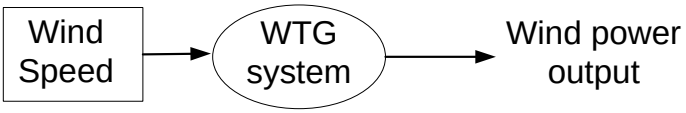

Fig. 3.1 Wind energy conversion system power output model

WECS model has been investigated for different utilizations [35, 46, 104]. An analytical method has been presented in [46] to model the WTG for reliability evaluation. However it did not include the chronological characteristics of wind speed and its effects on the output of the WTG. A sequential Monte Carlo method is capable of considering these factors in the adequacy evaluation of a power system containing WECS. Two time-series models of wind speed are given in [104] which is an essential step for the application of the sequential Monte Carlo method. A multistate model for a WTG unit and a WECS model containing many WTGs are built in [35] using the apportioning method. This model can be easily used in system adequacy analysis with many WTGs at different locations.

The time sequential model of WECS is developed in the following sub-sections. The novel contribution of this section is that a time series model of wind power has been developed which can be used in the short term or long term wind integration analysis described in Chapter 6.

3.1.1 Wind speed

The wind speed of the specific site indicates the energy that can be extracted from the wind. One of the critical steps in constructing the WECS model is to simulate the wind speed. The wind speed has been examined using an analytical method which cannot represent the chronological characteristic. A time-series model [104] which can simulate not only the auto-correlation of wind speed and the seasonal property, but also the diurnal distribution is adopted in this thesis to fulfill this step.

Auto-regressive and moving average (ARMA) model

The renewable power variations result from intermittent renewable sources like wind speed and solar radiation. The random behavior of wind speed and solar radiation characteristics correlate with climatic factors and shows chronological characteristics. Therefore they are hard to be modeled using analytical methods. The statistical method can model the time series variables and is adopted in analyzing the renewable sources.

The ARMA model that can represent the random and chronological characteristic of time series is utilized. ARMA model is widely used in modeling and prediction of time series. The utilization of ARMA model requires that the time series to be stationary and memoryless [105]. The wind speed and solar radiation all satisfy this requirement.

The general expression and theory of ARMA model is introduced first. For an observed time series with

OV_t = Observed value at time *t*,

μ_t = Mean value at time *t*,

σ_t = Standard deviation at time *t*.

The time series model can be developed from the above data. Let data series y_t be:

$$y_t = f\left(OV_t, \mu_t, \sigma_t\right) \tag{3.1}$$

The y_t is generated from the available data, and the transformation in *f* usually includes removing seasonal trends and removing means to produce a stationary data series. y_t can be modeled using *ARMA(p,q)* time series model:

$$y_t = c + \sum_{i=1}^{p} \phi_i y_t + \alpha_t + \sum_{i=1}^{q} \theta_i \alpha_{t-i} \tag{3.2}$$

Equation (3.2) contains an auto-regressive (AR) part $A(p) = c + \sum_{i=1}^{p} \phi_i y_t + \alpha_t$ and a moving average (MA) part $C(q) = \alpha_t + \sum_{i=1}^{q} \theta_i \alpha_{t-i}$ where $\phi_i \, (i = 1, 2, \ldots, p)$ and $\theta_j \, (j = 1, 2, \ldots, q)$ are the parameters of the model respectively. α_t is a normal white noise process with zero mean and a variance of σ_α^2 (i.e. $\alpha_t \in NID\left(0, \sigma_\alpha^2\right)$, where NID denotes Normally Independently Distributed).

After establishment of proper time series model for y_t, the simulated data SV_t of the examined time series can be calculated by:

$$SV_t = f^{-1}\left(y_t, \mu_t, \sigma_t\right) \tag{3.3}$$

where $f^{-1}(\cdot)$ is the inverse function of $f(\cdot)$.

The adequacy of the model is checked by a standard called Akaike's Information Criterion (AIC) which provides a way to measure the model quality by simulating the condition using a different data set. A smaller value indicates better estimation. In case studies, ARMA models with different orders were fitted and the one with smallest AIC value was chosen. Another is the fitness value which represents the percentage of the output that the model reproduces. Usually these two standards provide same results.

The simulated values produced from the ARMA model can capture the statistical characteristics of the original data such as mean and standard variation. Since the model is usually developed based on measurement data set, it is useful in generating data series that follows the characteristic of the measurement. With more simulated data, the behavior of the time series and its impacts on other systems can be examined.

ARMA model of wind speed

Let

OW_t = observed wind speed at hour *t*,

μ_t = mean observed wind speed at hour *t*,

σ_t = standard deviation of observed wind speed at hour *t*,

SW_t = the simulated wind speed at hour *t*.

A data series y_t is calculated from the measurement data as:

$$y_t = \left(OW_t - \mu_t\right) / \sigma_t \tag{3.4}$$

Based on the historical observed data of hourly average wind speed and variation, an ARMA (*n, m*) time-series model can be built as:

$$y_t = \phi_1 y_{t-1} + \phi_2 y_{t-2} + \ldots + \phi_n y_{t-n} + \alpha_t - \theta_1 \alpha_{t-1} - \theta_2 \alpha_{t-2} - \ldots - \theta_m \alpha_{t-m} \tag{3.5}$$

where $\phi_i (i = 1, 2, \ldots, \mathrm{n})$ and $\theta_j (j = 1, 2, \ldots, \mathrm{m})$ are the auto-regressive and moving average parameters of the model respectively. α_t and σ_α^2 are the same type of parameters as in Equation (3.2).

Through the ARMA model, data series of y_t can be predicted and generated. The simulated wind speed is calculated as:

$$SW_t = \mu_t + \sigma_t y_t \tag{3.6}$$

The wind data are obtained from [106]. Three years' wind speed data of ten minutes interval at height of 80 meters are examined using the ARMA model and presented in Equation (3.7). An ARMA model has been developed based on the measured data. The ARMA model's MA and AR orders are 4 and 3 respectively. The AIC of the model is 0.3678.

$$\begin{aligned} y_t = {} & 0.9235 y_{t-1} + 0.8603 y_{t-2} - 0.9331 y_{t-3} + 0.04418 y_{t-4} \\ & + \alpha_t - 0.8744 \alpha_{t-1} - 0.9039 \alpha_{t-2} + 0.867 \alpha_{t-3} \end{aligned} \tag{3.7}$$

where $\alpha_t \in NID\left(0, 1.2^2\right)$.

Fig. 3.2 shows the hourly predicted and measured wind speed. The prediction basically follows the measurement and represents the chronological characteristics.

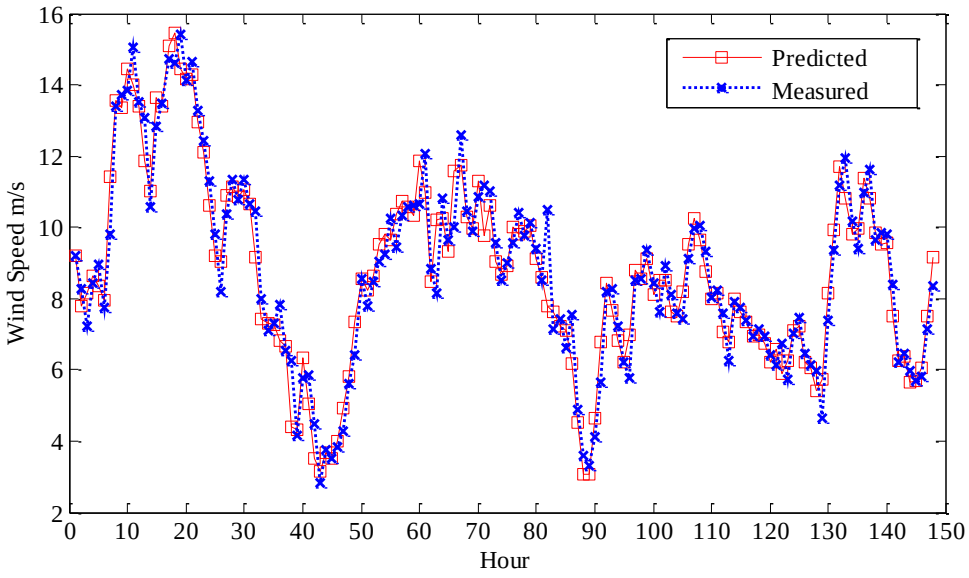

Fig. 3.2 Prediction and measurement of hourly wind speed

3.1.2 Relation between power output and wind speed

The power output characteristics of a wind turbine generator are quite different from those of conventional generators. The output of a wind turbine generator (WTG) depends strongly on the wind regime as well as the design parameters of the turbine. Generally it can be described by the plot of output power against the average wind speed as shown in Fig. 3.3.

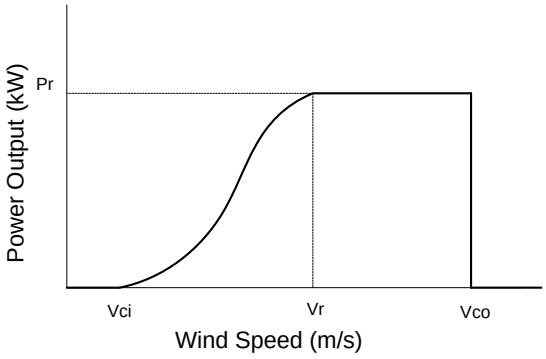

Fig. 3.3 Power output curve of wind turbine generator

In Fig. 3.3, there are three important parameters that determine the power output of the wind turbine. First is the cut-in speed V_{ci} which denotes the minimum wind speed for the turbine to generate power. Second is the rated speed V_r at which the generator generates rated power. Third is the cut-out speed V_{co} at which the generator will cut-off due to safety concerns. The hourly wind turbine power output can be calculated based on the simulated hourly wind speed:

$$PP(SW_T) = \begin{cases} 0 & 0 \le SW_T \le V_{ci} \\ (A + B \times SW_T + C \times SW_T) & V_{ci} \le SW_T \le V_r \\ P_r & V_r \le SW_T \le V_{co} \\ 0 & V_{co} \le SW_T \end{cases} \tag{3.8}$$

where P_r is the rated power output of the WTG.

The parameters *A*, *B* and *C* presented in [46] are determined by V_{ci}, V_r and V_{oc}.

$$A = \frac{1}{(V_{ci} - V_r)^2}\left[V_{ci}(V_{ci} + V_r) - 4V_{ci}V_r\left(\frac{V_{ci} + V_r}{2V_r}\right)^3\right] \tag{3.9}$$

$$B = \frac{1}{(V_{ci} - V_r)^2}\left[4(V_{ci} + V_r)\left(\frac{V_{ci} + V_r}{2V_r}\right)^3 - (3V_{ci} + V_r)\right] \tag{3.10}$$

$$C = \frac{1}{(V_{ci} - V_r)^2}\left[2 - 4\left(\frac{V_{ci} + V_r}{2V_r}\right)^3\right] \tag{3.11}$$

Given the WTG parameters and the input wind speed, the output power of WTG can be calculated. The calculated wind output power can be utilized in the time sequential analysis or Monte Carlo simulation and the multistate wind power generation model. For example, a three-state WTG model that includes the forced outage rate of WTG is developed in [49] and the Monte Carlo simulation method is utilized to evaluate the system adequacy with wind penetration in [107].

3.2 Solar Energy Conversion System

A solar energy conversion system (SECS) converts solar energy into electricity. The

solar radiation and the electric characteristic of Photovoltaic (PV) panels are examined to evaluate the performance of SECS, as depicted in Fig. 3.4.

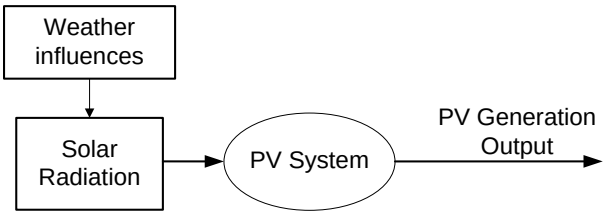

Fig. 3.4 Solar energy conversion system power output model

3.2.1 Solar radiation

The power output of the PV panel largely depends on the solar radiation. Different from wind speed, solar radiation is obtained from the sun and has a more obvious seasonal characteristic. Solar power is only available during the day time. The statistical characteristic of measured solar radiation data is important for PV system analysis.

Generation and prediction of synthesized hourly solar radiation data have been analyzed by many researchers. Overall, the analysis and model construction are based on the quality and availability of the measured data. Stochastic models based on hourly solar radiation obtained for one year in Singapore was proposed in [108]. The stochastic part was modeled using ARMA model. The determined part was obtained from the grand average over the entire recording period. A method for predicting the monthly mean solar radiation from the bright sunshine hours and other meteorological data was developed in [109]. A time dependent autoregressive Gaussian model was proposed in [110] to generate synthetic daily sequence of hourly solar radiation given the daily clearness index. The model considered two major factors that affect the hourly solar radiation: the solar hour and the daily clearness index. The model of 5 mins solar radiation probability density distribution was developed in [111] based on measurement of 5 mins global and beam solar radiation data. The objective was to evaluate the intra-hour variability of short-term solar radiation. A universal function

for calculating the hourly solar radiation for application in two locations in Greece was presented in [112]. The global daily solar radiation was predicted from the measurement using higher order statistical method [113]. Two statistical models were derived from the measurement: the clearness index and the loss radiation. The results showed that the prediction from the loss part model gave a more accurate prediction. Based on the measurement of mean hourly solar radiation values of 63 days and the meteorological data, a neural network was trained to predict the single step ahead hourly radiation [114]. Results showed that the prediction value captures the seasonal and stochastic characteristics of the solar radiation data. Further improvement was obtained with additional training data of meteorological parameters. Multiplicative ARMA models were developed from the monthly mean values of daily global radiation in [115] that can capture the seasonal characteristic of hourly series of solar radiation. It was applicable in areas with limited measurement data.

Based on previous research, the factors that determine the radiation include the determined part and the variation part. The determined parts are location of the site, solar hour of the day and day of the year. Determined factors are related to the position of the site with respect to the sun which is the source of the radiation. The variation factor is the meteorological condition which affects the percentage of radiation that can be received by the PV panel. The most widely used index representing the weather condition when determining the solar radiation is the clearness index [16, 108, 110, 114]. Clearness index is defined as the ratio of the average horizontal solar radiation at the site to the extraterrestrial insolation on a horizontal surface above the site just outside the atmosphere. Both environmental and meteorological factors can be reflected by the clearness index. The clear day solar radiation is used to determine the clearness index, instead of the extraterrestrial insolation in the examination. With determined factors, the clear day radiation can be calculated using the American Society of Heating, Refrigerating, and Air Conditioning Engineers (ASHRAE) Clear Day Solar Flux Model [16]. It is necessary to develop a model that can capture statistic characteristics of the solar radiations such

as the mean, variation and the autocorrelation function.

Due to its effectiveness in modeling chronological characteristic and random variations of data series, the ARMA time series model is developed to model the stochastic behavior of the solar radiation.

At hour *t*, the indices for solar radiation are as follows:

OSR^t = observation of solar radiation at hour *t*. CSR^t = clear day solar radiation at hour *t*.

μ^t = mean value of OSR^t.

σ^t = standard deviation of OSR^t.

CSR^t is determined using ASHRAE model instead of the extraterrestrial insolation [16]. The clearness index k^t and mean clearness index mk^t at hour *t*, and the daily clearness index for day *n*, dk_n are determined as:

$$k^t = OSR^t / CSR^t \tag{3.12}$$

$$mk^t = \mu^t / CSR^t \tag{3.13}$$

$$dk_n = \sum_{t \in n} OSR^t \Big/ \sum_{t \in n} CSR^t \tag{3.14}$$

In order to remove the diurnal effects, the hourly clearness index k^t is normalized first by subtracting mk^t and then divided by the standard deviation. The normalized data series y^t is:

$$y_t = \frac{k^t - mk^t}{\sigma^t} \tag{3.15}$$

The ARMA model of y_t is developed as:

$$y_t = \phi_1 y_{t-1} + \phi_2 y_{t-2} + \cdots + \phi_p y_{t-p} + \alpha_t - \theta_1 \alpha_{t-1} - \theta_2 \alpha_{t-2} - \cdots - \theta_q \alpha_{t-q} \tag{3.16}$$

where $\phi_i (i = 1, 2, \ldots, p)$ and $\theta_j (j = 1, 2, \ldots, q)$ are the auto-regressive and moving parameters of the model respectively. α_t and σ_α^2 are the same type of parameters as in (3.2).

Through the predicted series of y_t, the predicted clearness index sk^t and solar radiation SSR^t are obtained as:

$$sk^t = y_t \sigma^t dk + mk^t \tag{3.17}$$

$$SSR^t = sk^t CSR^t \tag{3.18}$$

Based on the solar radiation data obtained from the National Weather Study Project of Singapore, the ARMA model was developed. Since the available data are more detailed and comprehensive, more characteristics can be obtained to determine the parameters of the model. The ARMA model's MA and AR orders are 5 and 4 respectively. The AIC of the model is -13.23.

$$\begin{aligned} y_t = & -0.3944 y_{t-1} - 0.02011 y_{t-2} + 0.5122 y_{t-3} + 0.8906 y_{t-4} + 0.008758 y_{t-5} \\ & + \alpha_t + 0.413 \alpha_{t-1} + 0.02545 \alpha_{t-2} - 0.5224 \alpha_{t-3} - 0.9041 \alpha_{t-4} \end{aligned} \tag{3.19}$$

where $\alpha_t \in NID\left(0, 0.0013^2\right)$.

The predicted and measured values of the hourly solar radiation are shown in Fig. 3.5. For each day, the solar radiation is obtained for 11 hours from 8am to 7pm. Fig. 3.5 shows one week hourly solar radiation values. The prediction follows the measured values and the variations are due to the uncertainty of weather conditions.

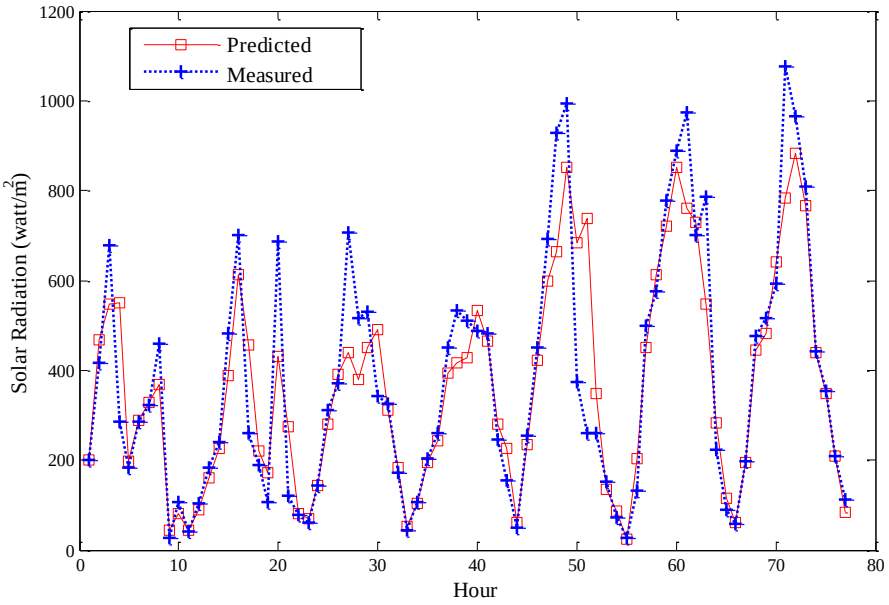

Fig. 3.5 Prediction and measurement of hourly solar radiations for one week

3.2.2 Electrical characteristic of PV panel

The power output of a PV panel is determined by I-V and P-V curves of the panel. Fig. 3.6 shows the I-V curves for different cell temperature and solar radiation levels. The mpp in the figure denotes the maximum power point of the PV panel. The Impp and Vmpp denote the current and voltage at the mpp respectively. The parameters of the two curves are affected mainly by the cell temperature and radiation level [16, 116].

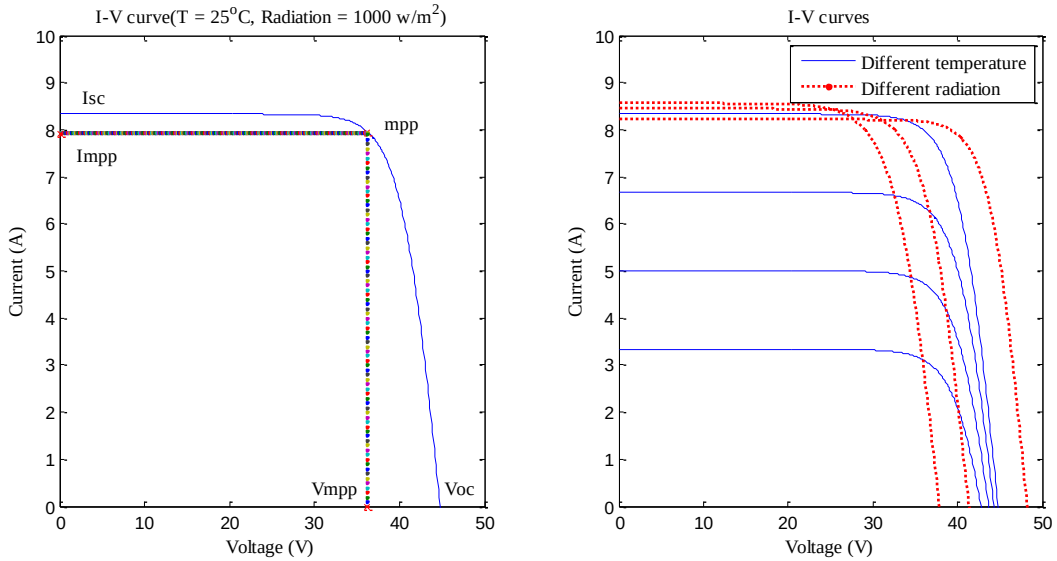

Fig. 3.6 PV panel output curves

Under solar radiation SR and temperature T, the maximum output power is calculated as:

$$P_{mp}^{T,SR} = I_{sc}^{T,SR} V_{oc}^{T,SR} ff \tag{3.20}$$

where $I_{sc}^{T,SR}$ and $V_{oc}^{T,SR}$ are the short circuit current and open circuit voltage respectively of the PV panel. The calculation procedures are described in [116], and the fill factor *ff* measures the ratio of the maximum power P_{mp} to the product of $I_{sc}^{T,SR}$ and $V_{oc}^{T,SR}$ is assumed to be a constant.

For PV panels with different electrical characteristics, the power output can be

calculated using the above process. For PV arrays that consist of many PV panels, the power output can thus be obtained by integrating the individual output of each PV panel.

3.3 Market Behavior of Wind Power

The existing power markets are mostly designed for conventional generations which are dispatchable. The day-ahead market and intra-hour market are cleared one day or several hours earlier before delivery. With deep penetration level, the variation of wind power can be very large and requires more balancing reserves and other services to maintain the energy balance.

In the Nordic market, the wind power providers may be charged the imbalance costs for unpredicted power variations through participating market operation [52, 53]. There are ways in which wind power owners can trade their generation. First is to take the balance responsibility themselves and pay the imbalance cost. Second is to trade wind power and sign contracts with balance providers to meet the mismatches. Third is to trade all the wind power through the balance responsible players [44]. In the second and third methods, the wind power owners pay a contract imbalance price which is usually lower than the market price. In California, the wind power receives extra-market treatment by receiving favorable feed-in tariffs and compulsory grid access [57]. The *Participating Intermittent Resources Program* (PIRP) legislation requires the system operators to accept all the wind power with contractual constraints [57]. The system takes all the wind power which is treated as negative load and the load serving entity is responsible for balancing the unpredicted wind power. In the United Kingdom, on the other hand, the large wind power providers are forced to participate in market operation and subject to penalty for mismatches from the contract power output [117].

The objective of the wind power traders is to optimize their revenue in the market.

Since wind power is perceived as the price taker in existing power markets, wind power traders can improve the accuracy of wind power forecast and minimize the imbalance cost. The bidding strategies of wind power in market operation have been the subject of much research [52, 53, 57, 118-120]. A bidding strategy with the objective to minimize imbalance cost was developed in [53] which performed better than bidding the forecast wind power in the Nordic power market. An explicit formula for optimal contract offerings was derived from the stochastic wind power generation model for the designed perfectly competitive market [57]. A generic methodology was developed considering wind forecast errors in the form of predictive distributions to design optimal participation strategies for wind power [118]. Different market strategies have been evaluated in [119] for competitive power markets including wind power. The market clearing prices with and without wind power were examined to optimize the total system benefits.

The bidding strategies of wind traders are associated with the market operation rules and penalty schemes for uncertainty. The behavior of wind power traders not only impacts the energy balance of the system, but also impacts the reliability operation due to bidding mismatch. The penalty scheme is designed to force the wind power producers to make more accurate power forecast and bid with fewer variations. However with high penetration, the bidding errors are unavoidable and their impacts on the economic and reliable operation of power market should be investigated and evaluated.

3.4 Conclusions

Renewable energy conversion systems and wind powers' participation in power market operation are introduced in this chapter. The random variation and intermittent characteristics of renewable energy have been investigated using the Auto-Regressive and Moving Average model. The models can be utilized in evaluating the benefits and risks of integrating renewable energy into power system and market operations.

Chapter 4 Impacts of Contingency Reserve on Energy Market

Reserves are important ancillary services in deregulated power systems for maintaining economic and reliable system operation. Variations of renewable energy affect the energy balance, which then needs to be balanced by reserves. The impacts and benefits of reserve on energy price and reliability need to be investigated to examine the impacts of renewable energy on power market operation.

In conventional power systems, reserves are procured by system operators for control zones or the entire system. The deregulation of power systems allows customers to participate in power market operation. In deregulated power systems, nodal price and nodal reliability are adopted to represent locational operation cost and reliability performance. Since contingency reserve (CR) plays an important role in reliable operation, the CR commitment should be considered in operational reliability analysis. In this chapter, a CR model based on customer reliability requirements has been formulated and integrated into power market settlement. A two-step market clearing process has been proposed to determine generation and CR allocation. Customers' nodal unit commitment risk (NUCR) and nodal energy interruption (NEI) have been evaluated through contingency analysis. Customers' reliability cost including reserve service cost and energy interruption cost have also been evaluated.

4.1 Introduction

In deregulated power systems, competition has been introduced to reduce operation cost and provide choices for participants to optimize their benefits [2]. Considering transmission cost, nodal price or locational marginal price has been adopted to charge customers in different locations in existing power systems like PJM [11].

Operating reserve is an important aspect of system reliable operation. The NERC

defines CR as the reserve to ensure the reliable operation of an interconnected power system when transmission or generation failures occur [121]. All committed reserves that can take up load in required time can be categorized as CR. Power markets like PJM and CASIO also include contingency reserve requirements in system operation process [122, 123]. Therefore CR should be considered in the operational reliability analysis in deregulated power systems.

Customer participation is also an important aspect of power system deregulation. In power market operation, customers can have different reliability levels based on their willingness to pay for CR to avoid being curtailed in contingency states. Some customers may be willing to be interrupted when facing the high CR cost while others need non-interruptible energy supply. Due to customer reliability selections and transmission constraints, nodal reliability thus is adopted to reflect customers' reliability performance at the load point in deregulated power system [66, 124, 125].

The integrated reserve and energy markets have been examined in many papers [77, 78, 126, 127]. The uniform security price scheme was proposed in [126] for different types of reserves, and customers provide interruptible services in the reserve market. An augmented optimal power flow (OPF) method has been adopted to determine the locational marginal pricing of energy and reserve [79]. However, only one energy price can be obtained at each node using the OPF method since there is only one energy balance equation at each node [126]. Therefore only energy can be charged by the nodal price while reserve should be charged separately. Different market types were analyzed in [77]. For most of the previous energy and reserve integrated markets, the reserve is cleared based on providers' bids and system or control zone total reserve requirement [78, 127] but individual customer reserve requirements are not explicitly considered. In deregulated power systems, it is important to provide more choices in the reserve market to improve nodal reliability and nodal prices. A new market clearing process therefore needs to be designed to achieve this goal. The reserve cost includes the capacity cost or availability cost, the opportunity cost and the energy cost

if delivered [77]. To charge the CR service considering its provision and utilization, capacity price plus the energy price scheme is adopted in this research. In the normal state, customers pay the capacity cost for CR purchased. In a contingency state where there is sufficient CR, the nodal price difference between the contingency state and the normal state reflects the cost for using reserve at the node. In this case, customers' reserve energy cost is calculated as the product of its load level in the normal state and the nodal price difference. In a contingency state where there is insufficient CR, customers pay interruption costs. Customers' reliability cost therefore includes reserve capacity cost, reserve energy cost, and the interruption cost.

Operational reliability performances of customers include the energy losses and the associated frequency or probability. The unit commitment risk (*UCR*) used by PJM is the most widely accepted index in evaluating the probability of energy losses [26, 63]. In order to consider the impacts of different reliability requirements from customers and network constraints to CR deliverability on the customer reliability, two nodal reliability indices are proposed in this thesis. The nodal UCR (*NUCR*) is used to evaluate the probability of energy interruption of customers at a node. The nodal energy interruption (*NEI*) is used to evaluate the energy loss of customers at a node.

This chapter proposes a method to investigate the impact of CR on customers' reliability benefit and cost. A two-step CR and energy integrated market clearing process is proposed to allocate CR and energy considering customers' reserve requirements. The expected nodal reliability and nodal reliability cost under the allocated CR are evaluated through contingency analysis. Two test systems were analyzed to illustrate the proposed method.

Nomenclature

0	Normal state index (Superscript)
j	Contingency state index (Superscript)
i, k	Bus index (Subscript)
g	Generator index (Subscript)
d	Load sector index (Subscript)
e	Energy index (Subscript)
r	Reserve index (Subscript)
N	Set of buses
N_g	Set of generator buses
N_d	Set of load buses
NG_i	Set of generators
NL_i	Set of load sectors
NOS	Set of all contingency states
NSN_i	Set of contingency states with no load curtailment
NSC_i	Set of contingency states with load curtailment
$P_{ig}^{\min}$	Minimum real power output of unit g
$P_{ig}^{\max}$	Maximum real power output of unit g
$P_{id(e)}^{\min}$	Minimum load level of load sector d
$Q_{ig}^{\min}$	Minimum reactive power output of unit g
$Q_{ig}^{\max}$	Maximum reactive power output of unit g
P_{ig}^{ramp}	Ramp limit of unit g
$\lvert V_i \rvert^{\min}$	Lower limit of voltage at bus i
$\lvert V_i \rvert^{\max}$	Upper limit of voltage at bus i

$\lvert S_{ik} \rvert^{\max}$	Limit of line apparent power from bus *i* to *k*
$P_{id(e)}^{0}$	Real power of load sector *d* at normal state
Q_{id}^{0}	Reactive power of load sector *d* at normal state
C_{ig}	Generation cost function for generator *g*
C_{id}	Customer cost function for customer sector *d*
$P_{ig(r)}^{bid}$	Real power of CR bid by generator *g*
$\rho_{ig(r)}$	Bidding price of CR by generator *g*
$P_{id(r)}^{req}$	Real power of CR requirement of customer *d*
$P_{ig(e)}$	Real power output of generator *g*
Q_{ig}	Reactive power output of generator *g*
$P_{ig(r)}^{0}$	Real power of CR allocation of unit *g*
$P_{id(e)}^{j}$	Real power of load sector *d* at contingency state *j*
Q_{id}^{j}	Reactive power of load sector *d* at contingency state *j*
P_{i}	Real injection power at node *i*
$V_i = \lvert V_i \rvert \angle \theta_i$	Bus voltage at bus *i*
$Y_{ik} = \lvert Y_{ik} \rvert \angle \delta_{ik}$	Element of admittance matrix
$\lvert S_{ik} \rvert$	Magnitude of line apparent power from bus *i* to *k*

4.2 Contingency Reserve and Energy Market Model

The contingency reserve and energy integrated market clearing process is designed to meet customers' demand for reserve and energy with minimum cost.

4.2.1 Contingency reserve pricing scheme

Contingency reserve and its location play important roles in maintaining customer reliability. Generation suppliers only provide reserve under the condition that it can make more profit than bid all the available capacity into the energy market. Customer reserve requirements relate to their reliability requirement, characteristics of load, demand level and the reserve cost.

CR is only delivered when generation or transmission failure occur. In the normal operation state, CR is just capacity (not output) from the committed units. CR capacity price is a call-like option on the energy that is generated by the reserve capacity in the future [74]. Customers purchase CR capacity to obtain the right to purchase CR energy in a contingency state.

In power markets like PJM, New York and New England, generators that provide reserves will receive availability or capacity cost and lost opportunity cost (LOC) [77]. Capacity cost refers to the payment the generator received for providing reserve capability. LOC refers to the revenue that generators lost in the energy market by preserving the reserve capacity. The coupling between energy and reserve is the marginal opportunity cost of dispatchable sources [128]. The designed energy and reserve market in [128] only considers the reserve price bid and not the capacity bid. It is up to the ISO to determine the capacity of cleared reserve and energy and the LOC. In this thesis, each provider is responsible for determining the proportion of energy and reserve they would like to provide by considering the LOC. Customers will bid CR based on their reliability requirements. As indicated in [77], spinning reserve generally will not generate LOC in such cases. The contingency reserve is modeled as spinning reserve in this thesis and should not generate LOC.

The CR capacity price is determined by clearing the CR bids from providers and CR offers from customers in the CR market. When a contingency occurs, the ISOs

dispatch energy from the CR units to meet the generation deficiency. In this case, the CR units which provide additional energy are also paid the energy price.

4.2.2 Market model

The procurement of reserve in most of the existing power markets is still mainly done by ISOs to maintain a uniform reliability level for secure and economic operation [77]. Reserve is procured zonally considering transmission limitations. A zonal price is applied to customers in the same reserve zone. Customers who have the higher load level share higher reserve capacity cost according to the load level proportional sharing method. However the CR allocation and prices are related to customers' reliability requirements and locations. In the proposed two-step market clearing process, energy market is cleared in the first step. Customers' reserve capacity requirements are incorporated in the second step to determine the CR allocation and CR capacity price. In this way, customers pay CR capacity cost according to their requirements.

The OPF method is adopted to model the two-step market clearing process. The objective is to minimize the total system cost while satisfying the energy and reserve requirement of customers. For each hour, generators bid into the market to supply energy and reserve. Customers bid into the market to purchase energy and reserve. It is assumed that each generator is responsible for determining the proportion of energy and CR bids to optimize their own benefits. The objective function is:

$$\min\ f^0 = \sum_{i \in N_g} \sum_{g \in NG_i} C_{ig} \left(P^0_{ig(e)} + P^0_{ig(r)} \right) \tag{4.1}$$

subject to the generation and transmission constraints:

$$\sum_{g \in NG_i} \left(P^0_{ig(e)} + P^0_{ig(r)} \right) - \sum_{d \in NL_i} \left(P^0_{id(e)} + P^{req}_{id(r)} \right) = \sum_{i=1}^{N} V_i^0 V_k^0 \left| Y^0_{ik} \right| \cos\left(\theta_i^0 - \theta_k^0 - \delta^0_{ik} \right) \tag{4.2}$$

$$\sum_{g \in NG_i} Q^0_{ig} - \sum_{d \in NL_i} Q^0_{id} = \sum_{i=1}^{N} V_i^0 V_k^0 \left| Y^0_{ik} \right| \sin\left(\theta_i^0 - \theta_k^0 - \delta^0_{ik} \right) \tag{4.3}$$

$$P_{ig}^{\min} \le P_{ig(e)}^{0} + P_{ig(r)}^{0} \le P_{ig}^{\max} - P_{ig(r)}^{bid} \tag{4.4}$$

$$0 \le P_{ig(r)}^{0} \le P_{ig}^{ramp} \tag{4.5}$$

$$0 \le P_{ig(r)}^{0} \le P_{ig(r)}^{bid} \tag{4.6}$$

$$Q_{ig}^{\min} \le Q_{ig}^{0} \le Q_{ig}^{\max} \tag{4.7}$$

$$\left|V_i\right|^{\min} \le \left|V_i^0\right| \le \left|V_i\right|^{\max} \tag{4.8}$$

$$\left|S_{ik}^{0}\right| \le \left|S_{ik}\right|^{\max} \tag{4.9}$$

Some constraints are only implemented for one step and should be set to zero if not used. In the first step, the generators are committed to supply load for the normal state. Customers' CR requirement $P_{id(r)}^{req}$ and the CR allocation $P_{ig(r)}^{0}$ are zero. The objective function is to minimize the energy cost. Equations (4.2) and (4.3) are the energy balance equations for supplying load $P_{id(e)}^{0}$ and Q_{id}^{0}. Equation (4.4) sets the generator energy output limits by excluding its CR bids $P_{ig(r)}^{bid}$ from the total capacity. Equations (4.5) and (4.6) are the reserve constraints and are not implemented. The Lagrangian function L_0 is formulated to solve the problems consisting of (4.1)-(4.4) and (4.7)-(4.9). The economic implication of the Lagrangian multipliers for energy balance constraint is marginal energy cost and therefore is the nodal price of supplying energy at each node. The output of unit ig $\left(P_{ig(e)}^{0}, Q_{ig(e)}^{0}\right)$ and the nodal price ρ_i^0 in normal state are determined.

$$\rho_i^0 = \frac{\partial L_0}{\partial P_i^0} \quad (\$ / MWh) \tag{4.10}$$

In the second step, the augmented OPF problem is formulated to allocate reserve. The CR bid $P_{ig(r)}^{bid}$ in generation constraint Equation (4.4) is set to zero. The objective function is to minimize the total energy cost considering the delivery of CR. Equation (4.2) is the energy balance constraint for supplying the augmented load ($P_{id(e)}^{0} + P_{id(r)}^{req}$). Equation (4.4) is generator's output limit considering its CR allocation. Equations (4.5)

and (4.6) ensure that each generator's CR allocation is within the limit of its ramp rate and bidding. Optimal CR allocation $P_{ig(r)}^{0}$ for each unit is determined by solving the augmented OPF problem using Equations (4.1)-(4.9). In this way, the deliverability of CR can be ensured to satisfy customers' CR requirement both physically and economically.

The accepted CR bids $\left(P_{ig(r)}^{0}, \rho_{ig(r)}\right)$ in step 2 are then arranged in an ascending order by prices. The CR capacity price ρ_r $\left(\$/MW/\mathrm{h}\right)$ is determined by the price of the last accepted bid. Customers pay according to ρ_r and share the total CR capacity cost proportionally by their CR requirement or by their reliability improvement, as discussed in Section 4.3.

4.3 Reliability Modeling

Under normal operation, customers' CR requirements are considered in the CR allocation. The delivery of CR in a contingency state should consider customers' reserve energy preferences, and it is also constrained by the physical limitations of the system. In this section, reliability risks for customers at each node are evaluated for each contingency state.

In system operation, repair can be neglected for a short operating period. The outage rates of units and transmission lines are the main concern. The outage replacement rate (*ORR*) of a component is defined as the probability that the component fails and cannot be replaced during operating period *T* which is referred to as the lead time [63]. The ORR_i for component *i* with failure rate λ_i is calculated as:

$$ORR_i = 1 - e^{-\lambda_i T} \approx \lambda_i T \left(if\ \lambda_i T << 1\right) \tag{4.11}$$

The probability A_i that the component is operating during lead time *T* is calculated as $A_i = 1 - ORR_i$. For a system with many components, the probability p^j of state *j* with

m_t operating components and s failed components is determined in Equation (4.12). Both generating units and transmission lines are considered in determining the system states.

$$p^j = \prod_{i=1}^{s} ORR_i \times \prod_{i=s+1}^{m_t} A_i \tag{4.12}$$

4.3.1 Customer cost

Customers purchase CR to avoid interruption under contingency states as explained in Section 4.2. However, purchase of CR capacity only entitles customers the right to purchase energy provided by CR in the contingency states. In a contingency state, the delivery of energy generated by CR is affected by the deliverability of the transmission system, contingency characteristics, and energy prices. If the energy price is very high, customers may choose to be interrupted. If energy cannot be delivered due to transmission constraints or if the CR unit fails to provide energy, customers may also be interrupted. Customers therefore need to know the market clearing information in contingency states, as well as their reliability performances to evaluate their reserve choices.

Energy interruption for a customer may or may not occur in a contingency state. Customer faces the interruption cost and the reliability energy cost respectively for the two cases. Reserve energy cost is ex post cost since it depends on the spot energy price. The reserve capacity cost and the reserve energy cost are categorized as reserve service cost.

Customer interruption cost in system operation depends on the load curtailment and duration of an interruption. Customers consume additional energy provided by CR to improve their reliability performance and reduce the interruption cost. Thus customer's reserve preference can be reflected indirectly by the load interruption cost. Customer damage functions $CDF_{id}\left(D^j\right)$ are used to evaluate the interruption cost of

different customers according to the duration of the outage [66, 125]. Customer cost function C_{id} is calculated as:

$$C_{id}\left(\Delta P_{id}^{j}\right)=\Delta P_{id}^{j}\times CDF_{id}\left(D^{j}\right) \tag{4.13}$$

where D^j is outage duration which equals system lead time T. $\Delta P_{id}^{j}=P_{id(e)}^{j}-P_{id(e)}^{0}$ is the load curtailment at contingency state j. It is assumed that the load curtailment at state j without reserve is $\Delta\hat{P}_{id}^{j}$. It is not necessary that $\Delta\hat{P}_{id}^{j}-\Delta P_{id}^{j}=P_{id(r)}^{req}$ since reserve delivery is also constrained by units availability and transmission cost in different contingency states.

4.3.2 Contingency formulation

In contingency state j, reserve is dispatched to meet the energy deficiency considering customers' reserve energy preferences. The objective function of the OPF problem for determining the CR utilization is as follows:

$$\min\ f^{j}=\sum_{i\in N_g}\sum_{g\in NG_i}C_{ig}\left(P_{ig(e)}^{j}\right)+\sum_{i\in N_d}\sum_{d\in NL_i}C_{id}\left(\Delta P_{id}^{j}\right) \tag{4.14}$$

subject to the generation and transmission constraints:

$$\sum_{g\in NG_i}P_{ig(e)}^{j}-\sum_{d\in NL_i}P_{id(e)}^{j}=\sum_{i=1}^{N}V_i^{j}V_k^{j}\left|Y_{ik}^{j}\right|\cos\left(\theta_i^{j}-\theta_k^{j}-\delta_{ik}^{j}\right) \tag{4.15}$$

$$\sum_{g\in NG_i}Q_{ig(e)}^{j}-\sum_{d\in NL_i}Q_{id(e)}^{j}=\sum_{i=1}^{N}V_i^{j}V_k^{j}\left|Y_{ik}^{j}\right|\sin\left(\theta_i^{j}-\theta_k^{j}-\delta_{ik}^{j}\right) \tag{4.16}$$

$$P_{ig(e)}^{0}-P_{ig}^{ramp}\le P_{ig(e)}^{j}\le P_{ig(e)}^{0}+P_{ig(r)}^{0} \tag{4.17}$$

$$Q_{ig}^{\min}\le Q_{ig(e)}^{j}\le Q_{ig}^{\max} \tag{4.18}$$

$$P_{id(e)}^{\min}\le P_{id(e)}^{j}\le P_{id(e)}^{0} \tag{4.19}$$

$$\left|V_i\right|^{\min}\le\left|V_i^{j}\right|\le\left|V_i\right|^{\max} \tag{4.20}$$

$$\left|S_{ik}^{j}\right|\le\left|S_{ik}\right|^{\max} \tag{4.21}$$

From Equation (4.17), each generating unit provides additional energy according to

its reserve allocation. The Lagrangian function L_j is formulated to solve the problems from Equations (4.14)-(4.21). The nodal price is determined using Equation (4.22).

$$\rho_i^j = \frac{\partial L_j}{\partial P_i^j} \quad (\$/MWh) \tag{4.22}$$

The generation units' outputs and load curtailment are then determined. The generation and reserve providers are paid nodal prices for supplying energy. The customers pay the nodal prices. The reserve provided by generator *ig* is $P_{ig(r)}^j = P_{ig(e)}^j - P_{ig(e)}^0$. From the OPF problem for each contingency state, the load level at contingency state $P_{id(e)}^j$ and load curtailment ΔP_{id}^j are results of the optimal schedule of available generations. A Customer may maintain its load level (ΔP_{id}^j =0) in a contingency state due to the CR utilized. The nodal prices increase since additional energy needs to be procured from high cost CR units, and the difference between the nodal price in state *j* and the normal state reflects the reserve energy cost. If load curtailment occurs (ΔP_{id}^j >0), the *NEI* and the nodal interruption cost are calculated. Reserve that customers at a certain node can obtain depends on the energy price and availability of CR, and it cannot be obtained directly from the solution. Customers' benefit from CR is evaluated in Section 4.4 through their reliability and price improvement.

4.3.3 Nodal price and nodal reliability risks

After obtaining results from the normal state and contingency state analysis, the nodal prices and nodal reliability risks of customers are evaluated.

The expected nodal price $\overline{\rho}_i$ and standard deviation of nodal price σ_i at node *i* are calculated using Equations (4.23) and (4.24) respectively:

$$\overline{\rho}_i = p^0 \rho_i^0 + \sum_{j \in NOS} p^j \rho_i^j \tag{4.23}$$

$$\sigma_i = \sqrt{p^0\left(\rho_i^0 - \overline{\rho}_i\right)^2 + \sum_{j \in NOS} p^j\left(\rho_i^j - \overline{\rho}_i\right)^2} \tag{4.24}$$

where p^0 is the probability of the normal state.

The nodal unit commitment risk (*NUCR*) at node *i* is evaluated using Equation (4.25). The *NUCR* is defined as the sum of the probabilities of states where demand is not satisfied: $\sum_{j \in NOS} p^j(\sum_{d \in NL_i} \Delta P_{id}^j > 0)$ and sum of probability of states where demand is just satisfied (reserve margin is zero): $\sum_{j \in NOS} p^j(\sum_{d \in NL_i} \Delta P_{id}^j = 0 \bigcap (P_{ig(e)}^j = P_{ig}^{\max}(\forall g)))$ during the system's lead time which is the period that generation cannot be replaced.

$$NUCR_i = \sum_{j \in NOS} p^j(\sum_{d \in NL_i} \Delta P_{id}^j > 0) \bigcup \sum_{j \in NOS} p^j(\sum_{d \in NL_i} \Delta P_{id}^j = 0 \bigcap (P_{ig(e)}^j = P_{ig}^{\max}(\forall g))) \tag{4.25}$$

For a contingency state where customers face load curtailment, the nodal energy interruption NEI_i^j is calculated as:

$$NEI_i^j = T \sum_{d \in NL_i} \Delta P_{id}^j \tag{4.26}$$

The nodal reserve capacity cost ($NRCC_i$), which is shared proportionally according to customers' CR requirement is:

$$NRCC_i = \frac{\sum_{d \in NL_i} P_{id(r)}^{req}}{\sum_{i \in N_d} \sum_{d \in NL_i} P_{id(r)}^{req}} \left(\rho_r \sum_{i \in N_g} \sum_{g \in NG_i} P_{ig(r)}^0 \right) (\$/h) \tag{4.27}$$

Reliability performance at some nodes cannot be improved by committing more reserve due to physical constraints. In such a case, customers at different load nodes share the CR capacity cost $NRCC_i'$ proportionally according to their reliability improvement.

$$NRCC_i' = \frac{\Delta NUCR_i}{\sum_{i \in N_d} \Delta NUCR_i} \left(\rho_r \sum_{i \in N_g} \sum_{g \in NG_i} P_{ig(r)}^0 \right) (\$/h) \tag{4.28}$$

where $\Delta NUCR_i$ is the percentage $NUCR_i$ reduction compared with the case without CR.

Expected nodal reserve energy cost ($ENREC_i$) and expected interruption cost $ENIC_i$ at node *i* are calculated as:

$$ENREC_i = \sum_{j \in NSN_i} \sum_{d \in NL_i} p^j P_{id}^0 \left(\rho_i^j - \rho_i^0 \right) \quad (\$/h) \tag{4.29}$$

$$ENIC_i = \sum_{j \in NSC_i} \sum_{d \in NL_i} p^j C_{id} \left(\Delta P_{id}^j \right) (\$/h) \tag{4.30}$$

4.4 Case Studies

The RBTS [98] and RTS [129] were used to illustrate the proposed method. The RBTS was modified by adding an identical parallel transmission line between bus 5 and bus 6. The peak load levels are used for the two systems in the analysis. Customers at each node are assumed to be comprised of same types of load and have the same priority for load curtailment. The system lead time is 1 hour and corresponding CDFs are 0.163, 2.990, 2.951, 0.295, 0.243 ($/kWh) for large users, industrial, commercial, agriculture and residential customers respectively [98]. The contingency states of up to second order failures were considered in the analysis.

4.4.1 RBTS Studies

The modified RBTS was studied using the proposed method. Fig. 4.1 shows the single line diagram of the modified RBTS. Customers' different CR requirements, generators' CR biddings and the resulting nodal price and nodal reliability risk indices have been analyzed and presented in this sub-section.

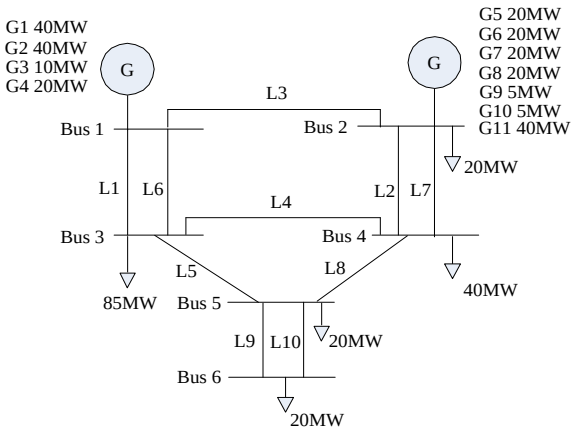

Fig. 4.1 Single line diagram of the modified RBTS

Two sets of customers' CR requirements denoted as CR 1 and CR 2 were evaluated and are shown in Table 4.1. In both cases, customers at node 6 have the highest CR requirement and customers at nodes 2 and 3 have the lowest.

Table 4.1 Customer CR requirement for the RBTS

Load Node	CR 1 (MW)	CR 2 (MW)
2	2	0
3	2	0
4	3	8
5	3	8
6	10	20

Assume that four CR biddings $\left(P_{ig(r)}^{bid}, \rho_{ig(r)}\right)$ from generators are submitted as shown in Table 4.2. The four bidding units are all high cost units. The nodal prices are mainly determined by the marginal cost of the marginal units [130]. If the low cost units are scheduled to provide CR, the high cost units will need to operate at their lower limits. The low cost units become the marginal units and the nodal price will be smaller than the marginal cost of high cost units. The nodal prices in the contingency states will then probably be lower than those under normal states except for the price spikes. Thus the high cost units are not willing to supply energy or reserve. The reserve bidding prices are usually very low and sometimes equal 0, because reserve

providers can also receive energy payment once the reserve is delivered.

Table 4.2 Generator Reserve bids

Generator	Quantity(MW)	Price($/MW/h)
1	15	0.7
2	15	0.7
3	4	1
4	6	1

The cleared CR bids $\left(P_{ig(r)}^{0}, \rho_{ig(r)}\right)$ for CR 1 and CR 2 are shown in Table 4.3 The reserve allocation for CR 2 was also investigated using the reserve capacity cost minimization (CCM) method designated as CR 2'. Without considering transmission limit, CCM allocates reserve from the cheapest bid to the most expensive bid according to the total system reserve requirement. The CR clearing prices determined from the last accepted bid are 1 $/MW/h for the three cases. The sum of reserve allocation for CR 2 is greater than that for CR 2' because the proposed reserve allocation method considers transmission losses for delivering reserve.

Table 4.3 CR allocation

Generator	CR 1 (MW)	CR 2 (MW)	CR 2'(MW)
1	5.80	13.88	15
2	5.80	13.88	15
3	4.00	4.00	4
4	5.06	6.00	2

Nodal prices without CR (W/O CR) and for the three different CR allocations were studied. Table 4.4 shows the nodal prices of normal state ρ_i^0 . ρ_i^0 with CRs are higher than those without CR. ρ_i^0 are the same for the three CRs since the generation capacity available for supplying normal state load are the same considering the reserve bids.

Table 4.4 Nodal price ρ_i^0 ($/MWh) for the normal state for the RBTS

Node	W/O CR	CR 1	CR 2	CR2’
1	14.086	14.406	14.406	14.406
2	13.297	13.599	13.599	13.599
3	14.510	14.840	14.840	14.840
4	14.454	14.782	14.782	14.782
5	14.609	14.941	14.941	14.941
6	14.673	15.007	15.007	15.007

Tables 4.5 and 4.6 show the expected nodal prices and standard deviation of nodal price respectively. Compared with the expected nodal prices without CR, $\overline{\rho}_i$ decreases for CR 1 and CR 2. σ_i for CR 1 and CR 2 show the same trends. The reason is that CR can reduce the prices spikes of some contingency states. $\overline{\rho}_i$ and σ_i for CR 2 are less than those for CR 2’. Therefore the proposed reserve allocation method performs better than the CCM method in improving the nodal price performances.

Table 4.5 Expected Nodal price $\overline{\rho}_i$ ($/MWh) for the RBTS

Node	W/O CR	CR 1	CR 2	CR2’
1	17.749	15.386	14.607	15.376
2	16.749	14.609	13.875	14.601
3	18.319	16.016	15.216	16.007
4	18.245	15.938	15.142	15.930
5	18.439	16.116	15.313	16.110
6	18.517	16.186	15.380	16.180

Table 4.6 Standard deviations of nodal price σ_i ($/MWh) for the RBTS

Node	W/O CR	CR1	CR 2	CR2’
1	534.405	225.887	130.488	164.178
2	505.779	245.399	157.515	186.993
3	577.088	316.266	222.718	252.796
4	571.232	306.944	213.341	243.624
5	580.157	315.091	220.942	251.426
6	582.653	316.705	222.305	252.895

Fig. 4.2 shows nodal unit commitment risks for five load nodes. $NUCR_2$ for each case is zero because node 2 is the generating node. With CR 1, $NUCR_4$ slightly decreases and $NUCR_3$, $NUCR_5$ and $NUCR_6$ also decrease. With CR 2, *NUCR* of all nodes decrease significantly. The reason is that CR can reduce the number of states with the load curtailment. Although the reserve requirement is the same, the improvement of $NUCR_4$, $NUCR_5$ and $NUCR_6$ for CR 2 is greater than those for CR 2'. The proposed reserve allocation method performs better than the CCM method in improving the nodal reliability according to customers' requirement.

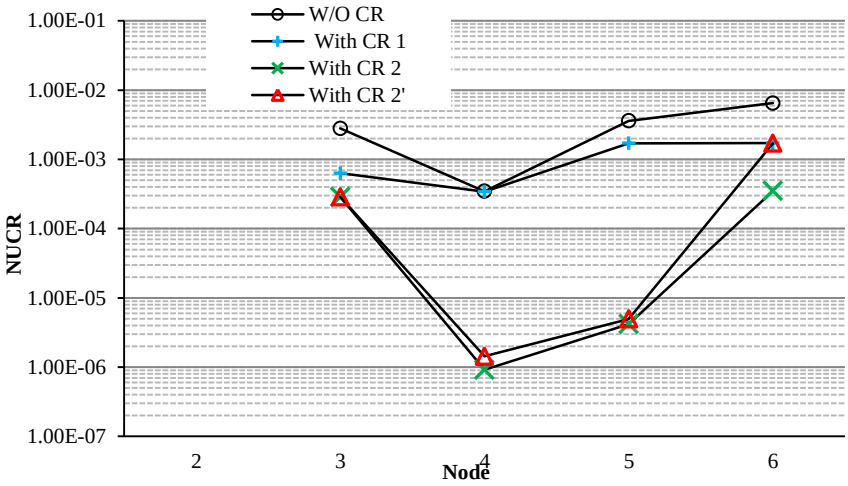

Fig. 4.2 *NUCR* for different CR allocation for the RBTS

Table 4.7 shows the percentages of *NUCR* reduction compared with the case without CR. For CR 1, $\Delta NUCR_6$ is slightly smaller than $\Delta NUCR_3$ although customers at node 6 purchase more CR than customers at node 3. For CR 2, customers located at nodes 4, 5 and 6 have greater reliability improvement than customers at node 3. It can be seen from the results that the reliability improvement is not proportional with the CR requirement because of transmission line limit. While customers at some nodes can greatly improve their reliability performance by purchasing small amount of reserve, customers at other nodes need to purchase more reserve to attain equivalent improvement.

Table 4.7 Percentage NUCR reduction $\Delta NUCR_i$ (%) for the RBTS

Node	With CR 1	With CR 2
2	0	0
3	77.47	89.74
4	1.03	99.74
5	52.45	99.88
6	73.60	94.61

For some states the *NUCR* may not decrease with the CR, but the energy interruption may be reduced for customers. Fig. 4.3 and 4.4 show the nodal energy interruption *(NEI)* for the representative outage states at nodes 3 and 6 respectively. NEI_3^j with CR 1 and CR 2 becomes 0 for most contingency states such as G2 and G10. For some states such as G1G11 NEI_3^j is reduced. For states such as state G2G3 and L2L3, NEI_3^j decrease more for CR 2 compared with that for CR 1. Similar conditions are seen at node 6. NEI_3^j for state L1G9 increase while NEI_6^j decreases to 0. This is because customers at node 6 have the priority of consuming CR.

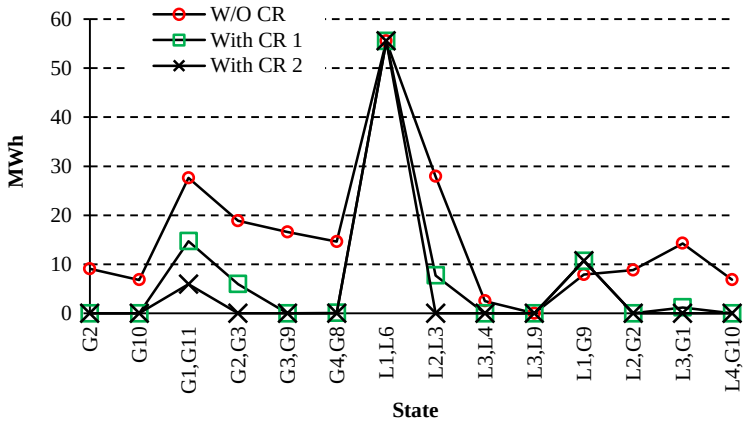

Fig. 4.3 NEI at node 3 for different contingency states for the RBTS

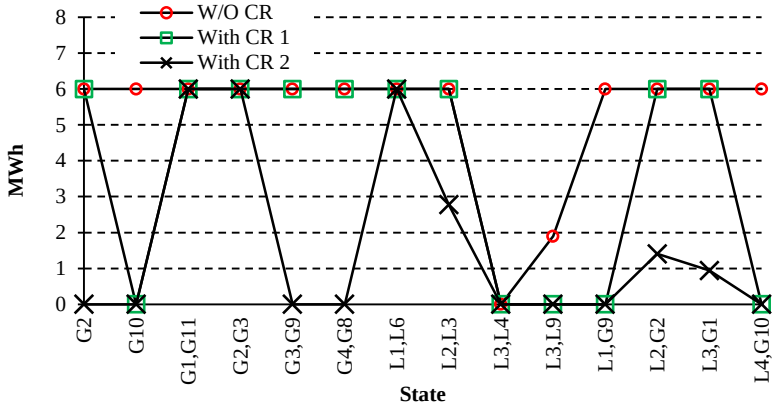

Fig. 4.4 *NEI* at node 6 for different contingency states for the RBTS

Table 4.8 shows the reserve capacity cost. For the reserve capacity cost shared proportionally according to the CR requirement ($NRCC_i$), customers at node 6 are charged the highest. However customers at other nodes also have comparable reliability improvement according to the nodal unit commitment risk analysis. When the reserve capacity cost is shared proportionally according to the reliability improvement ($NRCC_i$'), customers who have the greatest $\Delta NUCR_i$ are charged the highest. $NUCC_2$' equals 0 because reliability performance of customers at node 2 is not improved.

Table 4.8 Comparison of NRCC and NRCC' for the RBTS

Node	$NRCC_i$($/h)		$NRCC_i$'($/h)	
	With CR 1	With CR 2	With CR 1	With CR 2
2	2.066	0	0	0
3	2.066	0	7.825	8.825
4	3. 100	8.391	0.104	9.808
5	3.100	8.391	5.297	9.822
6	10.330	20.977	7.434	9.304

Tables 4.9 and 4.10 show *ENIC* and *ENREC* respectively. While customers' reliability performances are improved with CRs, customers have less energy interruption and *ENIC* decreases, but more CR energy is used and *ENREC* increases. The customer interruption cost is very high without CR. Since CR 2 performs better in improving nodal reliability, *ENIC* for CR 2 is less than that for CR 2'. *ENREC* is greater for CR

2 than that for CR 2'.

Table 4.9 $ENIC_i$ ($/h) for the RBTS

Node	W/O CR	CR 1	CR 2	CR 2'
2	0	0	0	0
3	8.141	0.514	0.077	0.079
4	0.366	0.134	0.001	0.002
5	5.321	1.294	0.006	0.007
6	8.146	3.034	0.074	1.000

Table 4.10 $ENREC_i$ ($/h) for the RBTS

Node	W/O CR	CR 1	CR 2	CR 2'
2	0	0.021	0.088	0.026
3	0	0.037	0.309	0.059
4	0	0.050	0.189	0.061
5	0	0.026	0.096	0.032
6	0	0.027	0.097	0.032

4.4.2 RTS Studies

The market clearing process and reliability analysis were also conducted using the IEEE-RTS. Representative results are presented to show the performance of the proposed method.

Two sets of reserve requirement denoted as CR 1R and CR 2R were examined and are shown in Table 4.11.

Table 4.11 Customer CR requirement for the RTS

Load Node	CR 1R (MW)	CR 2R (MW)
1	20	20
2	20	20
3	20	20
4	20	20
5	20	20
6	20	20
7	20	20
8	0	0
9	0	0
10	0	0
13	0	0
14	30	50
15	30	50
16	30	50
18	30	50
19	30	50
20	30	50

Assume that ten CR biddings $\left(P_{ig(r)}^{bid}, \rho_{ig(r)}\right)$ from generators are submitted. Bid 1 to Bid 3 from three 100MW generators at bus 7 are the same as (28 MW, 0.5$/MW/h). Bid 4 to Bid 6 from three 197MW generators at bus 13 are the same as (110 MW, 0.7$/MW/h). Bid 7 to Bid 10 from four 12MW generators at bus 15 are the same as (8MW, 0.8$/MW/h). The accepted CR bids $\left(P_{ig(r)}^{0}, \rho_{ig(r)}\right)$ for CR 1R are (12.73 MW, 0.5$/MW/h) for Bid 1 to Bid 3 respectively and (93.5 MW, 0.7$/MW/h) for Bid 4 to Bid 6 respectively. The CR clearing price is 0.7 $/MW/h. The accepted CR bids for CR 2R are (28 MW, 0.5$/MW/h) for Bid 1 to Bid 3 respectively, (93.5 MW, 0.7$/MW/h) for Bid 4 to Bid 6 respectively and (4.8 MW, 0.8$/MW/h) for Bid 7 to Bid 10 respectively. The CR clearing price is 0.8$/MW/h.

Expected nodal prices $\overline{\rho}_i$ and standard deviation of nodal prices σ_i are shown in Table 4.12. Like RBTS cases, $\overline{\rho}_i$ and σ_i all decrease as the CR requirement

increases. Without CR, $\overline{\rho}_i$ is nearly four times as that for CR 2R. After customers increase their CR requirement, $\overline{\rho}_i$ at nodes 14-20 decrease more than at nodes 1-7.

The nodal prices at node 18 for the representative system states are shown in Fig. 4.5. State 0 is the normal state. States 1- 19 and 20-44 are generator and transmission line outage states respectively. Without CR, nodal price spikes occur for all the generator outage states and some of the transmission line outage states. The CR can provide additional energy and reduce nodal prices. For states 12-15, the nodal price spikes decrease for CR 1R and decrease to normal level for CR 2R. For states 43-44, the nodal price spikes cannot be eliminated because of transmission constraints to the deliverability of CR.

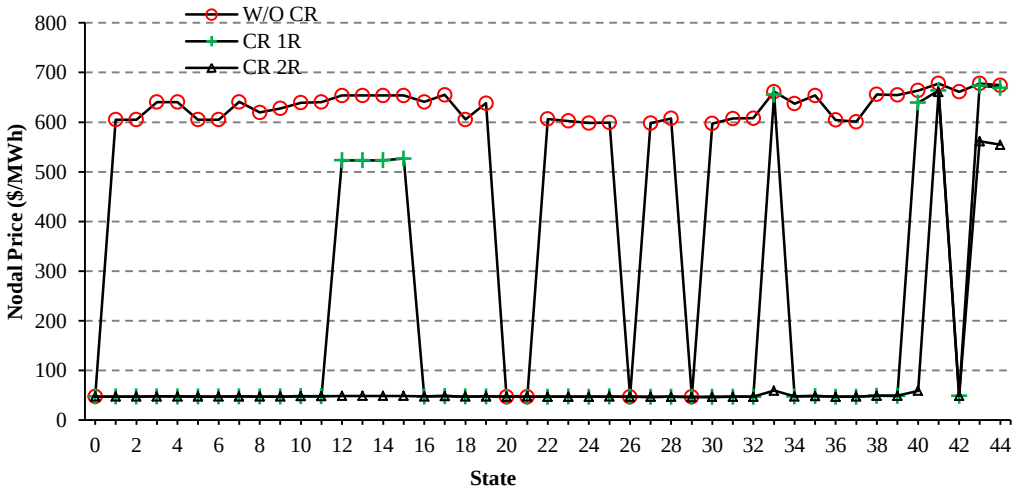

Fig. 4.5 Nodal prices of node 18 of RTS at representative contingency states

Table 4.12 Expected Nodal price $\overline{\rho}_i$ and corresponding standard deviation σ_i for the RTS

Node	$\overline{\rho}_i$ ($/MWh)			σ_i ($/MWh)		
	W/O CR	CR 1R	CR 2R	W/O CR	CR 1R	CR2R
1	238.3	65.57	60.31	5790	574.9	486.3
2	238.7	65.81	60.51	5810	583.7	494.0
3	240.4	65.96	60.29	5912	615.7	566.8
4	241.3	65.30	60.44	5831	522.9	444.2
5	238.6	64.01	59.42	5708	477.1	396.4
6	259.7	73.46	67.03	7962	551.5	459.7
7	216.0	48.25	48.16	5056	198.9	189.6
8	225.3	52.89	51.62	5277	106.3	84.34
9	238.3	64.44	59.68	5784	519.3	462.6
10	235.0	62.28	58.14	5579	424.3	364.3
11	243.2	67.46	61.96	5985	623.9	555.1
12	242.1	67.30	61.90	5946	620.4	549.1
13	241.5	68.12	62.32	5963	679.8	617.0
14	243.5	68.59	62.66	6061	693.0	647.3
15	234.8	66.41	60.63	5776	682.0	661.8
16	235.6	66.65	60.85	5811	685.1	666.2
17	230.8	65.44	59.73	5668	678.0	654.6
18	229.4	65.08	59.41	5625	675.9	658.0
19	236.9	67.14	61.31	5877	690.8	655.5
20	236.1	66.99	61.11	5863	696.1	646.3
21	228.5	64.83	59.18	5604	673.0	654.3
22	222.5	63.15	57.65	5453	658.6	640.4
23	234.9	66.70	60.77	5836	699.7	649.5
24	241.6	67.66	61.60	5964	682.5	637.6

The *NUCR* are shown in Fig. 4.6 where the values not denoted are zeros. *NUCR* decrease after CR is committed. $NUCR_1$ and $NUCR_2$ are higher for CR 2R than for CR 1R. Since more CRs are required by customers at nodes 14 -20 for case CR 2R, CRs are allocated in a way that they can deliver more to these nodes. Customers at 1 and 2 therefore cannot get as much CR in CR 2R as CR 1R. Although customers at nodes 8-10 have no CR requirement, their *NUCR* also decreases since the system reserve margin is increased by other customers' CR requirement. Due to transmission system limitation and generating units' unreliability, the *NUCR* improvements are not proportional to customers' CR requirement, a conclusion also reached for the RBTS.

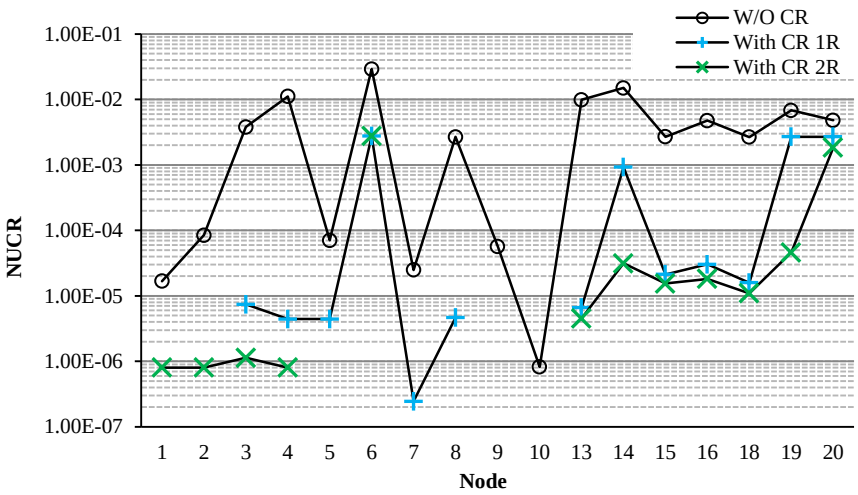

Fig. 4.6 *NUCR* for different CR allocation of the RTS

The *ENIC* and *ENREC* for the nodes are shown in Table 4.13. The *NRCC* is unrelated to the system size and therefore not shown. The *ENIC* is reduced because the CR reduces the price spikes during contingency states. Without CR the $ENIC_6$, $ENIC_{13}$, $ENIC_{14}$ and $ENIC_{19}$ are much higher. For case CR 2R, *ENIC* and *ENREC* both decrease compared with those for CR 1R.

Table 4.13 $ENIC_i$ and $ENREC_i$ for the *RTS*

Node	$ENIC_i$ ($/h)			$ENREC_i$ ($/h)		
	W/O CR	CR 1	CR 2	W/O CR	CR 1	CR 2
1	0.056	0	0.003	0	1.207	1.133
2	0.223	0	0.004	0	1.119	1.020
3	12.84	0.033	0.004	0	2.162	1.462
4	24.23	0.015	0.002	0	0.851	0.570
5	0.117	0.005	0	0	0.738	0.532
6	64.73	7.115	6.936	0	1.954	0.912
7	0.022	0	0	0	1.078	0.165
8	14.57	0.003	0	0	1.573	0.535
9	0.191	0	0	0	1.548	0.741
10	0.003	0	0	0	1.508	1.014
13	52.06	0.033	0.027	0	2.123	1.518
14	77.29	5.149	0.141	0	2.114	2.036
15	25.38	0.150	0.073	0	3.836	3.235
16	24.82	0.177	0.130	0	1.186	0.996
18	25.65	0.128	0.074	0	3.913	3.300
19	70.14	19.57	0.305	0	2.085	1.721
20	23.31	13.19	6.129	0	1.436	1.225

4.5 Conclusions

This chapter has examined the impacts of contingency reserve on nodal price and nodal reliability in deregulated power systems. A two-step clearing procedure has been developed to clear the energy market and to determine the reserve allocation according to customers' reserve requirement.

The customer reliability risks and nodal prices for two test systems have been evaluated. The results show that the proposed two-step market clearing process is effective in allocating CR to improve customers' reliability and prices. Under the market design, customers who have higher CR requirement can get higher reliability and price improvements. These improvements are also limited by the system topology which suggests that it is fairer to charge reserve cost according to customers' reliability improvement.

The proposed market clearing process provides a flexible way to optimize customers' reliability benefits through CR allocation in a deregulated power system. The results provide useful information for generation service providers and customers to optimize their benefits in the energy and reserve market.

Chapter 5 Impacts of Solar Power Penetration on Deregulated Power Systems

System reserves are necessary to maintain the economic and reliable operation of power systems. Due to the intermittent characteristic of solar radiation, power system reliability may be affected with high PV power penetration. Customers can choose their reliability level that is denoted by nodal reliability in deregulated power systems.

In order to reduce the impact of the large variation of PV power, additional balancing reserve would be needed in power system operation. In deregulated power systems, deployment of reserves and customer reliability requirements are correlated with energy and reserve prices. Under such conditions, to utilize PV power reliably and economically, a new method should be developed to evaluate the impacts of PV power on customer reliability and system reserve deployment.

In this Chapter, a method based on the pseudo-sequential Monte Carlo simulation technique has been proposed to evaluate the reserve deployment and customers' nodal reliability with high PV power penetration. The proposed method can effectively model the chronological aspects and stochastic characteristics of PV power and system operation while preserving the high computation efficiency of the non-sequential Monte Carlo simulation method. An auto-regressive and moving average (ARMA) model has also been developed for simulating the chronological characteristics of the solar radiation. Customers' reliability preferences have been considered in the generation and reserve deployment. Moreover, the correlation between PV power and load has been considered in the proposed method. Nodal reliability indices and reserve deployment have been evaluated by applying the proposed method to the IEEE Reliability Test System (RTS).

5.1 Introduction

In recent years, renewable energy sources have been rapidly adopted in many countries and regions as substitutes for traditional energy resources [20] for reducing environmental pollutants and global warming effects. Renewable energy has also been gradually competitive with conventional energy in markets because of the rising costs of conventional energy and government tariff policies [22]. Solar energy is a promising renewable energy source due to its abundance, accessibility and clean generation process. The application of photovoltaic (PV) panels for generating electric power also promotes the utilization of solar energy [20].

However, the power output of a PV generating system comprising a number of PV panels is mainly determined by the available solar radiations which vary chronologically. The fast fluctuation of the solar radiations makes the power output of the PV generating system intermittent and totally different from that of the conventional generators. The PV power is usually high around noon and not available during the night. In order to utilize solar power on a large scale effectively and efficiently, its chronological and intermittent characteristics have to be modeled [26, 43, 131, 132].

The high PV power penetration in electric power systems can impact the generation and reserves deployment, and therefore bring complexities in power system reliability assessment [26, 41, 43, 45, 60, 132-135]. In power system operation, operating reserve and contingency reserve are dispatched to meet load variation and capacity inadequacy in contingency state respectively [41, 135]. Both types of reserve can be provided by spinning reserve, online generating units, or fast start-up generating units with different synchronous times. With high renewable energy penetration, renewable power fluctuation may impact utilization of both types of reserves, and the differentiation between them is rather obscure [41]. Reference [133] illustrates that adequate reserve is necessary for balancing the high fluctuation of renewable power

output. Some research has shown that the requirement of reserve will ascend with the increase of wind power penetration for maintaining power system reliability levels [132, 134]. However, the reserve requirement in the new environment also depends on the correlation between renewable energy and load. If their correlation is positive, less reserve may be needed, and vice versa. The prediction errors of renewable power output can also impact the reserve deployment in deregulated power systems [60], where customers are more concerned about their own reliabilities than system reliabilities and also have their reliability preferences, which are evaluated by customers' nodal reliability indices [67]. The utilization of PV power will be affected by customers' reliability preferences. Therefore it is important to develop a method for evaluating customers' nodal reliabilities that can take into consideration customers' reliability preferences and high power fluctuation caused by PV penetration.

Typical methods that have been used for power system reliability studies can be classified into two categories, analytical methods and Monte Carlo simulation methods [63, 136, 137]. The analytical methods calculate system reliability indices for determined states using direct mathematical methods. Monte Carlo simulation methods, on the other hand, simulate the stochastic behavior of the power system operation for estimating reliability indices [63]. The analytical methods are relatively easy to implement. However, they are very sensitive to the system size, which usually takes significant computational efforts for evaluating reliabilities of large systems with complex generating conditions. On the other hand, when considering complex operating conditions or when the number of contingency events is large, Monte Carlo simulation is preferred as the number of samples required for a given accuracy level is independent of the system size [99]. Monte Carlo simulation methods can be further sub-divided into sequential and non-sequential methods. Sequential Monte Carlo simulation represents modeling the chronological aspects of system operation. However, it takes greater computation effort and sometimes a solution is impossible especially for large scale power systems. Non-sequential Monte Carlo simulation, on the other hand, takes less computational effort but cannot model the chronological

characteristics of power system operation. The pseudo-sequential Monte Carlo simulation preserves the high computation efficiency of the non-sequential Monte Carlo simulation and the chronological property of the sequential Monte Carlo simulation [138-140]. The pseudo-sequential Monte Carlo simulation techniques were initially developed for conventional power systems [138-140] and have been extended in this Chapter for reliability evaluation of deregulated power systems with high PV power penetration.

In this Chapter, a new method is proposed to evaluate the impact of high PV power penetration on customers' nodal reliability and system energy and reserve deployment. The new indices for assessing system reserve commitment and deployment have been developed through the proposed method. The ARMA model has been utilized to simulate the chronological characteristics of the solar radiation. Pseudo-sequential Monte Carlo simulation has been utilized in the proposed method for taking into account both chronological and stochastic characteristics of PV power as well as customer reliability preferences. The proposed method has also considered the correlation between PV power and load. Customers' nodal reliability and reserve deployment of generating units have been formulated and evaluated, respectively. The modified IEEE reliability test system - RTS [129] is used to illustrate the method. The modeling of PV generating system has been discussed in Section 5.2. In Section 5.3, optimal energy and reserve scheduling formulation for power system operation considering PV power penetration has been introduced. The proposed method based on the pseudo-sequential Monte Carlo simulation for nodal reliability and reserve evaluation has been introduced in Section 5.4. The system studies based on the modified RTS are given in Section 5.5.

Nomenclature

0	Normal state index (Superscript)
j	Contingency state index (Superscript)
i,k	Bus index (Superscript)

g	Generator index (Subscript)
d	Load sector index (Subscript)
N	Set of buses
N_g	Set of generator buses
N_d	Set of load buses
NG_i	Set of generators
ND_i	Set of load sectors
N_{PV}	Set of load buses containing PV power
$\hat{P}_{PV\,i}$	Predicted PV power at node i
$P^0_{PV\,i}$	Actual PV power at node i at normal state
$P^j_{PV\,i}$	Actual PV power at node i at state j
$\hat{P}^0_{NL\,i}$	Predicted net load at state 0
$P^0_{NL\,i}$	Actual net load at state 0
$P^j_{NL\,i}$	Actual net load at node i at state j
C_{ig}	Energy cost function
CR_{ig}	Secondary reserve real power cost function
C_{id}	Load interruption cost function
P^j_G	Generation power vector
P^j_{NL}	Net load power vector
B^j	Admittance matrix of transmission network
Θ^j	Bus voltage phase angle vector
x^j_{ik}	Line impedance from bus i to k
θ^j_i, θ^j_k	Voltage phase angle at buses i, k respectively
$\lvert S_{ik} \rvert^{\max}$	Maximum apparent power on transmission line from bus i to k
P^0_{ig}	Real power output of unit g at node i at normal state
ΔP^j_{ig}	Primary reserve real power provided by unit g at node i at state j

R_{ig}^{j} Secondary reserve real power provided by unit *g* at node *i* at state *j*

P_{id}^{0} Normal state load of load sector *d* at node *i*

ΔP_{id}^{j} Load curtailment of load sector *d* at node *i* at state *j*

$P_{ig}^{\min}$ Minimum real power output of unit g

$P_{ig}^{\max}$ Maximum real power output of unit g

$R_{ig}^{\max}$ Maximum secondary reserve real power provided by unit g

5.2 PV Generating System

PV generating system power output, reliability performance and its penetration are analyzed in this section.

5.2.1 PV panel output

The solar radiation modeling and electric characteristics of PV panel have been examined in Section 3.2. The PV panel produced by SUNTECH with model number STP280-VRM-1 was used. The parameters used are listed below. Cell area of the panel is about 1.65 m^2.

Table 5.1. Temperature Characteristics of PV Panel

Nominal Operating Cell Temperature (NOCT)	$45^{o} \pm 2^{o}C$
Temperature Coefficient of P_{max}	-0.44%/^{o}C
Temperature Coefficient of P_{max}	-0.33%/^{o}C
Temperature Coefficient of P_{max}	0.055%/^{o}C

Table 5.2. Electrical Characteristics

Operating condition	STC	NOCT
Open-circuit voltage (Voc)	44.8V	40.8V
Short-circuit current (Isc)	8.33A	6.74A
Maximum Power (Pmax)	280W	204W

STC: Irradiance 1000W/m^2, module temperature 25^{o}C, AM = 1.5;

NOCT: Irradiance 800W/m^2, module temperature 20^{o}C, AM = 1.5.

The power output of a PV panel can be obtained from Equation (3.20). Since solar radiation is the main factor that is random and impacts the PV panel power output, the relationship between solar radiation and PV panel output is of concern in the analysis.

Fig. 5.1 shows the relationship between PV panel output and solar radiation. The piecewise linear function is fitted for the aggregated power output curve using least-square fitting method.

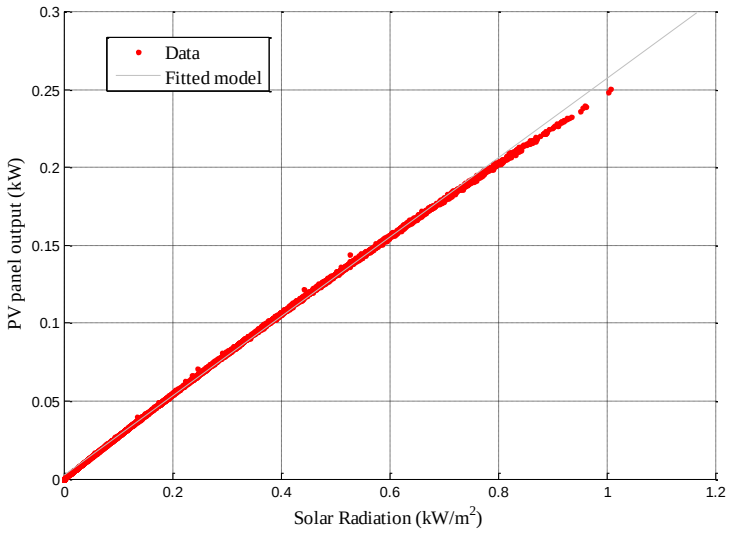

Fig. 5.1 Relation between PV panel output power and solar radiation

From the least-square fitting curve, the maximum PV panel power output P_{mp} and the PV array output P_{PV} are determined by Equations (5.1) and (5.2), respectively:

$$P_{mp}(SR) = 0.2548SR + 0.0027 \quad (kW) \tag{5.1}$$

where $P_{mp}(SR)$ is the maximum power of a PV panel under solar radiation level SR. The power of PV array consisting of N_{PV} modules P_{PV}:

$$P_{PV} = P_{mp}(SR) \cdot N_{PV} \tag{5.2}$$

It can be observed from Equation (5.1) that the power output of a PV panel is approximated as a linear function of solar radiation - the ratio of power output of the panel versus the solar radiation is: $P_{mp}(SR)/SR \approx 0.2548$ kW/Panel. Since the PV panel surface area is about 1.65 m^2 as shown in Appendix A, for 1 kW/m^2 solar radiation, the power output (kW) per m^2 of the panel is: **0.2548kW/1.65m^2= 0.152kW/m^2**. Therefore the conversion efficiency of the panel is 15.2%.

5.2.2 PV array power output

The real power output and the prediction of PV array are denoted as P_{PV} and $\hat{P}_{PV}$ respectively. The prediction error ΔP_{PV} is calculated as:

$$\Delta P_{PV} = P_{PV} - \hat{P}_{PV} \tag{5.3}$$

The predicted power and prediction error of a PV array with 1×10^5 PV panels were examined. The PDF of the PV array power output from predicted solar radiation and measurement are shown in Fig. 5.2. The fit of a *t*-distribution with freedom 1 to the PV array power output prediction errors is shown in Fig. 5.3.

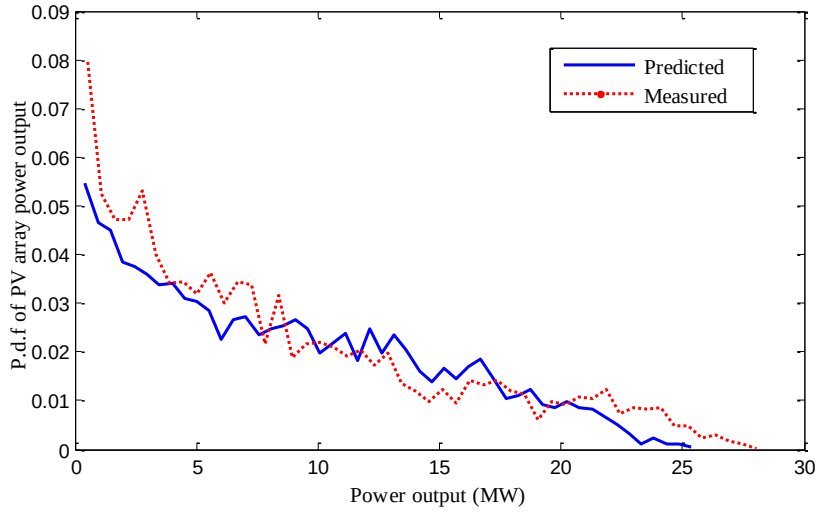

Fig. 5.2 PDF of PV array power output

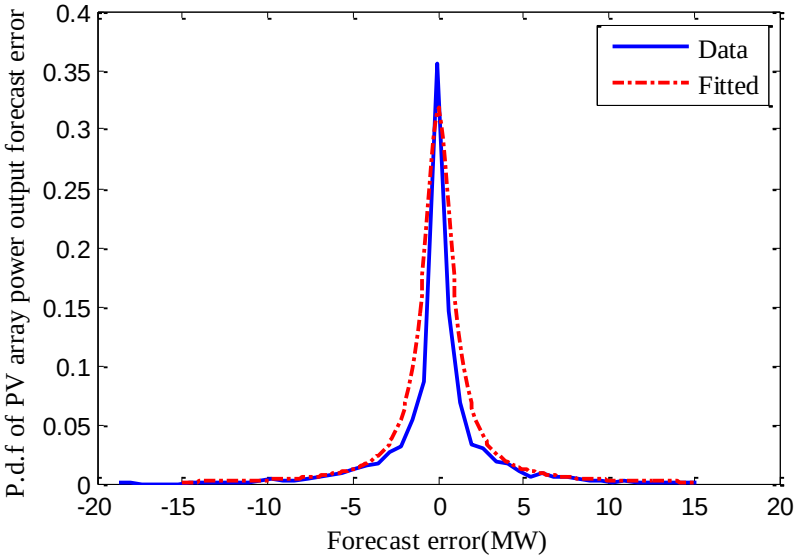

Fig. 5.3 PDF of PV array power output prediction error

5.2.3 PV array reliability

In reliability analysis, a PV array is modeled as a two-state Markov model. The failure rate and repair rate used are 0.000383 (1/hour) and 0.00381 (1/hour) respectively [141, 142].

5.2.4 PV power penetration

PV array located at the demand side will be utilized for supplying load directly. In

addition, from an economic point of view, PV power should be consumed first. It is assumed that customers will not use energy storage for storing PV power to make energy arbitrage. The load that cannot be fulfilled by PV energy is the net load (NL), which is supplied by the conventional generation.

Predicted NL $\hat{P}^0_{NL\,i}$ and actual NL $P^0_{NL\,i}$ at node i is determined by equations (5.4) and (5.3) respectively:

$$\hat{P}^0_{NL\,i} = \sum_{d \in ND_i} P^0_{id} - \hat{P}_{PV\,i} \tag{5.4}$$

$$P^0_{NL\,i} = \sum_{d \in ND_i} P^0_{id} - P^0_{PV\,i} \tag{5.5}$$

5.3 Problem Formulation

PV power is utilized in power system operation to substitute part of the conventional energy. However, the unpredicted PV power fluctuation needs to be balanced by system reserves within an acceptable time period (e.g, 10 minutes or intra-hour). PV power fluctuations may also require utilization of down reserves, which is seldom used in a conventional power system with low penetration of renewable energy resources [135]. Most electricity markets would provide balancing reserves with different synchronous times or various utilization purposes [143]. For example, in the Nordic power system, the frequency controlled normal operating reserve (FNR) and frequency controlled disturbance reserve (FDR) are procured to restore energy balances caused by demand variation and system disturbances respectively [143]. In this chapter, balancing reserves are modeled as primary reserve and secondary reserve. Primary reserve can be up reserve or down reserve and is mainly used to meet the unpredictable load variation or unpredictable PV power. Secondary reserve is the up reserve and is mainly used for contingency events when large generation inadequacy occurs. In deregulated power systems, customers may choose to interrupt their electricity consumption if the energy cost is higher than their reliability benefits. Customers' reliability benefits are difficult to be measured directly and are therefore

often evaluated indirectly using their interruption costs [63]. Therefore customers' interruption costs should be considered in the energy and reserve scheduling models.

The optimal energy and reserve scheduling problem in power system operation is formulated in two steps as shown in [41]. In the first step, the unit commitment (UC) is scheduled for each operating hour. The algorithm for determining UC is obtained from [144], which commits the available units at least operation cost. In the second step, the reserve utilization and load curtailment are determined for each contingency state during the real time operation. Since only real power is considered for the reserve and PV power, a DC optimal power flow (OPF) model has been developed, which is computationally efficient. The objective of the OPF model is to minimize the generation, reserve utilization and customer interruption cost for system state *j*:

$$\min_{P_{ig}^0,\Delta P_{ig}^j,R_{ig}^j,\Delta P_{id}^j} f^j = \sum_{i\in N_g^j}\sum_{g\in NG_i^j}\left(C_{ig}\left(\Delta P_{ig}^j + P_{ig}^0\right) + CR_{ig}\left(R_{ig}^j\right)\right) + \sum_{i\in N_d}\sum_{d\in ND_i} C_{id}\left(\Delta P_{id}^j\right) \quad (5.6)$$

subject to system security constraints:

DC power balance equation:

$$B^j\Theta^j - P_G^j + P_{NT}^j = 0 \quad (5.7)$$

where the i^{th} element of P_G^j is the generation power at node *i* at state *j* and equals $\sum_{g\in NG_i^j}\left(P_{ig}^0 + \Delta P_{ig}^j + R_{ig}^j\right)$, and the i^{th} element of P_{NL}^j is the net load at node *i* at state *j* and equals $\sum_{d\in ND_i}\left(P_{id}^0 - \Delta P_{id}^j\right) - P_{PV\,i}^j$.

Generating unit limits:

$$P_{ig}^{\min} \le \Delta P_{ig}^j + P_{ig}^0 \le P_{ig}^{\max} \quad (5.8)$$

$$0 \le R_{ig}^j \le R_{ig}^{\max} \quad (5.9)$$

Transmission line constraints:

$$\left|\frac{1}{x_{ik}^{j}}\left(\theta_i^j-\theta_k^j\right)\right|\le\left|S_{ik}^{j}\right|^{\max} \tag{5.10}$$

5.4 Proposed Method for Reliability and Reserve Evaluation

5.4.1 Markov Models

The reliability performance of conventional generating units, PV arrays and transmission lines were considered. The failure rate λ and the repair rate μ of a component are given by Equations (5.12) and (5.13) respectively [63]:

$$\lambda=\frac{1}{MTTF}\left(1/hour\right) \tag{5.11}$$

$$\mu=\frac{1}{MTTR}\left(1/hour\right) \tag{5.12}$$

where the *MTTF* and *MTTR* are the mean time to failure and mean time to repair respectively.

The availability of a component p_{in} and unavailability p_{out} are determined as:

$$p_{in}=\frac{\mu}{\lambda+\mu} \tag{5.13}$$

$$p_{out}=\frac{\lambda}{\lambda+\mu} \tag{5.14}$$

The generating unit, transmission lines and PV arrays were modeled as two-state Markov models. The pdf of each component was constructed using Equations (5.13) and (5.14).

5.4.2 Pseudo-Sequential Monte Carlo Simulation

In the pseudo-sequential Monte Carlo simulation process, a non-sequential Monte Carlo simulation method is used to select the load level and system state. If the selected state is a failure state, a sequence of neighboring states and the duration of

failure are determined utilizing the state transition method [138, 139]. The pseudo-sequential simulation process for evaluating customers' nodal reliability and reserve deployment considering PV power fluctuations is summarized in the following steps:

Step 1: Generate the hourly time varying sequences of PV power output of PV generating systems. Calculate predicted NL profile using (5.4).

Step 2: Sample a predicted NL level $\hat{P}_{NL\,i}^{0}$ from the predicted NL profile based on a uniform distribution. Do the first step of the problem defined in section 3 to determine the committed units and their power outputs P_{ig}^{0}.

Step 3: Sample system state *j* by sampling the states of committed units, transmission lines and PV generating systems based on their probability density function.

Step 4: Evaluate the system state *j*: if it is a success state (all the components are in their available state), go to Step 2; if it is a failure state, go to the next state.

Step 5: If the PV generating system failed at node i, the load at node i will be P_{id}^{0}. Otherwise the load is $P_{NL\,i}^{0}$ (NL) at node i, which considers the power contribution of the PV generating system.

Step 6: Calculate the failure states sequence starting from state *j* using the forward/backward simulation.

Step 7: Calculate the failure state duration D^{j} according to the failure sequence obtained in Step 6.

Step 8: Do the second step of the problem defined in section 3 to calculate the reserve deployments and load curtailment by solving problem (5.6) – (5.10). Calculate the

nodal reliability indices which are explained in part *C*.

Step 9: Check the convergence criteria. If satisfied, stop. If not, go to Step 3.

The first and second steps of the problem stated in Section 3 are implemented here in Steps 2 and 8 respectively. The method for generating forward/backward state sequences and failure duration $E(D)$ in Steps 6 and 7 are explained below [138, 139].

Forward/backward sequence simulation

The forward and backward sequences are sampled according to the probability distributions of the system transition states. The difference between the present state and the following state of the system is the operating state change of one component which can either be repaired or is failed. The forward sequence is to simulate a series of states following the examined state until a success state is found.

The frequency of departure from state *s* to state *j* f_{sj} is calculated as:

$$f_{sj} = p_s \lambda_{sj} \tag{5.15}$$

where p_s is the probability of state s, λ_{sj} is the transition rate from *s* to *j*.

For state *s* which can transit into *NFS* following states, the frequency of departure from state *s* is:

$$f_s^{dep} = p_s \sum_{j=1}^{NFS} \lambda_{sj} \tag{5.16}$$

The probability of the system transiting from state *s* to *j* is then determined as:

$$p_{sj} = f_{sj} / f_s^{dep} = \lambda_{sj} / \sum_{j=1}^{NFS} \lambda_{sj} \tag{5.17}$$

By sampling based on a uniform distribution, the following state is determined according to Equation (5.17).

The difference of previous state and present state is the same as that for the forward state transition. The backward sequence is identified by simulating a series of previous states of the examined state until a success state is found. The probability distribution of the previous state is determined by using the same method. The frequency that the system state *s* is transmitted from state *i* is:

$$f_{is} = p_i \lambda_{is} \tag{5.18}$$

For *NBS* possible previous states, the frequency that they arrive at state *s* is:

$$f_s^{arr} = \sum_{i=1}^{NBS} p_i \lambda_{is} \tag{5.19}$$

The probability that system has transited from state *i* to *s* is:

$$p_{is} = f_{is} / f_s^{arr} = p_i \lambda_{is} / \sum_{i=1}^{NBS} p_i \lambda_{is} \tag{5.20}$$

Assumes state *i* and *s* are differentiated by component k which is transformed from operating state to outage state. If k is represented by a two-state Markov model, then: $p_i / p_s = \left(\mu_k \middle/ \lambda_k + \mu_k \right) \middle/ \left(\lambda_k \middle/ \lambda_k + \mu_k \right) = \mu_k / \lambda_k$, and $\lambda_{is} = \lambda_k$. If all the components are represented using two-state Markov models, we have $\left(p_i / p_s \right) \lambda_{is} = \mu_k = \lambda_{si}$.

Dividing Equation (5.20) by p_s , we have:

$$p_{is} = \lambda_{si} / \sum_{i=1}^{NBS} \lambda_{si} \tag{5.21}$$

Note that Equation (5.21) is similar with Equation (5.17).

The duration of the outage state is determined by the combination of forward and backward sequences. The total duration *D* of the sequence is the sum of all duration D^j of each failure state *j*. For statistically independent components whose state durations follow the exponential distribution, the expected duration of state *j* is:

$$E\left(D^j\right) = 8760 / \sum_k \lambda_k \tag{5.22}$$

where λ_k is the transition rate between the examined state and any state it can transit to.

The expected duration of the sequence *I* is then:

$$E(D) = \sum_{j \in I} E\left(D^j\right) \tag{5.23}$$

5.4.3 Nodal Reliability and Reserve Indices

The nodal reliability and reserve indices evaluated in Step 8 are calculated as follows. The expected energy not supplied (*EENS*) is the estimator of energy not supplied (*ENS*):

$$EENS = \sum_{j=1}^{N} ENS^j \Big/ N \tag{5.24}$$

where $ENS^j = \begin{cases} 0 & j = success\ state \\ \sum_{i \in N_d} \sum_{d \in NL_i^j} \Delta P_{NL\,i}^j \times T & j = failure\ state \end{cases}$ where T is the examined period, e.g 8760 hours for annual analysis.

The loss of load probability (*LOLP*):

$$LOLP = \sum_{j=1}^{N} F^j \Big/ N \tag{5.25}$$

where $F^j = \begin{cases} 0 & j = success\ state \\ 1 & j = failure\ state \end{cases}$.

The expected energy interruption cost (*EEIC*):

$$EEIC = \sum_{j=1}^{N} EIC^j \Big/ N \tag{5.26}$$

where $EIC^j = \begin{cases} 0 & j = success\ state \\ \sum_{d \in NL^j} K_d / E(D) & j = failure\ state \end{cases}$ and K_d is the energy cost for

load sector d, NL^j is load sets. K_d is calculated as:

$$K_d = \sum_{k \in I^j} CDF_d\left(D^k\right) \times \Delta P_{id}^k \tag{5.27}$$

k is one of the states of the failure sequence I^t for choosing failure state j. $CDF_d\left(D^k\right)$ is the customer damage function of load sector d for duration D^k.

The expected committed primary reserve (*ECP*):

$$ECP = \sum_j^N CPR^j \Big/ N \tag{5.28}$$

where $CPR^j = \begin{cases} 0 & j = success\ state \\ \sum_{i \in N_g} \sum_{g \in NG_i^j} \left(P_{ig}^{\max} - P_{ig}^0\right) \times T & j = failure\ state \end{cases}$.

The expected committed secondary reserve (*ECS*):

$$ECS = \sum_j^N CSR^j \Big/ N \tag{5.29}$$

where $CSR^j = \begin{cases} 0 & j = success\ state \\ \sum_{i \in N_g} \sum_{g \in NG_i^j} R_{ig}^{\max} \times T & j = failure\ state \end{cases}$.

The expected utilization of primary reserve (*EUP*):

$$EUF = \sum_j^N FR^j \Big/ N \tag{5.30}$$

where $PR^j = \begin{cases} 0 & j = success\ state \\ \sum_{i \in N_g} \sum_{g \in NG_i^j} \left(P_{ig}^j - P_{ig}^0\right) \times T & j = failure\ state \end{cases}$.

The expected utilization of secondary reserve (*EUS*):

$$EUS = \sum_j^N SR^j \Big/ N \tag{5.31}$$

where $SR^j = \begin{cases} 0 & j = success\ state \\ \sum_{i \in N_g} \sum_{g \in NG_i^j} R_{ig}^j \times T & j = failure\ state \end{cases}$.

The uncertainty of *EENS* is evaluated by its variance coefficient. The coefficient of variance of *EENS* is used as the convergence criterion in Step 8.

$$\beta_{EENS} = \sqrt{V(EENS)} / EENS \tag{5.32}$$

where $V(EENS) = V(ENS)/N$ is the variance of *EENS*, $V(ENS)$ is the variance of *ENS*.

5.5 Case Studies

The modified IEEE RTS [129] is used to illustrate the proposed techniques. Three PV penetration levels of 0% (Case 0), 9.8% (Case 1) and 19.6% (Case 2) are studied. The nodal penetrations of PV power are shown in Table 5.3. In order to quantify the impact of PV power with or without additional reserve, the simulations for Cases 1 and 2 have been done under two conditions. Under condition (a), the UC of conventional units is determined based on the net load, which is the load minus the PV power output. Under condition (b), the UC for conventional units are only determined based on P_{id}^0 and PV powers are treated as additional power.

Table 5.3 Nodal PV install capacity (MW)

Node	Case 1 (9.8% PV penetration)	Case 2 (19.6% PV penetration)
1,2,3,4,5,6,7,8,9,10	28	28
13,15,18,	0	56
14,16,19,20	0	28

The *EENS* and *LOLP* at different load nodes are shown in Tables 5.4 and Fig. 5.4 respectively. Under condition (a), customers' reliabilities are impaired by PV power fluctuations and unreliability of PV generating systems. *EENS* and *LOLP* increase as

PV power penetration increases. For customers at node 1-4, 7-20, *EENS* increase more than 100% from Case 0 to Case 2(a), while for customers at nodes 5-6, *EENS* increase less than 100%. Customers' *LOLP* also have different variations after PV penetration. For condition (b), *EENS* and *LOLP* decrease after PV penetration increases since PV power served as an additional power source. Improvements of customers' *EENS* and *LOLP* are not uniform for each node under condition (b). For customers at nodes 13, 15 and 18 with higher PV power penetration, reliability improvement is less than other nodes.

In deregulated power systems, customers' reliability may be compromised by the PV penetration if there is insufficient reserve to account for the unpredictable PV power fluctuations. The impacts of PV power penetration on customers' nodal reliability also depend on customers' choices and should be evaluated after considering customers' reliability preferences. In an interconnected power system with high PV penetration, for customers located at nodes where PV power is penetrated, the variations of nodal reliability are not more significant than for other customers.

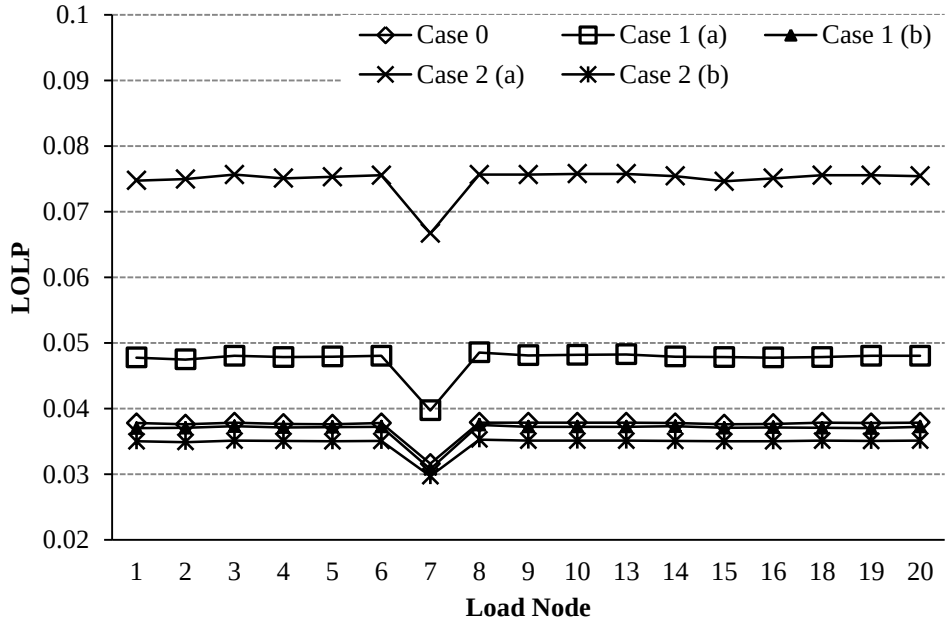

Fig. 5.4 *LOLP* at different load nodes

Table 5.4 EENS (MWh/yr)

Node	Case 0	Case 1(a)	Case 1(b)	Case 2(a)	Case 2(b)
1	2446.8	3120.9	2263.1	4936.3	2230.4
2	3041.8	3934.0	2789.0	6388.3	2774.8
3	3048.8	3937.2	2830.0	6224.5	2775.3
4	2380.0	3016.5	2207.3	4708.2	2161.2
5	2090.5	2648.1	1951.6	4081.3	1897.0
6	1943.5	2443.2	1821.8	3707.6	1761.2
7	2348.2	2932.4	2196.1	4865.7	2161.1
8	3986.7	5261.0	3709.9	8611.7	3651.8
9	3217.7	4171.2	2983.4	6642.8	2928.0
10	2903.0	3727.7	2684.7	5883.0	2626.8
13	3589.1	4815.6	3339.7	7637.5	3249.7
14	3250.4	4289.9	3062.8	6769.8	2981.0
15	3460.2	4773.2	3315.7	7384.9	3185.4
16	3142.7	4314.3	2987.9	6761.2	2885.3
18	3874.3	5301.4	3740.4	7883.0	3611.4
19	4173.6	5847.4	4001.3	9210.9	3860.8
20	2506.4	3338.6	2364.7	5266.6	2298.1

The *EEIC* are shown in Fig. 5.5. Customers' *EEIC* increases as PV penetration increases. *EEIC* increase by more than 400% from Case 0 to Case 2(a) while it increases less than 100% from Case 0 to Case 1(a). We can observe that with high PV penetration, the unreliability of PV arrays may increase the duration of the contingency events of the system, and customers' *EEIC* will increase. But for different customers, the increases in *EEIC* are not linear and may increase more dramatically when solar penetration increases.

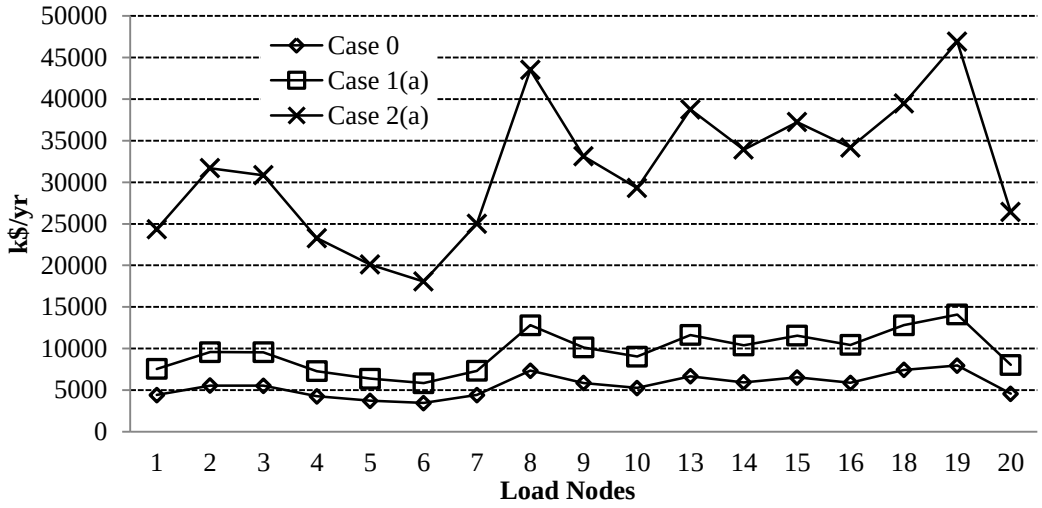

Fig. 5.5 *EEIC* at different load nodes

The reserve commitment and utilization are shown in Tables 5.5 and 5.6 respectively. From Table 5.5, ECP and ECS increase after PV power penetration especially under condition (b). Since PV penetration increases the power fluctuations, the EUP and EUS increase under condition (a) to balance the PV fluctuations. The reserve deployment is also affected by customers' reliability preferences. Without sufficient primary reserve, customers are more likely to be interrupted due to the slow response of secondary reserve. Under condition (b), the EUP increases and the EUS decreases. With sufficient primary reserve, customers can maintain or even improve their reliability.

It is therefore clear that in deregulated power systems, the benefits of solar power penetration on customers' reliability highly depend on whether the reserve markets can provide sufficiently fast response and relatively cheap reserve for balancing the fluctuations of PV power. The results shown in this chapter demonstrate that the RTS can have 20% PV power integration without affecting the customers' reliability if the PV power is integrated as additional energy sources in power system operations. However, under such conditions, the reserve deployment and utilizations will increase greatly.

Table 5.5 Reserve Commitments (MW)

	Case 0	Case 1(a)	Case 1(b)	Case 2(a)	Case 2(b)
ECF	183.85	286.19	323.99	315.72	395.44
ECS	168.04	254.05	263.29	276.20	293.29

Table 5.6 Reserve Utilization (MWh/yr)

	Case 0	Case 1(a)	Case 1(b)	Case 2(a)	Case 1(b)
EUF	811717.1	966988.9	1033253.9	1152290.9	1328220.3
EUS	265210.3	302340	260514.4	383276.73	261900.5
Total	1076927	1269329	1293768	1535568	1590121

5.6 Conclusions

In this Chapter, nodal reliability and reserve deployment have been investigated for deregulated power systems with PV power penetration. A technique using pseudo-sequential Monte Carlo simulation method has been developed which can take into consideration the stochastic and chronological fluctuations of PV power as well as customers' reliability preferences. The results show that nodal reliability is impaired with PV power penetration due to the intermittence of PV generation system. The impacts of PV generation also depend on customers' reliability preferences. Therefore PV power penetrations have non-uniform impacts on different customers. If more PV power is penetrated, the system should be able to meet the large power fluctuation by providing more fast response reserve without damaging customer reliability. The proposed technique provides a flexible method to evaluate these impacts on nodal reliability in deregulated power systems. This technique can also be extended to incorporate other intermittent renewable energy sources.

Chapter 6 Impacts of Wind Power Penetration on Deregulated Power Systems

Wind power can be generated on a large scale by wind farms. With high level penetration, more operating reserves are needed to balance wind power variations. The imbalance cost derived from the reserve utilization also increases. Wind power providers will adopt different bidding strategies to minimize the imbalance cost and to optimize their benefits. High penetrations of wind power may change the generation commitment since they should be consumed first due to economic and environmental concerns. Energy prices may therefore be affected. The variable wind power affects the deployment of balancing reserves which together with unreliability of wind turbine generators may affect adversely the customers' reliability in deregulated power systems. The behavior of wind power and their impacts on the existing power system operation should therefore be investigated for the efficient utilization of wind power.

In this chapter, the contingency reserve and its deployments are analyzed in a power market with wind power penetrations. Different bidding strategies of wind power providers are analyzed from the short-term wind power forecasting. The operational reliability is evaluated in terms of Nodal Unit Commitment Risk (*NUCR*) and nodal price of power systems. The impacts of wind power penetration on the nodal prices are also evaluated.

6.1 Introduction

Wind energy is a promising type of renewable energy due to its clean generating process and large potential. The development of wind power generation technology makes it possible to install large scale wind farms with great capacity. Wind power generation has been growing fast in recent decades. Many countries have set goals for

high level wind power penetration. By the end of 2011, the total global installed capacity has reached 238 GW [18]. While the penetration level of wind power increases, new challenges occur when integrating wind power into existing power systems and power markets. In many European countries like UK, Spain, Denmark, wind power can participate in power market operation [22]. The related issues include but are not limited to the responsibility for the cost induced from wind power variation, the pricing scheme and schedule of wind power.

The wind power fluctuates chronologically and cannot be scheduled like conventional generations due to its variability and forecast errors. However, wind power should be explicitly considered in the generation commitment and dispatch for optimizing the energy utilization [145-147]. By substituting part of conventional power, the spillage or shortage of wind power needs to be balanced by system reserve. The impacts of wind power forecast errors and forced outages on system operation was analyzed using a proposed mixed integer linear optimization scheduling model in [145]. In [25], a short-term electricity market clearing process was proposed with stochastic security that is capable of including stochastic wind power without damaging system operating security. The operating reserve requirement is optimized using stochastic programming to minimize the operating costs with different wind power penetration levels [41]. The impacts of wind penetration on the system operational reliability have been examined in [26]. The results show the benefits of integrating wind power in reducing the system UCR and increasing the load carrying capability.

The variability and intermittent nature of renewable power will affect the system energy balance [36, 148, 149]. The participation of renewable generation in the power market not only affects the system operation, but also influences the economic performance. Trading renewable power in the power market will influence the energy price and reserve price. The behavior of a wind power provider (WPP) or a wind farm (WF) has been investigated in [52, 53, 120]. A WPP in a power market can bid different amounts based on forecast, in order to optimize the profit under different

payment schemes for renewable power. However, this can adversely affect the system operation and market behavior.

Competition has been introduced in deregulated power systems to reduce the operation cost and to provide choices for participants to optimize their benefits [2]. Considering transmission network and related cost, nodal reliability and nodal price have been adopted to evaluate customer reliability and associated payment at different locations [66, 68, 125]. Since customers can choose different services to avoid interruption in a system contingency state, supply reliability to a customer will be affected by its reliability preferences. In short term market analysis, the operational reliability is evaluated, which is different from long term reliability analysis in the sense of time range, evaluation technique, and the outage property of units. The unit commitment risk (UCR) used by the PJM to evaluate operational reliability is the most widely used index in operational reliability [63]. Nodal price reflects not only the supply cost but also the reliability requirement of customer at the load point [66, 68, 125].

With wind power participation in power market operation, the variation of wind power and the bidding behavior of wind power providers should be accounted for in the generation and reserve deployment. In this chapter, a market clearing process has been developed with wind penetration. Wind power bidding strategies based on short term forecasting are explicitly incorporated in the market clearing and unit commitment process. Nodal operation reliability and nodal prices are examined through contingency analysis using the RBTS.

Nomenclature

0	Normal state index (superscript)
j	Contingency state index (superscript)
t	Time period index (superscript)

i,k	Bus index (subscript)
z	Reserve zone index (subscript)
g	Generating unit index (subscript)
d	Customer sector index (subscript)
r	Sign of reserve related parameters (subscript)
N	Set of buses
N_g	Set of buses containing generators
N_L	Set of load buses
NL	Set of load sectors
$\|V_i\|^{\min}$	Lower limit of voltage at bus i
$\|V_i\|^{\max}$	Upper limit of voltage at bus i
$P_{i\,g}^{\min}$	Minimum real power of generator g at bus i
$P_{i\,g}^{\max}$	Maximum real power of generator g at bus i
$Q_{i\,g}^{\min}$	Minimum reactive power of generator g at bus i
$Q_{i\,g}^{\max}$	Maximum reactive power of generator g at bus i
$P_{i\,d}^{t\,0}$	The real power demand of load sector d at bus i for normal state
$Q_{i\,d}^{t\,0}$	The reactive power demand of load sector d at bus i for normal state
$\Delta P_{i\,g}^{low}$	Lower limit on generation change $\Delta P_{i\,g}^{t\,j}$
$\Delta P_{i\,g}^{up}$	Upper limit on generation change $\Delta P_{i\,g}^{t\,j}$
$\Delta P_{i\,d}^{\max}$	Maximum load curtailment of load sector d at bus i

For state j and bus i at hour t:

$P_{i\,g}^{t\,j}$	Real power output of generator g
$Q_{i\,g}^{t\,j}$	Reactive power output of generator g

$R_{i\,g}^{t\,j}$	Reserve power provided by generator *g*
$\Delta P_{i\,d}^{t\,j}$	Real power curtailment of load sector *d*
$\Delta Q_{i\,d}^{t\,j}$	Reactive power curtailment of load sector *d*
$P_{i\,aw}^{t}$	Real wind power output at bus *i*
$P_{i\,bw}^{t}$	Bidding wind power at bus *i*
$C_{i\,g}$	Cost function of generator *g*
RC_{gr}	Reserve cost function of generator *g*
$CC_{i\,d}^{t\,j}$	Curtailment cost for customer sector *d*
$V_i^{t\,j} = \left\|V_i^{t\,j}\right\| \angle \theta_i^{t\,j}$	Bus voltage
$Y_{ik}^{t\,j} = \left\|Y_{ik}^{t\,j}\right\| \angle \delta_{ik}^{t\,j}$	Element of admittance matrix
$\Delta P_{i\,g}^{t\,j}$	Ramp up rate for generator *g*
$\Delta P_{i\,d}^{t\,j}$	Load curtailment of customer sector *d*
$\left\|S_{i\,k}^{j}\right\|$	Magnitude of apparent power from bus *i* to bus *k*
$\left\|S_{i\,k}^{j}\right\|^{\max}$	Magnitude of maximum apparent power from bus *i* to *k*

6.2 Penetration of Wind Power

The stochastic characteristics of wind power generation are analyzed in this section. Different bidding strategies based on the short term wind power forecasts have been analyzed.

6.2.1 Wind turbine power output

Multistate wind energy conversion system models which incorporate the wind speed variation and wind turbine outage probability have been proposed in [35]. This

method is more suitable in long term analytical and state sampling methods. In short term analysis, the wind power output model should account for the time correlation of wind speeds. The techniques for short-term wind power forecasting have been presented in [150, 151]. The numerical weather prediction models are capable of making accurate predictions for short term and long term time horizons [26]. ARMA model can be used in short term wind speed forecast since it can represent the time correlated stochastic characteristics of wind speed [26]. Using ARMA short term forecast, conditional wind power distribution proposed in [26] shows a strong correlation between the previous wind power and the present hour for the investigated hours. In our research, a strong correlation has been found between any hour and its next hour. Based on regression analysis, a linear regression model is fitted which can be used in short term wind speed forecast using the forecast data from the ARMA (Autoregressive and Moving Average) model.

The ARMA model for wind speeds and the electric characteristic of wind turbine generators are introduced in Section 3.1. Based on the prediction of the developed ARMA model, three years forecast data have been obtained. The correlation has been analyzed among hour $t-1$ and the following three hours from the prediction, and the results are shown in Table 6.1. It shows correlation coefficient near 1(1-highest correlation, 0-no correlation) for the next hour and decays for the second and third hours. Linear regression analysis has been conducted and the results are shown in Fig. 6.1. Fig. 6.1 shows strong and linear relationship of wind speed between the current hour and the next hour.

Table 6.1 Correlation Coefficients of Continuous Hours

Hour	t-1	t	t+1	t+2
	Correlation Coefficients			
t-1	1	0.915253	0.798026	0.692238
t	0.915253	1	0.915255	0.798028
t+1	0.798026	0.915255	1	0.915255
t+2	0.692238	0.798028	0.915255	1

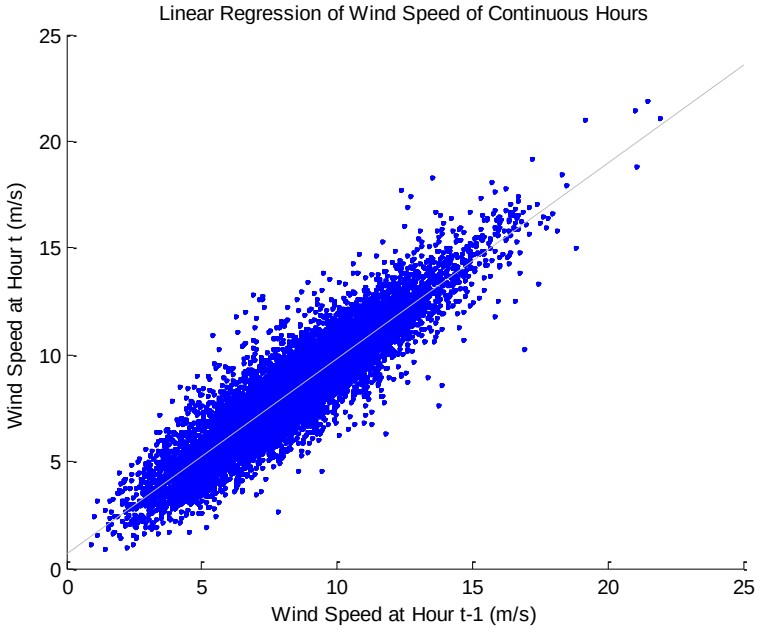

Fig. 6.1 The relation between wind speed at hour *t-1* and hour *t*

Based on the regression analysis results, the short term wind speed forecasting model using the probability distribution of wind speed variation has been derived. Given the observed wind speed V_{t-1} for hour *t-1*, the predicted wind speed $\tilde{V}_t$ for hour *t* can be obtained as:

$$\tilde{V}_t = SV_t \left(V_{t-1}^l \le SV_{t-1} \le V_{t-1}^u \right) \tag{6.1}$$

where SV_t is the simulated wind speed at hour *t*, $V_{t-1}^l = \min(V_{t-1})$ and $V_{t-1}^u = \max(V_{t-1})$ represent the lower bound and upper bound respectively of V_{t-1}.

To obtain the probability distribution of variation of $\tilde{V}_t$, $\tilde{V}_t$ are equally grouped according to its numeric range. The predicted wind speed $\tilde{V}_t^x$ and its probability $p\left(\tilde{V}_t^x\right)$ for group *x* are calculated as:

$$\tilde{V}_t^x = \frac{1}{2}\left(\tilde{V}_t^{xl} + \tilde{V}_t^{xu}\right) \tag{6.2}$$

$$p\left(\tilde{V}_t^x\right) = \frac{num(SV_t \mid \tilde{V}_t^{xl} \le SV_t \le \tilde{V}_t^{xu})}{num\left(SV_t\right)} \tag{6.3}$$

where $\tilde{V}_t^{xl}$ and $\tilde{V}_t^{xu}$ are the lower and upper bounds respectively of $\tilde{V}_t^{x}$, and num is the number of samples with given conditions in parentheses.

The forecast wind power output for a wind turbine is calculated using the method introduced in Section 3.1.2. The probability distribution of forecast wind power can be derived correspondingly.

The short term forecast error of wind speed was analyzed using a statistical method by previous researchers [44, 53]. In our analysis, the bidding error is used in evaluating the impacts of WPP bidding strategies on the system reserve requirement. The wind power forecast error and WPP bidding strategy are combined to determine the bidding error.

6.2.2 Trading wind power

In addition to the variation of forecast wind power, bidding strategies of WPP also impact the market behavior. The bidding strategies are based on the forecast wind power, the payment scheme from the market and the price pattern of regulation market.

In [52], a method of minimizing the imbalance cost has been proposed to determine the optimal energy sold on the advance market. The imbalance cost is caused by the difference between bidding power and real power. The energy provider will be paid a down regulation price for under-bid power and it will pay for an up regulation price for over-bid power. Here the down regulation price is lower while the up regulation price is higher than the energy price. Reference [53] further evaluated the imbalance cost of wind generation by examining the optimal bidding strategy. The results confirmed that suggested bidding strategy would obtain equal or higher revenue than the strategy that the player bids the forecast wind power and pay for the imbalance cost. These analyses provide a thorough examination of different bidding strategies of

the WPP. The benefits that WPP can procure from the bidding strategy in [53] is limited and the results in [52] show that the imbalance price and its relativity to the contract price determine the total revenue of the WPP. Therefore, the behavior of WPP in our analysis is only based on the wind power forecast.

In our analysis, based on the obtained probability distribution of wind power forecast, different wind power bidding strategies are considered. The impacts of different bidding strategies on system price and reliability are also examined. Since the wind power penetration is relatively low in many countries, they are assumed to be the price-taker in market operation [24, 52, 53, 118]. It is further assumed that the WPP is paid according to the real output power regardless of its imbalance, and that the WPP will not make use of previous price patterns to make its bidding strategy.

Under these assumptions, two bidding strategies for WPP have been evaluated in this thesis. Strategy S1 assumes that the WPP bids the power with the highest forecast probability. Strategy S2 assumes that the WPP bids the expected forecasted wind power.

6.3 Contingency Reserve Modeling

In a contingency state, system operators reschedule generation or make load curtailments to ensure the secure operation of the power system. Customers can purchase operating reserve to avoid load curtailment. The structure of the CR market can affect the reserve cost. Based on the pay-as-used policy, a CR market is formulated and cleared simultaneously with the energy market.

The energy market and reserve market can be cleared simultaneously or sequentially in different market structures [15]. The sequential approach clears markets in a sequence and requires one market's result as the starting point of the next market. The simultaneous market simplifies the market auction process and dispatch as the energy

and reserve at the same time. The reserve price can be determined according to the reserve capacity committed or the reserve power delivered [76]. The main function of the CR market is to provide reserve economically when a unit outage occurs. In a CR market, generators scheduled to provide CR will be paid according to dispatch capacity and zonal reserve price. Customers would purchase reserve from the market by weighting the reserve cost with the interruption cost.

6.3.1 Customer reserve requirements

The customer interruption cost in system operation depends on the time, load curtailment and duration of an interruption, and is also related to CR purchased by the customer.

The reserve purchased by a customer is determined by weighting the interruption cost and reserve cost. Customer interruption costs are indirectly determined by the customer damage functions (CDFs). The reserve cost depends on reserve price. In operating period *t*, the objective function of reserve purchase of a customer at bus *i* at reserve zone *z* for contingency state *j* is to minimize its net cost represented as:

$$\prod_{i\,d}^{t\,j} = CC\left(\Delta P_{i\,d}^{t\,j}\right) + \rho_{e\,i}^{t\,j} P_{i\,d}^{t\,j} \tag{6.4}$$

where $\Delta P_{i\,d}^{t\,j} = P_{i\,d}^{t\,0} - P_{i\,d}^{t\,j}$ is the load curtailment, $P_{i\,d}^{t\,0}$ and $P_{i\,d}^{t\,j}$ are demand for normal and contingency states respectively, $\rho_{e\,i}^{t\,j}$ is the nodal price.

Customer cost function $CC_{i\,d}^{t\,j}$ is calculated as:

$$CC_{i\,d}^{t\,j} = \left(\Delta P_{i\,d}^{t\,j}\right) \times CDF_{i\,d}\left(OD^{t\,j}\right) \tag{6.5}$$

where customer damage function $CDF_{i\,d}\left(OD^{t\,j}\right)$ is a function of outage duration $OD^{t\,j}$.

6.3.2 Contingency reserve deployment

A customer submits reserve biddings based on its net cost and a CR provider submits

offers according to the reserve cost in the reserve market. The objective of CR dispatch is to minimize the total system reserve cost. The total reserve cost $\Gamma_z^{t\,j}$ for state *j* and time *t* at zone *z* is determined by:

$$\Gamma_z^{t\,j} = \sum_{i \in z} \left[\sum_{d \in NL_i^j} \prod_{i\,d}^{t\,j} + \sum_{g \in NG_i^{t\,j}} RC_{gr}\left(R_{i\,g}^{t\,j}\right) \right] \tag{6.6}$$

where NL_i^j and $NG_i^{t\,j}$ are the number of load sectors and the number of generators at bus *i* respectively. $RC_{gr}\left(\mathrm{R}_{i\,g}^{t\,j}\right)$ is the cost function for generator *g* providing reserve $R_{i\,g}^{t\,j}$.

6.4 Reliability Modeling

In power system operation, the outage rate of units is the only concern because the repair can be neglected for a short operating period. The outage replacement rate (ORR) of a unit is defined as the probability that the unit fails and is not replaced during operating period *T* [63]. The ORR_i for unit *i* with failure rate λ_i is calculated as:

$$ORR_i = 1 - e^{-\lambda_i T} \approx \lambda_i T \left(if\ \lambda_i T << 1\right) \tag{6.7}$$

The probability A_i that the unit is operating during operating period *T* is calculated as $A_i = 1 - ORR_i$. For an operating period *t*, the probability $p^{t\,j}$ of state *j* with m_t operating components and *s* failed components is determined as:

$$p^{t\,j} = \prod_{i=1}^{s} ORR_i \times \prod_{i=s+1}^{m_t} A_i \tag{6.8}$$

The reliabilities of transmission lines and generating units are considered in determining the system operating states.

6.5 Problem Formulation

The OPF problem is formulated to determine the nodal energy price, regional reserve

price, the optimal reserve allocation and the nodal operational reliability. The objective of the OPF problem is to minimize the total system cost. For a system with N_z reserve zones, the objective function for period *t* and state *j* can be formulated as:

$$\begin{aligned}\min\ f_{t,j} = &\sum_{i\in N_g^{t\,j}}\sum_{g\in NG_i^{t\,j}} C_{i\,g}\left(P_{i\,g}^{t\,j}, Q_{i\,g}^{t\,j}\right) \\ &+\sum_{z\in N_z}\sum_{i\in z}\left[\sum_{d\in NL_i^j} CC\left(\Delta P_{i\,d}^{t\,j}\right)+\sum_{g\in NG_i^{t\,j}} RC_{gr}\left(R_{i\,g}^{t\,j}\right)\right]\end{aligned} \tag{6.9}$$

subject to the following constraints:

Power flow constraints:

$$\begin{aligned}&\sum_{g\in NG_i^{t\,j}}\left(P_{i\,\mathrm{g}}^{t\,j}+R_{i\,g}^{t\,j}\right)+WP_{i\,a}^{t}-\sum_{d\in NL_i^j}\left(P_{i\,d}^{t\,0}-\Delta P_{i\,d}^{t\,j}\right) \\ &\qquad=\sum_{i=1}^{N} V_i^{t\,j}V_k^{t\,j}\left|Y_{ik}^{\mathrm{t}\,j}\right|\cos\left(\theta_i^{t\,j}-\theta_k^{t\,j}-\delta_{ik}^{t\,j}\right)\end{aligned} \tag{6.10}$$

$$\begin{aligned}&\sum_{g\in NG_i^{t\,j}} Q_{i\,g}^{t\,j}-\sum_{d\in NL_i^j}\left(Q_{i\,d}^{t\,0}-\Delta Q_{i\,d}^{t\,j}\right) \\ &\qquad=\sum_{i=1}^{N} V_i^{t\,j}V_k^{t\,j}\left|Y_{ik}^{\mathrm{t}\,j}\right|\sin\left(\theta_i^{t\,j}-\theta_k^{t\,j}-\delta_{ik}^{t\,j}\right)\end{aligned} \tag{6.11}$$

where $WP_{i\,a}^{t}$ is actual wind power production of WPP.

Generating unit limits:

$$P_{i\,g}^{\min}\le P_{i\,g}^{t\,j}+R_{i\,g}^{t\,j}\le P_{i\,g}^{\max} \tag{6.12}$$

$$Q_{i\,g}^{\min}\le Q_{i\,g}^{t\,j}\le Q_{i\,g}^{\max} \tag{6.13}$$

$$\Delta P_{i\,g}^{low}\le \Delta P_{i\,g}^{t\,j}+R_{i\,g}^{t\,j}\le \Delta P_{i\,g}^{up} \tag{6.14}$$

Load curtailment limits, voltage limits and transmission line limits are given by (6.15), (6.16)and (6.17) respectively:

$$0\le \Delta P_{i\,d}^{t\,j}\le \Delta P_{i\,d}^{\max} \tag{6.15}$$

$$\left|V_i^{j}\right|^{\min}\le\left|V_i^{t\,j}\right|\le\left|V_i^{j}\right|^{\max} \tag{6.16}$$

$$\left|S_{i\,k}^{j}\right|\le\left|S_{i\,k}^{j}\right|^{\max} \tag{6.17}$$

Zonal reserve constraints:

$$\sum_{i \in z} R_{i\,d}^{t\,j} - \sum_{i \in z} R_{i\,g}^{t\,j} = 0 \tag{6.18}$$

Rserve capacity limit for a reserve provider:

$$0 \le R_{i\,g}^{t\,j} \le R_{i\,g}^{\max} \tag{6.19}$$

where $R_{i\,g}^{\max}$ is the maximum reserve bidding.

A Lagrangian function $L_{t\,j}$ was formulated to solve the problem. The energy output $\left(P_{i\,g}^{t\,j}, Q_{i\,g}^{t\,j}\right)$ and the reserve generation $R_{i\,g}^{t\,j}$, and the customer's load curtailment $\Delta P_{i\,d}^{t\,j}$ can be determined by solving $L_{t\,j}$.

The nodal price $\rho_{e\,i}^{t\,j}$, expected nodal price $\overline{\rho}_{e\,i}^{t}$ and standard deviation $\sigma_{e\,i}^{t}$ can also be determined as:

$$\rho_{e\,i}^{t\,j} = \frac{\partial L_{t\,j}}{\partial P_i^{t\,j}} \quad (\$ / MW) \tag{6.20}$$

$$\overline{\rho}_{e\,i}^{t} = \sum_{j \in NOS^t} p^{t\,j} \rho_{p\,i}^{t\,j} \tag{6.21}$$

$$\sigma_{e\,i}^{t} = \sqrt{\sum_{j=1}^{NOS^t} p^{t\,j} \times \left(\rho_{e\,i}^{t\,j} - \overline{\rho}_{e\,i}^{t}\right)^2} \tag{6.22}$$

The nodal unit commitment risk (*NUCR*) at node *i* and time *t* are determined as:

$$\begin{aligned} NUCR_i^t = & \sum_{j \in NOS^t} p^{t\,j} \left(\Delta P_{i\,c}^{t\,j} > 0\right) \\ & \bigcup \sum_{j \in NOS^t} p^{t\,j} \left(\Delta P_{i\,c}^{t\,j} = 0 \bigcap \left(P_{i\,g}^{t\,j} + R_{i\,g}^{t\,j} = P_{i\,g}^{\max} \left(\, for \forall g \,\right)\right)\right) \end{aligned} \tag{6.23}$$

The simulation procedure for the problem is shown in Fig. 6.2. The bidding wind powers are explicitly considered in the unit commitment process. In the real time dispatch, the real wind powers are dispatched. In this way, the wind power bidding errors impact the market operations.

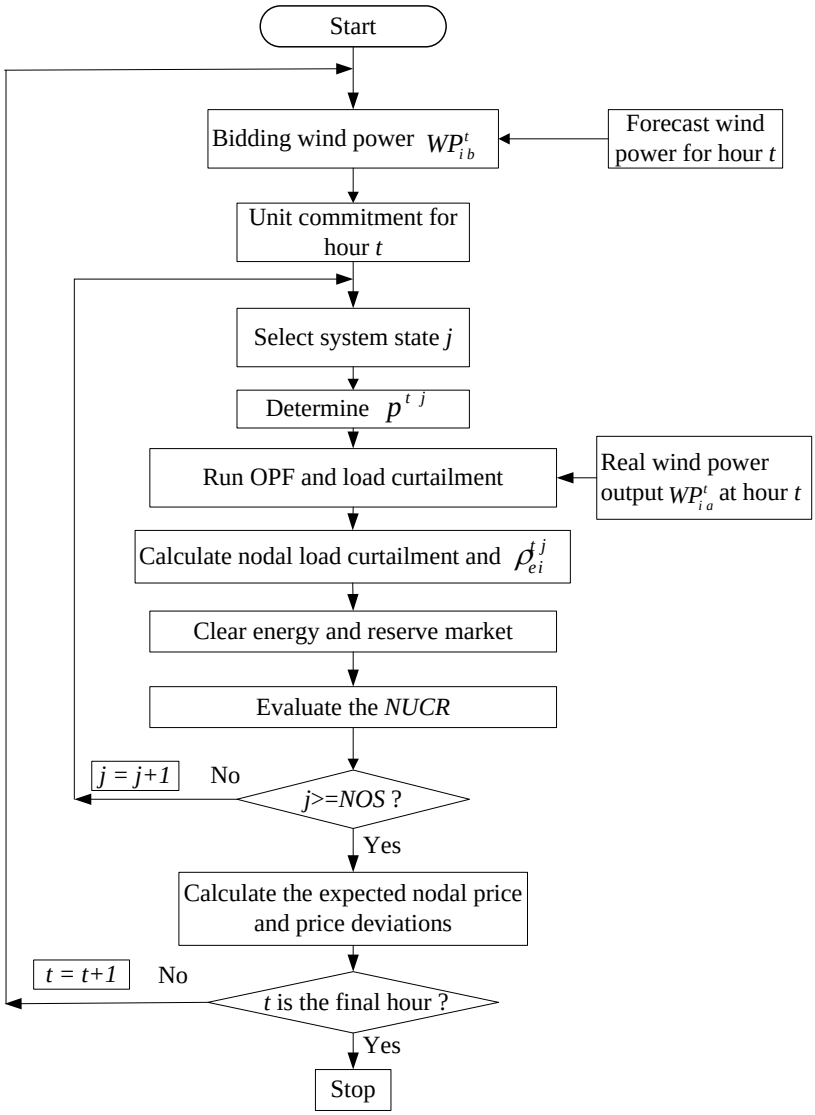

Fig. 6.2 Flowchart of the simulation to determine wind power impacts on power market

6.6 Case Studies

The RBTS [98] was used to illustrate the proposed method. The system has been modified by adding an identical parallel transmission line between bus 5 and bus 6. The market clearing period is assumed to be 1 hour. The nodal reliability and nodal price for 24 hours of the 361th day of the RBTS are evaluated to illustrate the proposed technique. The load profile of the day is obtained from [98].

6.6.1 Nodal indices without reserve and wind power

The nodal prices and reliability performance of the energy market without emergency reserve have been analyzed. The expected hourly nodal prices for each node were obtained and are shown in Fig. 6.3. The nodal prices represent the expected values of energy considering different outage states at each node. The price profiles are similar for each node. Price is high when the load level is high at hour 18-20. Bus 2 has the lowest price compared with other nodes at any hour because it is a generation node.

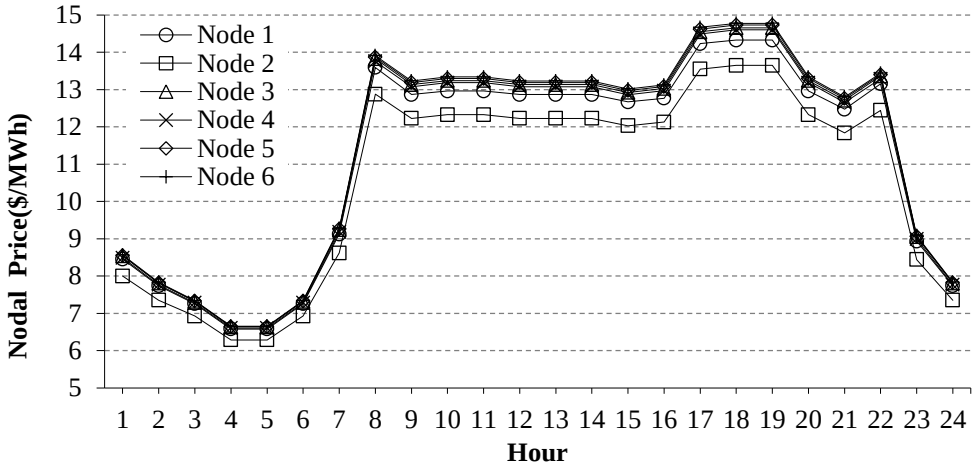

Fig. 6.3 Nodal energy prices of different nodes for 24 hours

The load curtailment for each node is different due to the system configuration and the customer reliability requirements. The *NUCR* are evaluated and shown in Fig. 6.4. *NUCR* at node 2 are lower than those of other nodes. The differences of *NUCR* between nodes are due to the location and reliability requirements of corresponding customers. The variation of *NUCR* between hours is caused by the load variation and corresponding generation dispatch at different hours.

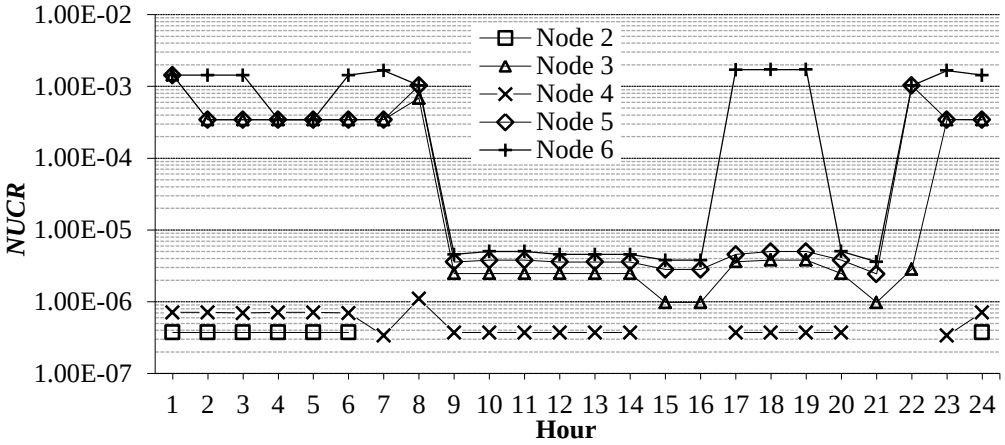

Fig. 6.4 *NUCR* for 24 hours

The nodal price and *NUCR* show the overall energy cost and reliability of each load node in the system. The integration of contingency reserve market and wind power are expected to reduce price fluctuation and improve system reliability.

6.6.2 Impacts of contingency reserve

The nodal price and nodal reliability depend on generation and reserve deployment and customer reliability requirements. Fig. 6.5 shows the expected nodal prices at node 3 with and without CR. The expected nodal price for each hour is reduced when CR is committed. The expected nodal price reduction for hours 8-16 is more significant because more reserve is available. The same trend can be observed at other nodes.

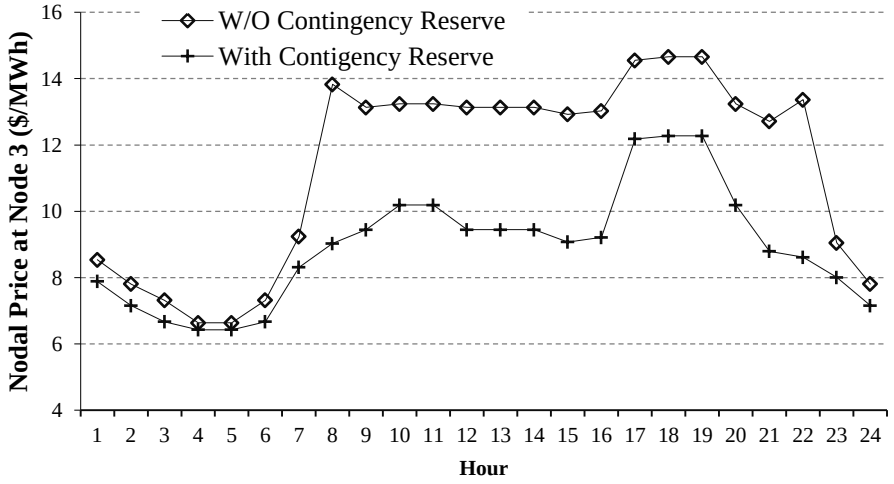

Fig. 6.5 Nodal Price at node 3 for 24 hours

Fig. 6.6 shows the *NUCR*s for node 3. The *NUCR*s for 24 hours are reduced after contingency reserve is added. *NUCR* is also improved at the other nodes.

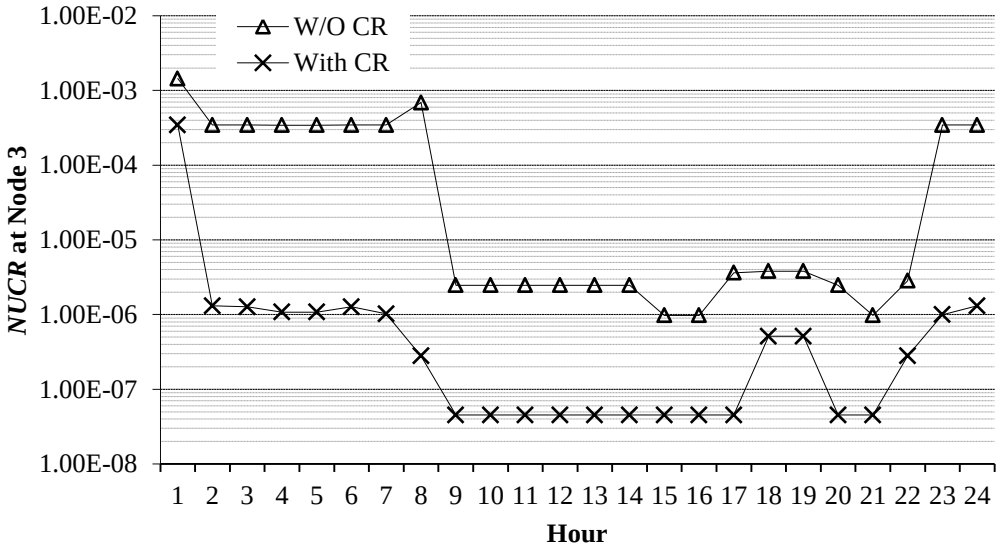

Fig. 6.6 *NUCR* at node 3

The nodal prices at node 3 for some representative states are shown in Fig 6.7. Without CR, there are nodal price spikes for some contingencies due to generator outages (states 12-19) and combinational outages of generators and transmission lines (states 85-95). Therefore those price spikes are removed after committing CR. However, the price spikes still exist for some transmission outages (states 47-57) such as state 49 (L2 and L3 are out of service) even after committing CR due to transmission constraints. CR cannot reduce the price spikes of some contingency states caused by transmission line outages.

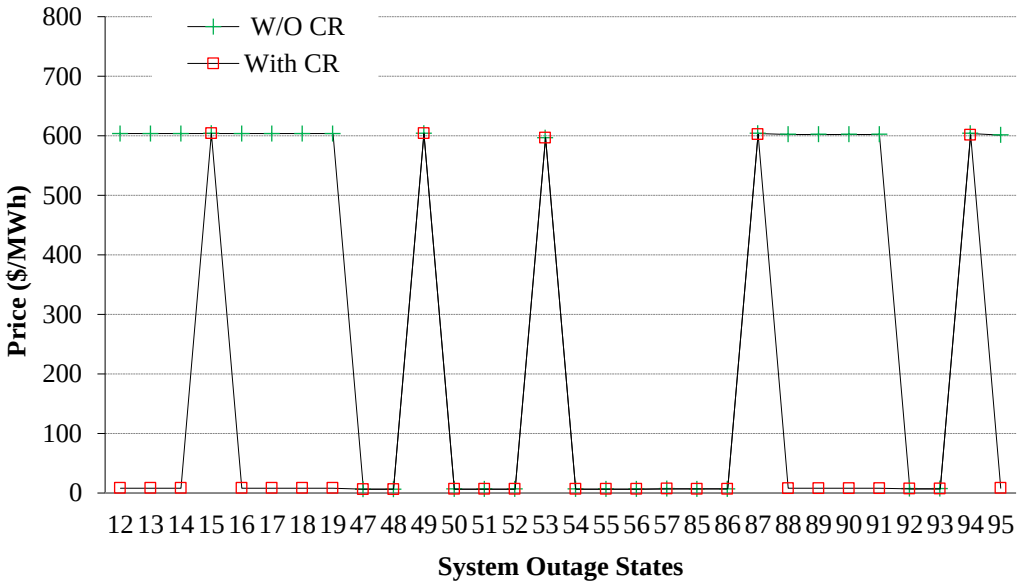

Fig. 6.7 Nodal Prices for node 3 at hour 6

6.6.3 Impacts of wind power

20×1.5MW WTGs are assumed to be installed at node 3 of the RBTS. The specifications of the WTG are shown below. The cut-in, cut-out and rated wind speeds are 3.5m/s, 20m/s and 11.5m/s respectively. The parameters of GE's 1.5 MW WTG were obtained from GE's website and are shown below [152].

Table 6.2. Technical Data

Operating Data	
Rated Capacity	1,500 kW
Temperature Range: Operation: Survival: (with Cold Weather Extreme Package)	-30°C-+40°C -40°C-+50°C
Cut-in Wind Speed	3.5m/s
Cut-out Wind Speed	20 m/s
Rated Wind Speed	11.5 m/s
Wind Class – IEC	IIIb($V_{e50} = 52.5\,m/s$, $V_{ave} = 8.0\,m/s$)
Electrical Interface	

Frequency	50/60Hz
Voltage	690V
Rotor	
Rotor Diameter	82.5m
Swept Area	5346 m^2
Tower	
Hub Heights:	80m
Power Control	Active Blade Pitch Control

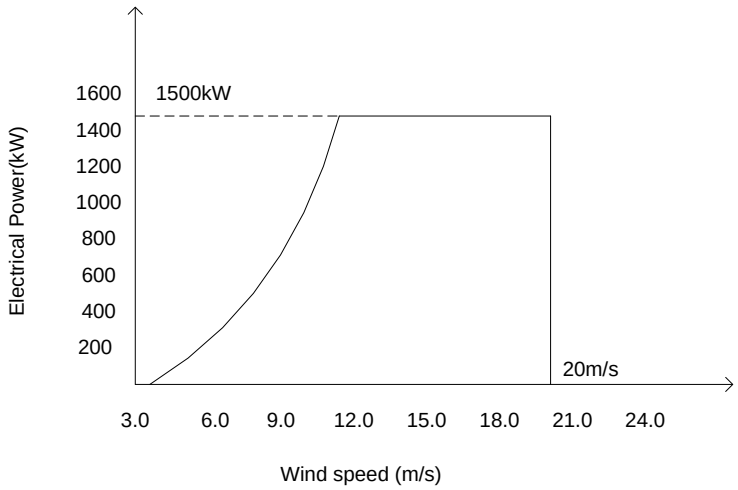

Fig. 6.8 Power curve of GE 1.5 MW WTG

The wind speed data obtained from [106] have been utilized. An ARMA model has been developed based on three years' wind speed data at ten minutes interval. Three years forecast data have been obtained through the model.

The wind speeds at two representative hours (5 and 14) were observed as 7.89-8.95m/s and 10.55-12.08 m/s. The forecast wind power distribution for hour 6 and hour 15 are shown in Table 6.3. The actual wind power production for each wind turbine at hour 6 and hour 15 are 0.56 MW and 1.5 MW respectively.

Table 6.3 Probability Density Distribution of Wind Power at Hour 6 and Hour 15

Wind Power (MW)	Hour 6	Hour 15
	Probability	Probability
0.1	0.014412	0
0.2	0.032826	0.000934
0.3	0.079263	0.002801
0.4	0.152122	0.001867
0.5	0.142781	0.006536
0.6	0.15052	0.013072
0.7	0.141446	0.023343
0.8	0.096878	0.045752
0.9	0.072858	0.052288
1	0.044035	0.072829
1.1	0.029624	0.093371
1.2	0.016813	0.11578
1.3	0.010408	0.112045
1.4	0.005604	0.102708
1.5	0.010408	0.356676

15 groups of wind power have been generated for the two bidding strategies S1 and S2 from the forecast wind speed data. According to the bidding strategies of S1 and S2, the bidding powers of S1 are 0.4MW and 1.5MW for each WTG, and the bidding powers for S2 are 0.63 MW and 1.25MW for each WTG for hours 6 and 15 respectively. The unit commitment is based on the principle that the wind energy should be consumed first. Bidding wind power of S1 and S2 and the real wind power output for 24 hours are also shown in Table 6.4.

Table 6.4 Wind power providers' bidding power and real power output

Hour	Bidding Power		Real Power
	S1(MW)	S2(MW)	(MW)
1	8	11.054	12.600
2	12	13.392	9.320
3	6	9.422	9.876
4	8	10.254	13.622
5	14	14.066	11.658
6	8	12.604	11.202
7	12	13.038	29.544
8	30	24.366	30
9	30	29.624	30
10	30	29.534	30
11	30	29.940	30
12	30	29.750	30
13	30	29.650	30
14	30	26.158	28.264
15	30	25.036	30
16	30	29.580	30
17	30	29.632	30
18	30	30	30
19	30	30	30
20	30	29.938	30
21	30	29.770	30
22	30	29.722	30
23	30	29.500	30
24	30	27.957	23.832

The expected nodal prices and their standard deviations under different wind power bidding strategies are shown in Table 6.5. Reduction of the expected nodal prices for wind power bidding strategy S2 is larger than that of S1. The increase of price deviation is larger for S2 than that for S1. This is because bidding wind power of S1 is more close to the real wind power production at this hour and resulting committed units and CR deviate less from the real condition.

Table 6.5 Expected Nodal Price $\overline{\rho}_{ei}^{t}$ and Standard Deviation σ_{ei}^{t} at Hour 15

Nodes	$\overline{\rho}_{ei}^{t}$ ($/MWh)			σ_{ei}^{t} ($/MWh)		
	W/O Wind	S1	S2	W/O Wind	S1	S2
1	8.9093	7.6152	7.3720	10.8070	17.0130	18.8689
2	8.3717	7.2303	7.0118	10.0852	16.2757	17.6754
3	9.0726	7.7067	7.4628	13.8980	17.2708	19.0878
4	9.0166	7.6831	7.4421	13.1677	17.2579	19.0128
5	9.1026	7.7435	7.4994	13.8375	17.3747	19.1889
6	9.1316	7.7678	7.5229	13.9991	17.4395	19.2746

Fig. 6.9 shows the expected prices of node 3. The figure shows that the nodal prices have been reduced after the wind power penetration. For most periods, the two bidding strategies provide similar results. The prices for S1 and S2 at hours 14 and 15 are different since the wind power bidding errors of S1 lead to the reduction of reserve margin.

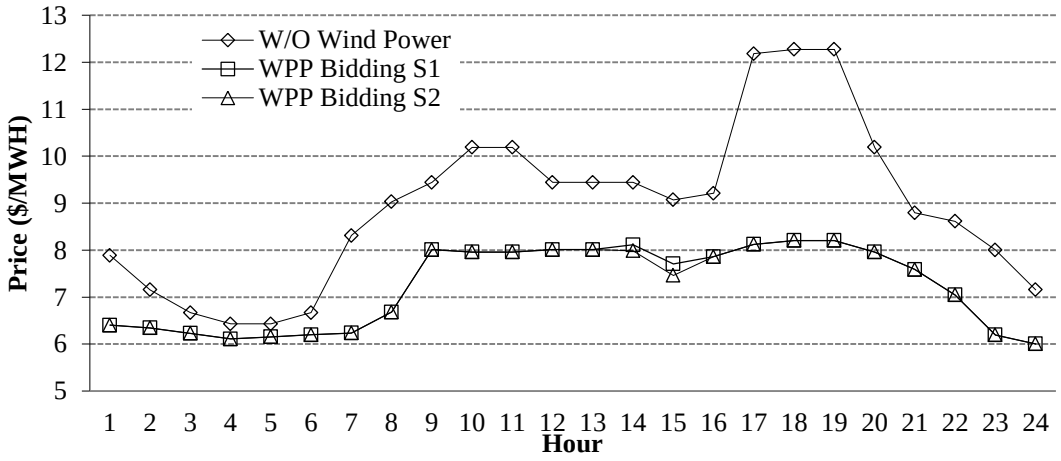

Fig. 6.9 Expected nodal prices at node 3 with different WPP bidding strategy

Fig. 6.10 shows the *NUCR* of node 3 for 24 hours. It shows that the penetration of wind power cannot always improve nodal reliability. Reliability improvement depends on many factors such as wind speed, load level, wind power bidding strategy, units committed, CR committed and the correlation among them. For hours 7-23, the

integration of bidding wind power reduces the committed units and CR, and the *NUCR* is improved for hours 7-8, 15-16, 18-19, 23 but not improved for the rest. At hour 15, the *NUCR* is reduced because the wind power bid with S1 is more close to the real wind power production, while the *NUCR* is increased if wind power bids with S2. Therefore, integration of wind power is a very complicated issue in market operation due to the intermittent and uncertain nature of wind speed.

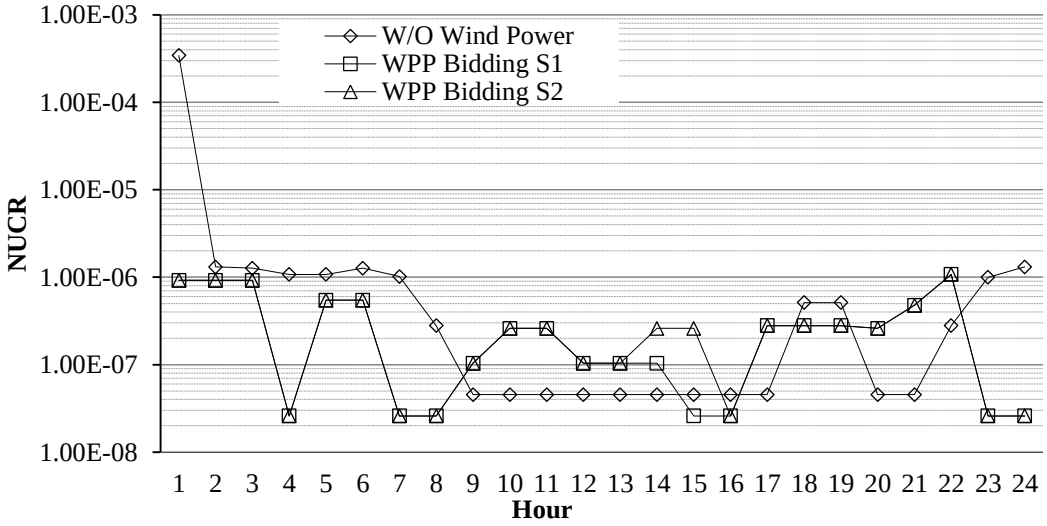

Fig. 6.10 *NUCR* at node 3 with different WPP bidding strategies

Fig. 6.11 shows the nodal prices at node 3 for the representative states at hour 6 considering bidding strategy S1. The number of price spikes has reduced after wind power penetration. Although wind powers are also paid according to the nodal price, customers still benefit from reduced nodal prices due to wind power penetration. Similar results are obtained when wind power bidding is with S2.

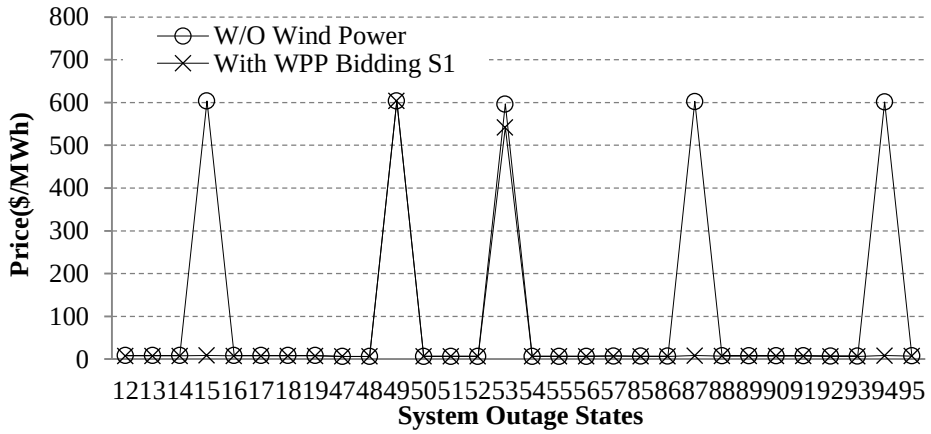

Fig. 6.11 Nodal Price at node 3 for different outage states at hour 6

6.7 Conclusions

This chapter has investigated the impacts of CR and wind power on nodal price and nodal reliability in deregulated power systems. CR market model has been developed with participation of customers. A simultaneous market for energy and CR has been formulated. The wind farm's bidding strategies have been analyzed based on short term wind power forecast. Hourly bidding wind power has been incorporated into the market clearing process. The operational reliability for each node has been evaluated using the *NUCR*.

NUCR and expected nodal price at all nodes decreased to some degree with CR integration. Price spikes are also reduced after the integration of CR. CR is important to improve the economic and reliable operation of power systems. The penetration of wind power reduces the expected nodal prices. But the variation of nodal price increases due to the intermittent characteristic of wind energy and WPP bidding strategies. The impacts of wind power on NUCR are affected by the wind power bidding errors, the load level and their correlations. The results provide very useful information for system operators and customers to make optimal decisions in a deregulated power market with wind penetration.

Chapter 7 Conclusions and Recommendations

7.1 Conclusions

In this thesis, the impacts of renewable energy on the power market operation have been investigated in terms of system reliability, electricity price and system reserve deployments. New techniques that can evaluate these impacts are important for policy makers, system operators, renewable energy providers and market participants to optimize the total or individual benefits in the competitive power market operation.

The background of the research work has been described in Chapter 1. The deregulation process of power system and existing power system structures have been introduced. The renewable energy application and penetration in power system have also been presented.

The state of the art of power system economic operation and reliability evaluation methods has been introduced in Chapter 2, which provide the theoretical basis for the reliability and power market analysis. The economic dispatch is the basis for the optimal energy dispatch in both conventional and deregulated power systems. The OPF techniques implement the economic and security constraints in energy dispatch and are the basic techniques widely used in existing power systems to determine locational energy prices. The nodal price and nodal reliability are adopted in deregulated power systems to evaluate the locational energy cost and reliability levels. New evaluation techniques need to be developed for examining the impacts of renewable energy on locational customer energy cost and reliability.

The intermittent and chronological characteristics of renewable energy sources have been investigated in Chapter 3, which provides the basis for research work in Chapter 5 and 6. The time series models of wind speed and solar radiation have been

developed using ARMA model. The outputs of the renewable energy conversion systems have been obtained. The unpredictable random variation of solar and wind power need to be accounted for when integrating renewable power into existing power market operation.

The stochastic variations of renewable energy need to be balanced by the system reserve. In the power market, reserves are unbundled from energy and are important ancillary services. Therefore firstly the issue of reserve pricing and deployments has been investigated through co-optimized energy and reserve market in Chapter 4. In the proposed two-step energy and reserve market clearing process, the optimal energy and contingency reserves allocation have been determined. Customers' reserve requirements are explicitly considered in the reserve allocation. The reserve costs and reliability risks of customers have also been evaluated for different reserve requirements. Customers who choose higher reliability levels by purchasing more reserve can utilize more energy at contingency states and have less load interruptions; however, they will pay higher prices for both the energy and reserve. The designed market ensures the allocation of reserve in favor of customers who have higher reliability requirements.

Considering the random variation and chronological characteristics of solar power, a technique using pseudo-sequential Monte Carlo simulation is proposed in Chapter 5 to evaluate the penetration of solar power in deregulated power systems. The solar power generation has been examined using the PV array. The PV array power output variations are examined through the probability density function in the Monte Carlo simulation. Two types of spinning reserves are modeled to meet the requirements of solar power variation and generation deficit in contingency states. To utilize solar power more reliably, the solar power can penetrate as additional energy and the solar power variation should be accounted for by enough reserves.

Renewable energy sources also participate in the power market operation by bidding

into the energy market to optimize their benefits. The impacts of wind farms' bidding strategies on nodal price and nodal reliability in deregulated power systems have been investigated in Chapter 6. The bidding strategies of wind farms have been analyzed based on the short term wind power forecasts. The energy and reserve dispatch have explicitly considered different wind farms' biddings. The bidding errors of wind power increase the uncertainty of wind power and may impair customer reliability when the power output is relatively high. Participation of wind power producers as price-takers in the market operation reduces the energy prices. It is necessary to quantify the impacts of wind power penetration on reliability and energy prices for the economic and reliable utilization of wind power.

The research work described in Chapter 4 has analyzed the reliability issues in power markets, which is the primary work needed for the objective of thesis to evaluate the impacts of renewable power on power market operation. The research works described in Chapters 5 and 6 have evaluated the impacts of renewable energy on power market operation, which is another objective of the thesis, from the viewpoint of reliability, reserve and energy dispatch, customer cost and energy prices. The techniques for analyzing impacts of renewable energy on market price and system reliability are useful for policy makers, system operators and market participants in order to make optimal decisions in power market operation with renewable energy.

7.2 Future Work

The micro-grid or smart grid with renewable energy penetrations are hot topics. The small scale distributed renewable energy generations are finding favor in many countries. The distributed renewable energy can be consumed by local customers directly. The energy storage plays an important role in balancing energy in smart grids. The renewable energy providers or users can make energy replacements through energy storage. The interactions between smart grids and power system provide energy and information exchanges. Customers can sell back energy to power systems

when load level is low and make load shifting using energy storage to profit from the system energy price variations. In smart grids, coordinating different renewable energy considering their correlations can increase the efficiency of energy utilizations.

For future work considering economic and reliable operation in smart grids with renewable penetrations, some suggestions are as follows:

1. In smart grids, correlation between different renewable sources should be considered in designing an optimal energy management scheme to improve customer reliability and energy prices.

2. In order to optimize customer benefits, the energy replacements using renewable energy and energy storage can be considered to sell back energy when the energy prices are high and purchase energy when the energy prices are low.

3. The reliability of smart grids can be improved through energy exchanges with the power system. The impacts of renewable energy variations on smart grid reliability should also be evaluated.

References

[1] M. Shahidehpour and M. Alomoush, *Restructured Electrical Power Systems: Operation, Trading, and Volatility*. New York: Marcel Dekker, 2001.

[2] M. D. Ilic, F. D. Galiana, and L. H. Fink, *Power Systems Restructuring : Engineering and Economics*. Boston: Kluwer, 1998.

[3] D. S. Kirschen, G. Strbac, and I. Ebrary, *Fundamentals of Power System Economics*. Chichester, West Sussex, England: Hoboken, NJ :John Wiley & Sons, 2004.

[4] J. D. Weber, "Individual Welfare Maximization in Electricity Maeket including Consumer and Full Transmission System Modelling," Ph.D Thesis, University of Illinois at Urbana-Champaign, 1999.

[5] U. S. E. I. Administaraion. *Energy Policy Act of 1992*. Available: http://www.eia.gov/oil_gas/natural_gas/analysis_publications/ngmajorleg/enrgypolicy.html

[6] F. E. R. Commission. (1996). *FERC Order No.888 : Transmission Open Access. Promoting Wholesale Competition Through Open Access Non-discriminatory Transmission Services by Public Utilities; Recovery of Stranded Costs by Public Utilities and Transmitting Utilities (Final Rule)*. Available: http://www.ferc.gov/legal/maj-ord-reg/land-docs/order888.asp

[7] F. E. R. Commission. (1996). *FERC Order No.889 : Open Access Same-Time Information System (formerly Real-Time Information Networks) and Standards of Conduct*. Available: http://www.ferc.gov/legal/maj-ord-reg/land-docs/order889.asp

[8] F. E. R. Commission. (1999). *FERC Order No.2000 : Establishment of Regional Transmission Organizations proposals (Final Rule)*. Available: http://www.ferc.gov/legal/maj-ord-reg/land-docs/RM99-2A.pdf

[9] F. E. R. Commission. (2005). *Energy Policy Act (EPAct) of 2005*. Available: http://www.ferc.gov/legal/fed-sta/ene-pol-act.asp

[10] F. E. R. Commission. (2007). *FERC Order No.890 : Preventing Undue Discrimination and Preference in Transmission Service (Final Rule)*. Available: http://www.ferc.gov/whats-new/comm-meet/2007/021507/E-1.pdf

[11] *PJM - Markets & Operations*. Available: http://www.pjm.com/markets-and-operations.aspx

[12] E. I. Administration. *Electricity Reform Abroad and U.S. Investment*. Available: http://www.eia.gov/emeu/pgem/electric/

[13] K. Bhattacharya, M. H. J. Bollen, and J. E. Daalder, *Operation of Restructured Power Systems*. Boston: Kluwer Academic Publishers, 2001.

[14] E. M. Authority. (2009). *Introduction to the National Electricity Market of Singapore*. Available: http://www.ema.gov.sg/media/files/books/intro_to_nems/Introduction%20to%20the%20NEMS_Jul%2009.pdf

[15] M. Shahidehpour, H. Yamin, and Z. Li, *Market Operations in Electric Power Systems*: Wiley Online Library, 2002.

[16] G. M. Masters, *Renewable and Efficient Electric Power Systems*. Hoboken, NJ: John Wiley & Sons, 2004.

[17] *RenewableUK - The Technology of Turbines*. Available: http://www.bwea.com/ref/tech.html

[18] *European Wind Energy Association - EWEA*. Available: http://www.ewea.org/

[19] *NREL: Learning - Solar Energy Basics*. Available: http://www.nrel.gov/learning/re_solar.html

[20] (2010). *2008 Solar Technologies Market Report*. Available: http://www.nrel.gov/analysis/pdfs/46025.pdf

[21] *Renewables 2011 Global Status Report*. Available: http://www.ren21.net/

[22] L. Bird, R. Wüstenhagen, and J. Aabakken, "A Review of International Green Power Markets: Recent Experience, Trends, and Market Drivers," *Renewable and Sustainable Energy Reviews*, vol. 6, pp. 513-536, 2002.

[23] C. Weber, "Adequate Intraday Market Design to Enable the Integration of Wind Energy into the European Power Systems," *Energy Policy*, vol. 38, pp. 3155-3163, 2010.

[24] B. C. Ummels, M. Gibescu, E. Pelgrum, W. L. Kling, and A. J. Brand, "Impacts of Wind Power on Thermal Generation Unit Commitment and Dispatch," *IEEE Transactions on Energy Conversion*, vol. 22, pp. 44-51, 2007.

[25] F. Bouffard and F. D. Galiana, "Stochastic Security for Operations Planning With Significant Wind Power Generation," *IEEE Transactions on Power Systems*, vol. 23, pp. 306-316, 2008.

[26] R. Billinton, B. Karki, R. Karki, and G. Ramakrishna, "Unit Commitment Risk Analysis of Wind Integrated Power Systems," *IEEE Transactions on Power Systems*, vol. 24, pp. 930-939, 2009.

[27] R. Rajagopal, E. Bitar, P. Varaiya, and F. Wu, "Risk-Limiting Dispatch for Integrating Renewable Power," *International Journal of Electrical Power & Energy Systems*, vol. 44, pp. 615-628, 2013.

[28] R. Boqiang and J. Chuanwen, "A Review on the Economic Dispatch and Risk Management Considering Wind Power in the Power Market," *Renewable and Sustainable Energy Reviews*, vol. 13, pp. 2169-2174, 2009.

[29] T. J. Hammons, "Integrating Renewable Energy Sources into European Grids," *International Journal of Electrical Power & Energy Systems*, vol. 30, pp. 462-475, 2008.

[30] L. Soder, L. Hofmann, A. Orths, H. Holttinen, W. Yih-Huei, and A. Tuohy, "Experience From Wind Integration in Some High Penetration Areas," *IEEE Transactions on Energy Conversion*, vol. 22, pp. 4-12, 2007.

[31] C. Munoz, E. Sauma, J. Contreras, J. Aguado, and S. de la Torre, "Impact of High Wind Power Penetration on Transmission Network Expansion Planning," *IET Proceedings, Generation, Transmission & Distribution*, vol. 6, pp. 1281-1291, 2012.

[32] Y. M. Atwa and E. F. El-Saadany, "Reliability Evaluation for Distribution System With Renewable Distributed Generation During Islanded Mode of Operation," *IEEE Transactions on Power Systems,* vol. 24, pp. 572-581, 2009.

[33] T. Ackermann, *Wind Power in Power Systems*. Chichester, UK: John Wiley, 2005.

[34] R. Billinton, Y. Gao, and R. Karki, "Composite System Adequacy Assessment Incorporating Large-scale Wind Energy Conversion Systems Considering Wind Speed Correlation," *IEEE Transactions on Power Systems,* vol. 24, pp. 1375-1382, 2009.

[35] R. Billinton and Y. Gao, "Multistate Wind Energy Conversion System Models for Adequacy Assessment of Generating Systems Incorporating Wind Energy," *IEEE Transactions on Energy Conversion,* vol. 23, pp. 163-170, 2008.

[36] M. H. Albadi and E. F. El-Saadany, "Overview of Wind Power Intermittency Impacts on Power Systems," *Electric Power Systems Research,* vol. 80, pp. 627-632, 2010.

[37] K. R. Voorspools and W. D. D'Haeseleer, "An Analytical Formula for the Capacity Credit of Wind Power," *Renewable Energy,* vol. 31, pp. 45-54, 2006.

[38] P. Hu, R. Karki, and R. Billinton, "Reliability Evaluation of Generating Systems Containing Wind Power and Energy Storage," *IET Proceedings, Generation, Transmission & Distribution,* vol. 3, pp. 783-791, 2009.

[39] J. Skea, D. Anderson, T. Green, R. Gross, P. Heptonstall, and M. Leach, "Intermittent Renewable Generation and the Cost of Maintaining Power System Reliability," *IET Proceedings, Generation, Transmission & Distribution,* vol. 2, pp. 82-89, 2008.

[40] Y. V. Makarov, P. V. Etingov, J. Ma, Z. Huang, and K. Subbarao, "Incorporating Uncertainty of Wind Power Generation Forecast into Power System Operation, Dispatch, and Unit Commitment Procedures," *IEEE Transactions on Sustainable Energy,* vol. 2, pp. 433-442, 2011.

[41] A. Papavasiliou, S. S. Oren, and R. P. O'Neill, "Reserve Requirements for Wind Power Integration: A Scenario-based Stochastic Programming Framework," *IEEE Transactions on Power Systems,* vol. 26, p. 2197, 2011.

[42] J. M. Morales, A. J. Conejo, and J. Pérez-Ruiz, "Economic Valuation of Reserves in Power Systems with High Penetration of Wind Power," *IEEE Transactions on Power Systems,* vol. 24, pp. 900-910, 2009.

[43] Y. Ding, P. Wang, L. Goel, P. C. Loh, and Q. Wu, "Long-Term Reserve Expansion of Power Systems With High Wind Power Penetration Using Universal Generating Function Methods," *IEEE Transactions on Power Systems,* vol. 26, pp. 766-774, 2011.

[44] H. Holttinen, "The Impact of Large Scale Wind Power Production on The Nordic Electricity System," *Doctor Thesis, VTT,* 2004.

[45] A. da Silva, W. S. Sales, L. A. da Fonseca Manso, and R. Billinton, "Long-term Probabilistic Evaluation of Operating Reserve Requirements with Renewable Sources," *IEEE Transactions on Power Systems,* vol. 25, pp. 106-116, 2010.

[46] P. Giorsetto and K. Utsurogi, "Development of A New Procedure for Reliability Modeling of Wind Turbine Generators," *IEEE Transactions on Power Apparatus and Systems*, pp. 134-143, 1983.

[47] R. Karki, P. Hu, and R. Billinton, "A Simplified Wind Power Generation Model for Reliability Evaluation," *IEEE Transactions on Energy Conversion*, vol. 21, pp. 533-540, 2006.

[48] R. Karki and R. Billinton, "Reliability/cost Implications of PV and Wind Energy Utilization in Small Isolated Power Systems," *IEEE Transactions on Energy Conversion*, vol. 16, pp. 368-373, 2001.

[49] P. Wang and R. Billinton, "Reliability Benefit Analysis of Adding WTG to A Distribution System," *IEEE Transactions on Energy Conversion*, vol. 16, pp. 134-139, 2001.

[50] A. Mehrtash, P. Wang, and L. Goel, "Reliability Evaluation of Power Systems Considering Restructuring and Renewable Generators," *IEEE Transactions on Power Systems*, vol. 27, pp. 243-250, 2012.

[51] A. Leite da Silva, L. Manso, S. Flávio, M. da Rosa, and L. Resende, "Composite Reliability Assessment of Power Systems with Large Penetration of Renewable Sources," in *Reliability and Risk Evaluation of Wind Integrated Power Systems*, R. Billinton, R. Karki, and A. K. Verma, Eds., ed: Springer India, 2013, pp. 107-128.

[52] G. N. Bathurst, J. Weatherill, and G. Strbac, "Trading Wind Generation in Short Term Energy Markets," *IEEE Transactions on Power Systems*, vol. 17, pp. 782-789, 2002.

[53] J. Matevosyan and L. Soder, "Minimization of Imbalance Cost Trading Wind Power on the Short-term Power Market," *IEEE Transactions on Power Systems*, vol. 21, pp. 1396-1404, 2006.

[54] F. Sensfuß, M. Ragwitz, and M. Genoese, "The Merit-order Effect: A Detailed Analysis of the Price Effect of Renewable Electricity Generation on Spot Market Prices in Germany," *Energy Policy*, vol. 36, pp. 3086-3094, 2008.

[55] E. Bitar, K. Poolla, P. Khargonekar, R. Rajagopal, P. Varaiya, and F. Wu, "Selling Random Wind," in *System Science (HICSS), 2012 45th Hawaii International Conference on*, 2012, pp. 1931-1937.

[56] A. Subramanian, E. Bitar, P. Khargonekar, and K. Poolla, "Market Induced Curtailment of Wind Power," in *IEEE Power and Energy Society General Meeting*, San Diego, California, USA, 2012.

[57] E. Y. Bitar, R. Rajagopal, P. P. Khargonekar, K. Poolla, and P. Varaiya, "Bringing Wind Energy to Market," *IEEE Transactions on Power Systems*, vol. 27, pp. 1225-1235, 2012.

[58] D. T. Ho, J. Frunt, and J. M. A. Myrzik, "Photovoltaic Energy in Power Market," in *Energy Market, 2009. EEM 2009. 6th International Conference on the European*, 2009, pp. 1-5.

[59] B. Elliston, M. Diesendorf, and I. MacGill, "Simulations of Scenarios with 100% Renewable Electricity in the Australian National Electricity Market," *Energy Policy*, vol. 45, pp. 606-613, 2012.

[60] A. Fabbri, T. GomezSanRoman, J. RivierAbbad, and V. MendezQuezada, "Assessment of The Cost Associated With Wind Generation Prediction Errors in A Liberalized Electricity Market," *IEEE Transactions on Power Systems*, vol. 20, pp. 1440-1446, 2005.

[61] R. Green and N. Vasilakos, "Market Behaviour with Large Amounts of Intermittent Generation," *Energy Policy*, vol. 38, pp. 3211-3220, 2010.

[62] H. H. Zeineldin, T. H. M. El-Fouly, E. F. El-Saadany, and M. M. A. Salama, "Impact of Wind Farm Integration on Electricity Market Prices," *IET Proceedings, Renewable Power Generation*, vol. 3, pp. 84-95, 2009.

[63] R. Billinton and R. N. Allan, *Reliability Evaluation of Power Systems*, 2nd ed. New York: Plenum Press, 1996.

[64] R. Billinton, M. Fotuhi-Firuzabad, and L. Bertling, "Bibliography on The Application of Probability Methods in Power System Reliability Evaluation 1996-1999," *IEEE Transactions on Power Systems*, vol. 16, pp. 595-602, 2001.

[65] R. Allan, R. Billinton, A. Breipohl, and C. Grigg, "Bibliography on The Application of Probability Methods in Power System Reliability Evaluation: 1987-1991," *IEEE Transactions on Power Systems*, vol. 9, pp. 41-49, 1994.

[66] P. Wang, L. Goel, and Y. Ding, "The Impact of Random Failures on Nodal Price and Nodal Reliability in Restructured Power Systems," *Electric Power Systems Research*, vol. 71, pp. 129-134, 2004.

[67] P. Wang, Y. Ding, and Y. Xiao, "Technique to Evaluate Nodal Reliability Indices and Nodal Prices of Restructured Power Systems," *IEE Proceedings, Generation, Transmission and Distribution*, vol. 152, pp. 390-396, 2005.

[68] Y. Ding, "Nodal Reliability and Nodal Price in Deregulated Power Markets," Ph.D Thesis, Nanyang Technological University, Singapore, 2006.

[69] P. Wang, Y. Xiao, and Y. Ding, "Nodal Market Power Assessment in Electricity Markets," *IEEE Transactions on Power Systems*, vol. 19, pp. 1373-1379, 2004.

[70] D. S. Kirschen, "Demand-Side View of Electricity Markets," *IEEE Transactions on Power Systems*, vol. 18, pp. 520-527, 2003.

[71] S. S. Oren, "Design of Ancillary Service Markets," in *Proceedings of the 34th Annual Hawaii International Conference on System Sciences*, 2001, pp. 769-777.

[72] M. Flynn, W. P. Sheridan, J. D. Dillon, and M. J. O'Malley, "Reliability and Reserve in Competitive Electricity Market Scheduling," *IEEE Transactions on Power Systems*, vol. 16, pp. 78-87, 2001.

[73] W. Peng and R. Billinton, "Reliability Assessment of A Restructured Power System Considering the Reserve Agreements," *IEEE Transactions on Power Systems*, vol. 19, pp. 972-978, 2004.

[74] J. F. Prada. (1999). *The Value of Reliability in Power Systems-Pricing Operating Reserves*. Available: http://web.mit.edu/energylab/www/pubs/el99-005wp.pdf

[75] Y. Liu, Z. Alaywan, M. Rothleder, S. Liu, and M. Assadian, "A Rational

Buyer's Algorithm Used for Ancillary Service Procurement," in *IEEE Power Engineering Society Winter Meeting* 2002, pp. 855-860.

[76] E. Allen and M. Ilic, "Reserve Markets for Power Systems Reliability," *IEEE Transactions on Power Systems,* vol. 15, pp. 228-233, 2002.

[77] D. Gan and E. Litvinov, "Energy and Reserve Market Designs with Explicit Consideration to Lost Opportunity Costs," *IEEE Transactions on Power Systems,* vol. 18, pp. 53-59, 2003.

[78] W. Tong, M. Rothleder, Z. Alaywan, and A. D. Papalexopoulos, "Pricing Energy and Ancillary Services in Integrated Market Systems by An Optimal Power Flow," *IEEE Transactions on Power Systems,* vol. 19, pp. 339-347, 2004.

[79] J. Chen, J. S. Thorp, R. J. Thomas, and T. D. Mount, "Locational Pricing and Scheduling For An Integrated Energy-Reserve Market," in *Proceedings of the 36th Annual Hawaii International Conference on System Sciences*, 2003, pp. 56-63.

[80] J. Wang, X. Wang, and Y. Wu, "Operating Reserve Model in the Power Market," *IEEE Transactions on Power Systems*, vol. 20, pp. 223-229, 2005.

[81] Z. Song, L. Goel, and P. Wang, "Optimal Spinning Reserve Allocation in Deregulated Power Systems," *IEE Proceedings, Generation, Transmission and Distribution,* vol. 152, pp. 483-488, 2005.

[82] M. Ortega-Vazquez and D. Kirschen, "Optimizing the Spinning Reserve Requirements using a Cost/Benefit Analysis," *IEEE Transactions on Power Systems,* vol. 22, pp. 24-33, 2007.

[83] S. N. Siddiqi and M. L. Baughman, "Reliability Differentiated Pricing of Spinning Reserve," *IEEE Transactions on Power Systems,* vol. 10, pp. 1211-1218, 1995.

[84] H. Gooi, D. Mendes, K. Bell, and D. Kirschen, "Optimal Scheduling of Spinning Reserve," *IEEE Transactions on Power Systems,* vol. 14, pp. 1485-1492, 2002.

[85] H. Singh and A. Papalexopoulos, "Competitive Procurement of Ancillary Services by An Independent System Operator," *IEEE Transactions on Power Systems,* vol. 14, pp. 498-504, 1999.

[86] M. Najafi, M. Ehsan, M. Fotuhi-Firuzabad, A. Akhavein, and K. Afshar, "Optimal Reserve Capacity Allocation with Consideration of Customer Reliability Requirements," *Energy,* vol. 35, pp. 3883-3890, 2010.

[87] R. Billinton, H. Chen, and R. Ghajar, "Time-series Models for Reliability Evaluation of Power Systems Including Wind Energy," *Microelectronics and Reliability,* vol. 36, pp. 1253-1261, 1996.

[88] B. Gen, "Reliability and Cost/Worth Evaluation of Generating Systems Utilizing Wind and Solar Energy," Ph.D Thesis, University of Saskatchewan, 2005.

[89] Y. Gao, "Adequacy Assessment of Electric Power Systems Incorporating Wind and Solar Energy," MSc Thesis, University of Saskatchewan, 2006.

[90] H. Saadat, *Power System Analysis*. Boston: WCB/McGraw-Hill, 1999.

[91] J. D. Weber, "Implementation of A Newton-Based Optimal Power Flow into A Power System Simulation Environment," MSc Thesis, University of Illinois at Urbana-Champaign, 1997.

[92] A. J. Wood and B. Wollenberg, *Power Generation Operation & Control*. New York: John Wiley & Sons, 2006.

[93] M. L. Baughman and S. N. Siddiqi, "Real-time Pricing of Reactive Power: Theory and Case Study Results," *IEEE Transactions on Power Systems,* vol. 6, pp. 23-29, 1991.

[94] W. Yu-Chi, A. S. Debs, and R. E. Marsten, "A Direct Nonlinear Predictor-Corrector Primal-dual Interior Point Algorithm for Optimal Power Flows," *IEEE Transactions on Power Systems,* vol. 9, pp. 876-883, 1994.

[95] J. A. Momoh, M. E. El-Hawary, and R. Adapa, "A Review of Selected Optimal Power Flow Literature to 1993. II. Newton, Linear Programming and Interior Point Methods," *IEEE Transactions on Power Systems,* vol. 14, pp. 105-111, 1999.

[96] S. Storen and T. Hertzberg, "The Sequential Linear Quadratic Programming Algorithm for Solving Dynamic Optimization Problems-A Review," in *European Symposium on Computer Aides Process Engineering - 5*, UK, 11-14 June 1995, pp. 495-500.

[97] K. Schittkowski, "NLPQL: A FORTRAN Subroutine Solving Constrained Nonlinear Programming Problems," *Annals of Operations Research,* vol. 5, pp. 485-500, 1986.

[98] R. Billinton, S. Kumar, N. Chowdhury, K. Chu, K. Debnath, L. Goel, E. Khan, P. Kos, G. Nourbakhsh, and J. Oteng-Adjei, "A Reliability Test System for Educational Purposes-Basic Data," *IEEE Transactions on Power Systems,* vol. 4, pp. 1238-1244, 1989.

[99] R. Billinton and W. Li, *Reliability Assessment of Electric Power Systems using Monte Carlo Methods*. New York: Plenum Press, 1994.

[100] L. Goel, P. Viswanath, and P. Wang, "Monte Carlo Simulation Based Reliability Evaluation in A Multi-bilateral Contracts Market," *IEE Proceedings, Generation, Transmission and Distribution,* vol. 151, pp. 728-734, 2004.

[101] W. Peng and R. Billinton, "Time Sequential Distribution System Reliability Worth Analysis Considering Time Varying Load and Cost Models," *IEEE Transactions on Power Delivery,* vol. 14, pp. 1046-1051, 1999.

[102] F. C. Schweppe, *Spot Pricing of Electricity*. Boston: Kluwer Academic, 1988.

[103] F. Ding and J. D. Fuller, "Nodal, Uniform, or Zonal Pricing: Distribution of Economic Surplus," *IEEE Transactions on Power Systems,* vol. 20, pp. 875-882, 2005.

[104] R. Billinton, H. Chen, and R. Ghajar, "A Sequential Simulation Technique for Adequacy Evaluation of Generating Systems Including Wind Energy," *IEEE Transactions on Energy Conversion,* vol. 11, pp. 728-734, 1996.

[105] G. E. P. Box and G. M. Jenkins, *Time Series Analysis : Forecasting and Control*, Rev. ed. San Francisco: Holden-Day, 1976.

[106] *NREL: Wind Integration Datasets - About the Wind Integration Datasets*. Available: http://www.nrel.gov/wind/integrationdatasets/about.html

[107] R. Billinton and G. Bai, "Generating Capacity Adequacy Associated with Wind Energy," *IEEE Transactions on Energy Conversion,* vol. 19, pp. 641-646, 2004.

[108] T. N. Goh and K. J. Tan, "Stochastic Modeling and Forecasting of Solar Radiation Data," *Solar Energy,* vol. 19, pp. 755-757, 1977.

[109] H. P. Garg and S. N. Garg, "Prediction of Global Solar Radiation from Bright Sunshine Hours and Other Meteorological Data," *Energy Conversion and Management,* vol. 23, pp. 113-118, 1983.

[110] R. Aguiar and M. Collares-Pereira, "TAG: A Time-dependent, Autoregressive, Gaussian Model for Generating Synthetic Hourly Radiation," *Solar Energy,* vol. 49, pp. 167-174, 1992.

[111] A. Skartveit and J. A. Olseth, "The Probability Density and Autocorrelation of Short-term Global and Beam Irradiance," *Solar Energy,* vol. 49, pp. 477-487, 1992.

[112] S. N. Kaplanis, "New Methodologies to Estimate the Hourly Global Solar Radiation; Comparisons with Existing Models," *Renewable Energy,* vol. 31, pp. 781-790, 2006.

[113] S. Safi, A. Zeroual, and M. Hassani, "Prediction of Global Daily Solar Radiation using Higher Order Statistics," *Renewable Energy,* vol. 27, pp. 647-666, 2002.

[114] A. Sfetsos and A. H. Coonick, "Univariate and Multivariate Forecasting of Hourly Solar Radiation with Artificial Intelligence Techniques," *Solar Energy,* vol. 68, pp. 169-178, 2000.

[115] L. Mora-Lopez and M. Sidrach-De-Cardona, "Multiplicative ARMA Models to Generate Hourly Series of Global Irradiation," *Solar Energy,* vol. 63, pp. 283-291, 1998.

[116] F. M. González-Longatt, "Model of Photovoltaic Module in Matlab," *II CIBELEC,* vol. 2005, pp. 1-5, 2005.

[117] J. Rivier Abbad, "Electricity Market Participation of Wind Farms: The Success Story of The Spanish Pragmatism," *Energy Policy,* vol. 38, pp. 3174-3179, 2010.

[118] P. Pinson, C. Chevallier, and G. N. Kariniotakis, "Trading Wind Generation From Short-Term Probabilistic Forecasts of Wind Power," *IEEE Transactions on Power Systems,* vol. 22, pp. 1148-1156, 2007.

[119] S. N. Singh and I. Erlich, "Strategies for Wind Power Trading in Competitive Electricity Markets," *IEEE Transactions on Energy Conversion,* vol. 23, pp. 249-256, 2008.

[120] A. Dukpa, I. Duggal, B. Venkatesh, and L. Chang, "Optimal Participation and Risk Mitigation of Wind Generators in An Electricity Market," *IET Proceedings, Renewable Power Generation,* vol. 4, pp. 165-175, 2010.

[121] *Reliability Standards*. Available: http://www.nerc.com/page.php?cid=2|20

[122] *PJM Manual 12: Balancing Operations*. Available:

http://www.pjm.com/documents/~/media/documents/manuals/m12.ashx

[123] *Ancillary Service Procurement and Availability Validation*. Available: http://www.caiso.com/Documents/1340.pdf

[124] Y. Ding, P. Wang, L. Goel, P. C. Loh, and Q. Wu, "Long-Term Reserve Expansion of Power Systems With High Wind Power Penetration Using Universal Generating Function Methods," *Power Systems, IEEE Transactions on*, vol. 26, pp. 766-774, 2011.

[125] Y. Ding and P. Wang, "Reliability and Price Risk Assessment of A Restructured Power System with Hybrid Market Structure," *IEEE Transactions on Power Systems*, vol. 21, pp. 108-116, 2006.

[126] J. M. Arroyo and F. D. Galiana, "Energy and Reserve Pricing in Security and Network-Constrained Electricity Markets," *IEEE Transactions on Power Systems*, vol. 20, pp. 634-643, 2005.

[127] T. Zheng and E. Litvinov, "Contingency-Based Zonal Reserve Modeling and Pricing in a Co-Optimized Energy and Reserve Market," *IEEE Transactions on Power Systems*, vol. 23, pp. 277-286, 2008.

[128] T. Zheng and E. Litvinov, "Ex Post Pricing in The Co-optimized Energy and Reserve Market," *IEEE Transactions on Power Systems*, vol. 21, pp. 1528-1538, 2006.

[129] I. P. M. Subcommittee, "IEEE Reliability Test System," *IEEE Transactions on Power Apparatus and Systems*, vol. PAS-98, pp. 2047-2054, 1979.

[130] L. Chen, H. Suzuki, T. Wachi, and Y. Shimura, "Components of Nodal Prices for Electric Power Systems," *IEEE Transactions on Power Systems*, vol. 17, pp. 41-49, 2002.

[131] R. Billinton and R. Karki, "Capacity Expansion of Small Isolated Power Systems Using PV and Wind Energy," *IEEE Transactions on Power Systems*, vol. 16, pp. 892-897, 2001.

[132] R. Doherty and M. O'Malley, "A New Approach to Quantify Reserve Demand in Systems with Significant Installed Wind Capacity," *IEEE Transactions on Power Systems*, vol. 20, pp. 587-595, 2005.

[133] D. Lew, D. Piwko, N. Miller, G. Jordan, K. Clark, and L. Freeman. (2010). *How Do High Levels of Wind and Solar Impact the Grid? The Western Wind and Solar Integration Study*. Available: http://www.nrel.gov/wind/systemsintegration/pdfs/2010/lew_wwsis_grid_impact.pdf

[134] H. Holttinen, "Impact of Hourly Wind Power Variations on The System Operation in The Nordic Countries," *Wind Energy*, vol. 8, pp. 197-218, 2005.

[135] E. Ela, M. Milligan, and B. Kirby. (2011). *Operating Reserves and Variable Generation*. Available: www.nrel.gov/docs/fy11osti/51978.pdf

[136] Y. Ding, P. Wang, L. Goel, R. Billinton, and R. Karki, "Reliability assessment of restructured power systems using reliability network equivalent and pseudo-sequential simulation techniques," *Electric Power Systems Research*, vol. 77, pp. 1665-1671, 2007.

[137] R. Karki and R. Billinton, "Cost-effective Wind Energy Utilization for

Reliable Power Supply," *IEEE Transactions on Energy Conversion*, vol. 19, pp. 435-440, 2004.

[138] J. C. O. Mello, A. M. Leite da Silva, and M. V. F. Pereira, "Efficient Loss-of-Load Cost Evaluation by Combined Pseudo-sequential and State Transition Simulation," *IEE Proceedings, Generation, Transmission and Distribution*, vol. 144, pp. 147-154, 1997.

[139] A. M. Leite da Silva, L. A. Da Fonseca Manso, J. C. De Oliveira Mello, and R. Billinton, "Pseudo-chronological Simulation for Composite Reliability Analysis with Time Varying Loads," *IEEE Transactions on Power Systems*, vol. 15, pp. 73-80, 2000.

[140] J. C. O. Mello, M. V. F. Pereira, and A. M. Leite da Silva, "Evaluation of reliability worth in composite systems based on pseudo-sequential Monte Carlo simulation," *Power Systems, IEEE Transactions on*, vol. 9, pp. 1318-1326, 1994.

[141] C. Singh and A. Lago-Gonzalez, "Reliability Modeling of Generation Systems Including Unconventional Energy Sources," *IEEE Transactions on Power Apparatus and Systems*, pp. 1049-1056, 1985.

[142] L. Stember, W. Huss, and M. Bridgman, "A Methodology for Photovoltaic System Reliability & Economic Analysis," *IEEE Transactions on Reliability*, vol. 31, pp. 296-303, 2009.

[143] C. University, Elia, E. TSO, H. Transmission, REE, and RTE. (2011). *D22; D331; D332; D32 Current Designs and Expected Evolutions of Day-ahead, Intra-day and Balancing Market/ Mechanisms in Europe*. Available: http://www.optimate-platform.eu/downloads/

[144] R. D. Zimmerman and C. E. Murillo-Sanchez, "Matpower 4.1 User's Manual."

[145] P. Meibom, R. Barth, B. Hasche, H. Brand, C. Weber, and M. O'Malley, "Stochastic Optimization Model to Study the Operational Impacts of High Wind Penetrations in Ireland," *IEEE Transactions on Power Systems*, pp. 1-12, 2010.

[146] H. Holttinen, P. Meibom, A. Orths, F. van Hulle, B. Lange, M. O'Malley, J. Pierik, B. Ummels, J. O. Tande, and A. Estanqueiro, *Design and Operation of Power Systems with Large Amounts of Wind Power: Final report, IEA WIND Task 25, Phase One 2006-2008*: VTT Technical Research Centre of Finland, 2009.

[147] M. A. Matos and R. J. Bessa, "Setting the Operating Reserve Using Probabilistic Wind Power Forecasts," *IEEE Transactions on Power Systems*, vol. 26, pp. 594-603, 2011.

[148] M. A. Ortega-Vazquez and D. S. Kirschen, "Estimating the Spinning Reserve Requirements in Systems With Significant Wind Power Generation Penetration," *IEEE Transactions on Power Systems*, vol. 24, pp. 114-124, 2009.

[149] Y. V. Makarov, C. Loutan, M. Jian, and P. de Mello, "Operational Impacts of Wind Generation on California Power Systems," *IEEE Transactions on Power Systems*, vol. 24, pp. 1039-1050, 2009.

[150] G. Giebel, R. Brownsword, G. Kariniotakis, M. Denhard, and C. Draxl. (2011). *The State-of-The-Art in Short-Term Prediction of Wind Power: A Literature Overview*. Available: http://www.anemos-plus.eu/

[151] C. Monteiro, R. Bessa, V. Miranda, A. Botterud, J. Wang, and G. Conzelmann. (2009, Wind Power Forecasting : State-of-The-Art 2009. Available: http://www.osti.gov/energycitations/servlets/purl/968212-IMKXCO/

[152] *GEA14954C15-MW-Brochure*. Available: http://site.ge-energy.com/prod_serv/products/wind_turbines/en/downloads/GEA14954C15-MW-Broch.pdf

Author's Publications

- Q. Zhao, P. Wang, L. Goel and Y. Ding, "Impacts of Contingency Reserve on Nodal Price and Nodal Reliability Risk in Deregulated Power Systems", *Accepted by IEEE Transactions on Power Systems, 2013*.
- Q. Zhao, P. Wang, L. Goel and Y. Ding, "Evaluation of Nodal Reliability and Reserve in Deregulated Power System with Solar Power Penetration", *Accepted by IET Proceedings, Generation, Transmission and Distribution, 2013.*
- Q. Zhao, P. Wang, L. Goel and Y. Ding, "Reserve Optimization to Improve Operational Reliability in Deregulated Power System with PV Power Penetration", *Probabilistic Methods Applied to Power Systems (PMAPS), The 12th International Conference Proceedings, 10-14 June, 2012, Istanbul, Turkey.*
- Q. Zhao, P. Wang, L. Goel and Y. Ding, "Impacts of Renewable Energy Penetration on Nodal Price and Nodal Reliability in Deregulated Power System", *Proceedings of the Power and Energy Society General Meeting, 2011 IEEE, pp.1-6, 24-29 July, 2011 Detroit, Michigan, USA.*
- Q. Zhao, P. Wang, Y. Ding and Lalit Goel, "Impacts of Solar Power Penetration on Nodal Prices and Nodal Reliability", *The 9th International Power and Energy Conference(IPEC), 2010 Conference Proceedings, pp.1134-1139, 27-29 Oct., 2010, Singapore.*
- Q. Zhao, P. Wang and L. Goel, "Optimal PV Panel Tilt Angle Based on Solar Radiation Prediction", *Probabilistic Methods Applied to Power Systems (PMAPS), 2010 IEEE 11th International Conference Proceedings, pp.425-430, 14-17 June, 2010, Singapore.*